F. W. Klaiber, T. J. Wipf, F. S. Fanous,
T. E. Bosch, H. El-Arabaty

Strengthening of an Existing Continuous-Span, Steel-Stringer, Concrete-Deck Bridge

Sept. 1993

Sponsored by the
Iowa Department of Transportation Highway Division
and the Iowa Highway Research Board

FINAL REPORT

Iowa DOT Project HR-333
ISU-ERI-Ames-94403

Iowa Department of Transportation

report

College of Engineering
Iowa State University

The opinions, findings, and conclusions expressed in this publication are those of the authors and not necessarily those of the Highway Division of the Iowa Department of Transportation.

F. W. Klaiber, T. J. Wipf, F. S. Fanous,
T. E. Bosch, H. El-Arabaty

Strengthening of an Existing Continuous-Span, Steel-Stringer, Concrete-Deck Bridge

Sponsored by the
Iowa Department of Transportation Highway Division
and the Iowa Highway Research Board

FINAL REPORT

Iowa DOT Project HR-333
ISU-ERI-Ames-94403

engineering research institute
iowa state university

ABSTRACT

The need to upgrade understrength bridges in the United States has been well documented in the literature. The concept of strengthening steel stringer bridges in Iowa has been developed through several Iowa DOT projects. The objective of the project described in this report was to investigate the use of one such strengthening system on a three-span continuous steel stringer bridge in the field. In addition, a design methodology was developed to assist bridge engineers with designing a strengthening system to obtain the desired stress reductions.

The bridge selected for strengthening was in Cerro Gordo County near Mason City, Iowa on County Road B65. The strengthening system was designed to remove overstresses that occurred when the bridge was subjected to Iowa legal loads. A two part strengthening system was used: post-tensioning the positive moment regions of all the stringers and superimposed trusses in the negative moment regions of the two exterior stringers at the two piers. The strengthening system was installed in the summer of 1992. Instrumentation was installed in the summers of 1992 and 1993.

In the summer of 1993, the bridge was load tested before and after the strengthening system was activated. The load test results indicate that the strengthening system was effective in reducing the overstress in both the negative and positive regions of the stringers.

The design methodology that was developed includes a procedure for determining the magnitude of post-tensioning and truss forces required to strengthen a given bridge. This method utilizes moment and force fractions to determine the distribution of strengthening axial forces and moments throughout the bridge. Finite element analysis and experimental results were used in the formulation and calibration of the methodology. A spreadsheet was developed to facilitate the calculation of these required strengthening forces.

TABLE OF CONTENTS

LIST OF FIGURES

LIST OF FIGURES

LIST OF FIGURES

LIST OF TABLES

1. INTRODUCTION

1.1. General Background

A significant increase in legal loads as well as increases in the volume of traffic has left many of the nation's older bridges structurally deficient. In addition, inadequate maintenance over many years has complicated the problem. An alternative to posting or replacing the under-capacity bridges is to strengthen them. The goal of the strengthening process is to increase the rated strength of the bridge enough to eliminate the need for posting.

1.2. Objectives

The primary objective of this study was the development of a design methodology for designing strengthening systems for overstressed continuous span bridges. A secondary objective of the research program was to design, install, and test a strengthening system for both the negative moment regions and positive moment regions of a given continuous span bridge. In HR-308 [1], only positive moment regions were post-tensioned which was successful in reducing critical stresses below inventory level at all locations except in the vicinity of the piers, where a slight overstress still existed. Users of the proposed design methodology developed in this investigation should be aware that post-tensioning positive moment regions of a continuous span bridge may not, in all cases, reduce overstresses below inventory level in the negative moment regions. This investigation presents a method of eliminating the overstresses in the negative moment regions using post-tensioning of the positive moment regions and superimposed trusses at the piers.

Theoretical investigations of several negative moment region strengthening techniques were completed in a previous research project HR-302 [2]. Post-compression of negative moment regions and the use of superimposed trusses (trusses or truss system) in the negative moment regions has been investigated in the laboratory. A summary of the results of these laboratory tests will be presented here. The laboratory negative moment region mockup utilized in HR-302 was very similar to the negative moment region of the bridge strengthened in the current investigation. A description of the current bridge will be presented later in this report.

Although several locations on the laboratory mockup were instrumented with electrical-resistance strain gages (strain gages), only two locations will be discussed here. The reader is encouraged to consult HR-302 [2] for a more complete examination of the experimental result. Location A was approximately one ft from the simulated pier support and Location B was near the end of the coverplate. Post-compression of the stringer resulted in a 36% and 58% reduction in bottom-flange compressive strain at Location A and Location B, respectively. The corresponding bottom-flange compressive strain reduction for the truss system was 48% for Location A and 30% for Location B. However, the post-compression technique also resulted in an undesirable top flange tensile strain increase of approximately 20% at each location. Based on the laboratory tests and theoretical analysis, the trusses were selected for use in the negative moment regions along with post-tensioning of the positive moment regions for the current research work.

1.3. Research Program

The research program consisted of two parts: Part 1 - Development of a Design Manual, Part 2 - Field Tests. Parts 1 and 2 will be discussed separately in the following subsections. In conjunction with the two main parts of the research program, several additional tasks were also performed.

The researchers have performed several comprehensive literature reviews pertaining to the strengthening of bridges. Section 1.4 of this report refers to the previous literature reviews along with literature reviews of current research. Because the previous literature reviews are readily available, they have not been duplicated here.

The supplemental literature review is presented in Sec. 1.4. Chapter 2 describes the bridge and layout of the strengthening system applied to the bridge. The instrumentation and field test procedure used are discussed in Chp. 3. Chapter 4 presents the development of the strengthening design methodology. Results of the field tests and the finite element analysis are summarized in Chp. 5. Following the results, are the summary and conclusions in Chp. 6 and recommended further research in Chp. 7.

1.3.1. Development of a design manual

The development of a design manual involved the development of a practical procedure for determining the magnitude and location of post-tensioning and truss forces required to strengthen a given bridge. A more complete discussion of the design manual can be found in Ref. 3. Finite element analysis and experimental results from previous projects HR-308,HR-287 [1,4] were used in the formulation and

calibration of the developed design methodology. A sensitivity study using the finite element analysis was conducted to determine the effects of the design variables on the distribution of the post-tensioning forces. Factors such as number of spans, span lengths, angle-of-skew, stringer spacing, deck thickness, concrete strength, etc. were considered. From these analyses it was determined which variables could be eliminated from the analytical models. The design methodology is similar to the one developed for simple spans bridges, HR-238 Part III [5] which involved moment fractions and force fractions. However, because of the longitudinal distribution of force exhibited by continuous bridges, the resulting design methodology for continuous span bridges is considerably more complex.

A spreadsheet was developed to facilitate the calculation of the required strengthening forces. This will enable the practicing engineer to design the strengthening system with avoiding the use of a more complex analysis such as finite element analysis.

1.3.2. Field tests

The field tests involved the implementation of a strengthening system for application to a three-span continuous, steel-girder, concrete-deck bridge. Vertical load testing of the bridge was performed prior to and after the strengthening system was implemented to investigate the effectiveness of the strengthening system.

The bridge selected for strengthening in this study was chosen by the research team in coordination with the Office of Bridge Design at the Iowa DOT. The bridge selected was similar to the bridge strengthened in 1988 by the research team (HR-308) [1]. The bridge is a three-span continuous,

steel stringer, concrete deck bridge from the V12 (1957) series. Chapter 2 contains a detailed discussion of the bridge selected.

Once the bridge was selected the analytical work necessary to determine the extent to which the bridge was overstressed when subjected to Iowa legal loads was performed. The strengthening system could then be designed to eliminate these overstresses. A two part strengthening system was used involving post-tensioning as utilized in 1988 (HR-308) [1] and a superimposed truss system to further reduce negative moment overstresses at the pier supports. The specifics of the strengthening system are detailed in Chp. 2.

The strengthening system was installed on the bridge in the summer of 1992. Instrumentation of the bridge was accomplished in the summers of 1992 and 1993. The instrumentation included strain gages on the stringer flanges and displacement instruments to measure vertical and longitudinal displacements.

In the summer of 1993, after all of the instrumentation was completed and checked, the bridge was load tested both prior to and subsequent to the strengthening system being activated. The bridge was subjected to the following loading conditions:

1. Heavily loaded truck(s) at predetermined locations on the bridge prior to providing the strengthening system.
2. Implementation of the truss strengthening system.
3. A heavily loaded truck at several locations on the bridge.
4. The remaining stages of the strengthening sequence.

5. The same heavily loaded truck(s) at the locations given in step 1 to determine the effectiveness of the strengthening system.

Approximately every three months after the strengthening for a one year period, the bridge will be inspected to monitor the bridge's behavior.

1.4. Literature Review

The literature review presented here is not intended to be a complete examination of existing strengthening techniques but rather to be a supplement to the previous literature reviews performed for the Iowa DOT. The previous literature reviews are available in the following references:

- post-tensioning of simple span bridges [5,6,7,8]
- post-tensioning of continuous span bridges [1]
- strengthening of highway bridges [2,9,10]

The articles summarized in this section deal with recent strengthening methods for simple and continuous span bridges which are no in the literature reviews previously noted. Several related experimental studies have been documented in the literature. Some of these studies have included developing analytical models to confirm the experimental results.

A flexural design and analysis methodology for prestressed composite beams was proposed by Saadatmanesh et al. [11]. The methodology incorporates both working stress design and load factor design principles. Its application is limited to the following construction sequences. For positive moment regions, the steel stringer must be prestressed prior to the concrete deck being cast. For negative moment regions,

the steel stringer should be prestressed, then compositely connected to a precast, prestressed concrete deck.

Five prestressed, composite, welded girders were tested to failure under negative bending moment by Ayyub et al. [12]. The test setup approximated the support region between the inflection points of a continuous girder. The steel girders had varying proportions with some elements being non-compact in an attempt to determine the effect of compactness on prestressed composite girders. In addition, the study involved comparing the structural behavior of the prestressed composite girders under several different deck prestressing conditions and prestressing sequences for the deck and girders.

In a companion paper to the preceding article, Ayyub et al. [13] reported on an analytical study of two of the prestressed composite girders mentioned in Ref. 12. An incremental deformation technique was used in the analysis. A detailed comparison of experimental and analytical results was included in the study.

In another investigation by Ayyub et al. [14], three composite steel-concrete beams with varying tendon types and profiles were tested to failure under positive bending moment. Analytical models of the beams were developed in an attempt to predict stresses in the tendons, concrete deck, and steel beams. The investigators also attempted to predict deflections with their models which were developed using the strain compatibility method. The theoretical stresses and deflections determined with the model agreed quite well with the experimental results. Comparisons between tendon types (bar vs. strand) and tendon profiles (straight vs. draped) were also made.

The results indicated that strands are the preferable tendon type because of the savings in steel weight. It was also shown that straight tendons were better than draped tendons because of the higher yield load experienced and their lower construction cost.

The elastic behavior of continuous prestressed beams was investigated by Tong and Saadatmanesh [15]. The investigators presented two methods of analysis for the beams. For straight discontinuous tendons the stiffness method was used. A combination of stiffness and flexibility methods was used for draped continuous tendon profiles.

Two girders were modeled using these methods. The first model was a two-span, continuous, prestressed, composite girder. With this model, the effect of prestress force, eccentricity, tendon profile, and tendon length were investigated.

A three-span, continuous, prestressed, composite girder model was also developed. The effect that different tendon profiles had on the model's behavior was examined. Also, pattern loading of both models was investigated to determine its effect on the change in tendon force in each span.

Mancarti [16] has presented design criteria and strengthening methods for short span bridges. These criteria are currently being used by the California Department of Transportation (Caltrans).

The State of California has designated specific routes for permit vehicles. Many of the bridges on these routes, however, were deficient with respect to moment capacity for the permit vehicles. Caltrans has used post-tensioning to

strengthen many of these bridges. They have had success post-tensioning both steel girder and concrete girder bridges.

Albrecht and Li [17] investigated the fatigue strength of prestressed composite beams in 1989. The beams tested were prestressed prior to the deck being cast and had the following fatigue prone details: prestressing strands, shear studs, and coverplates. The prestressed composite beams were stress cycled until a fatigue crack developed at the end of the coverplates. The beam was repaired using the first of three repair methods investigated and was stress cycled again. When the first repair failed, the beam was repaired using a second method. The beam was stress cycled a third time until fatigue failure once again occurred. The final repair method investigated increased the initial prestressing force until the bottom flange was no longer experiencing tensile stresses during the cyclic loading. Increasing the prestressing force changed the stress cycle in the bottom flange from tension-compression to low compression-high compression. The third repair procedure was found to be a very effective means of repairing fatigue cracked beams.

The remaining articles in this literature review pertain to strengthening techniques used in strengthening reinforced concrete members. A strengthening method for reinforced concrete beams was examined in the papers authored by Saadatmanesh and Ehsani [18] and by An and Saadatmanesh [19]. The strengthening technique employed involved the use of fiber composite plates. Fiber composite plates were epoxy-bonded to the exterior of the reinforced concrete beams. The use of fiber composites as a method of strengthening bridge beams has several advantages. Among them are the high strength-to-weight ratio of fiber composites and their resistance to corrosion.

In the paper by Saadatmanesh and Ehsani [18], six simply supported beams were tested to failure under two concentrated loads near midspan. Deflections were measured in addition to strains in the reinforced steel, concrete beam, and fiber reinforced plate. For each beam, plots of deflection and strain vs. load were made up to failure. In the companion paper by An and Saadatmanesh [19], analytical methods were developed to predict the behavior of the externally reinforced beams. With these analytical models, the researchers were able to make comparisons between experimental and predicted values. The investigators also calculated values for beams that were not externally reinforced with fiber composite plates. The results of this study showed that the yield and ultimate loads of the reinforced steel could be increased by 33% and 65%, respectively.

Seible et al. [20] investigated strengthening techniques on a test specimen taken from a cast in place 25 year old reinforced concrete T-beam bridge. Three different strengthening techniques were utilized on the test section. Substantial flexural cracking existed in the positive moment regions of the section. These cracks were repaired using an epoxy injection technique. Subsequent testing revealed that epoxy injection of the flexural cracks increased the longitudinal stiffness of the member. The remaining two strengthening techniques had to be investigated in conjunction with the epoxy injection because it was not possible to remove the epoxy after the first test was performed. Test results showed that external post-tensioning of the epoxy injected bridge section did not increase the longitudinal or transverse flexural stiffness characteristics of the section. However, longitudinal and transverse stiffnesses were increased with the use of a concrete bottom soffit panel attached to the T-beam stems in conjunction with the epoxy injection.

2. BRIDGE DESCRIPTION AND STRENGTHENING DESIGN

2.1. Bridge Description

As mentioned earlier, a group comprised of the research team and representatives of the Office of Bridge Design at the Iowa DOT selected the bridge for this research project. Ten three-span continuous bridges requiring posting were considered by this group. Factors considered included: bridge location, distance from ground to bridge at the midspans, and an available power source. The bridge selected, hereafter referred to as the bridge, is located in north central Iowa in Cerro Gordo county approximately 12 miles south of Mason City, Iowa and seven miles east of Thornton, Iowa on County Road B65.

The bridge framing plan and cross section are shown in Figs. 2.1a and 2.1b, respectively. Photographs of the bridge side view and top view are shown in Figs. 2.2a and 2.2b, respectively. The bridge is three-span continuous with exterior spans of 45 ft 9 in. and a middle span of 58 ft 6 in. for a total length of 150 ft. The four bridge stringers are spliced at the nominal dead load inflection points in the center span. In addition, there are coverplates on both the top and bottom flanges of the stringers at the pier supports.

Steel wide-flange diaphragms are located at the one-third points of the middle span and at the midpoints of the end spans. Diaphragms consist of channel sections at the abutments and standard I-shapes at the piers.

The bridge section is 26 ft wide with a 24 ft roadway providing two 12 ft traffic lanes according to AASHTO [21]. The concrete deck has a variable thickness from 6 7/16 in.

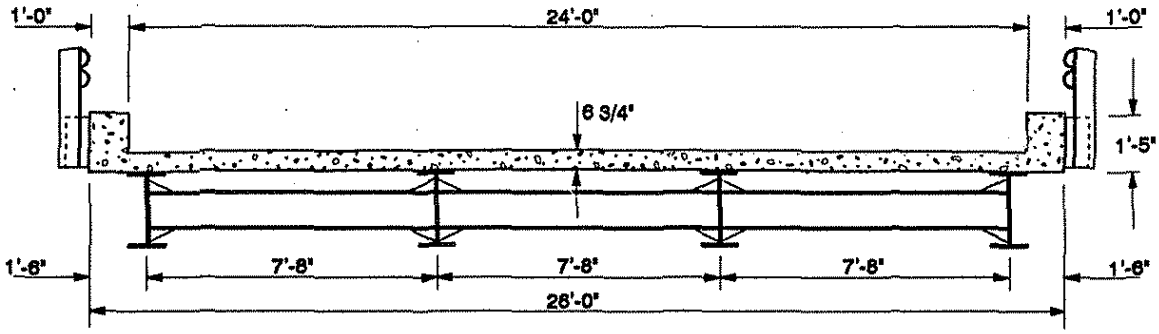

a. BRIDGE SECTION

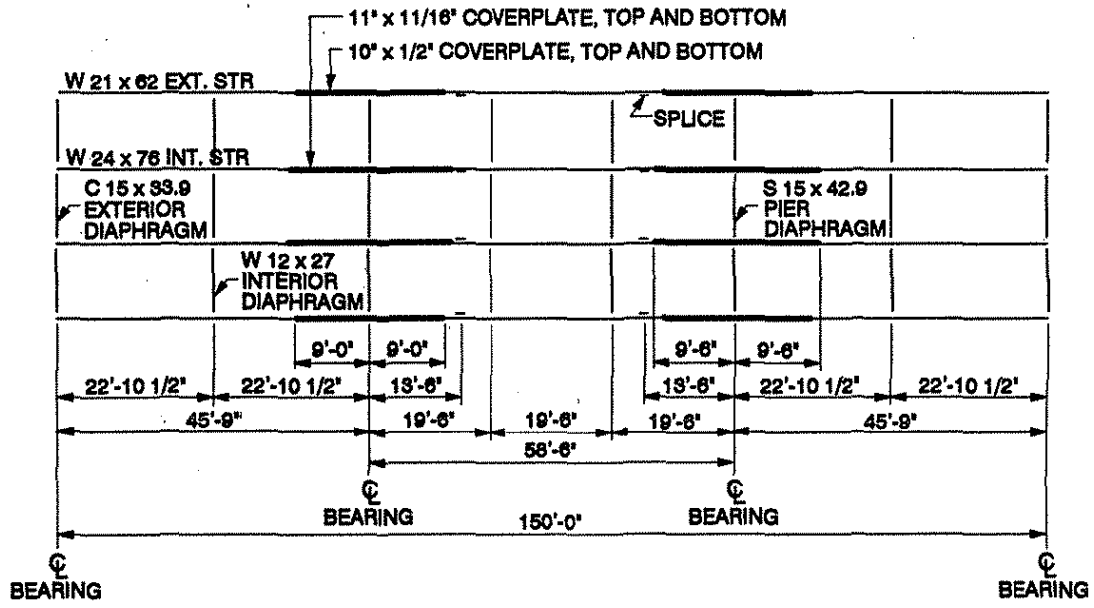

b. BRIDGE FRAMING PLAN

Fig. 2.1. Framing plan of Mason City bridge.

a. SIDE VIEW

b. END VIEW

Fig. 2.2. Photographs of Mason City bridge.

over the stringers to 6 3/4 in. between the stringers. A three-in. crown for positive drainage of the roadway surface results from the difference in height of the interior and exterior stringers. A guardrail is bolted along each integral curb and consists of a 10-gauge formed steel beam rail bolted to L5x5-1/2x3/8 posts spaced at six ft. Continuity of the beam rail sections is provided at alternating angle posts by a bolted one ft overlap. The result of this construction technique is that the beam rail and stringer bottom flange simulates the top and bottom chords of a Vierendeel truss.

Several concrete cores were tested to determine the concrete compressive strength of the deck. Cores had to be removed from the deck for the additional shear connectors required between the deck and stringers. The cores were approximately six in. long with a four in. diameter and were selected such that they did not contain deck reinforcement. Compressive strength tests on six cores were performed in accordance with ASTM Standards and yielded an average compressive strength of 5820 psi, which includes a correction factor for non-standard core dimensions.

Figure 2.3 shows reference sections along the bridge length. These reference sections will be used to refer to locations along the bridge length throughout the remainder of this report. Table 2.1 is a description of the reference sections shown in Fig. 2.3. Only one half of the bridge has been included here because of the symmetry that exists.

2.2. Strengthening Design

This section has been divided into two subsections. In Sec. 2.2.1, the need for and method of providing additional shear connection is presented. In Sec. 2.2.2, the

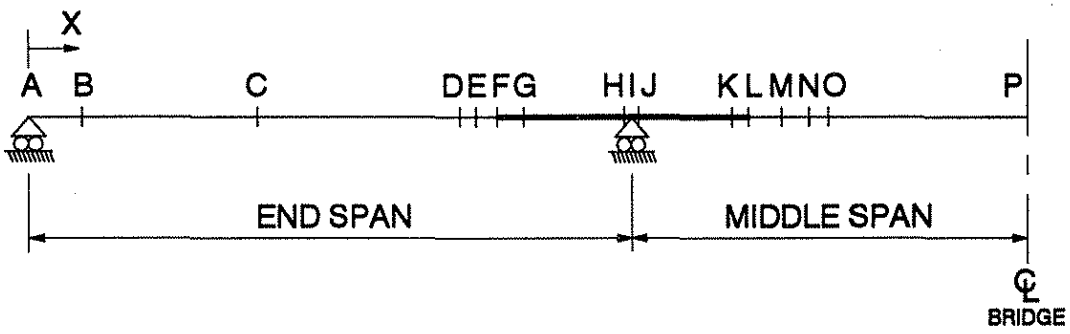

Fig. 2.3. Reference sections along half bridge length.

Table 2.1. Description and location of reference sections.

Section	Description	X, in.	
		Exterior Stringer	Interior Stringer
A	Abutment bearing	0	0
B	Tendon anchorage at Bracket A	66	66
C	Nominal maximum positive moment	220	220
D	Nominal dead-load inflection point and anchorage at Bracket A	400	400
E	Location of truss bearing	412	412
F	Actual coverplate end	431	435
G	Theoretical coverplate end	456	462
H	Pin anchorage at Bracket B	544	544
I	Pier bearing	549	549
J	Pin anchorage at Bracket B	554	554
K	Theoretical coverplate end	642	647
L	Actual coverplate end	657	663
M	Location of truss bearing	686	686
N	Splice and nominal dead-load inflection point	711	711
O	Tendon anchorage at Bracket A	727	727
P	Nominal maximum positive moment and center line of bridge	900	900

development of the strengthening system (post-tensioning and trusses) is discussed.

2.2.1. Shear connector design

According to the current AASHTO design specification [21] the bridge did not have sufficient shear capacity for composite action between the concrete deck and the steel stringers. Thus, additional shear connectors were required to increase the shear capacity.

The original shear connectors are the angle plus bar type. Typically, for the V12 series bridge, a three in. length of L5x5x3/8 is welded vertically to the top flange of the stringer. A small bar is welded across the top of the angle to prevent lift up of the concrete deck.

The number of additional shear connectors required was computed based on Sec. 10.38.5.1 of AASHTO [21]. Existing and new shear connector ultimate strength capacities were obtained from shear strength tests conducted in the Iowa State University Structures Laboratory; results from these tests are reported in Refs. 6 and 22.

For the additional shear capacity, one in. diameter high-strength bolts were added at the locations shown in Fig. 2.4a on the exterior stringers and Fig. 2.4b on the interior stringers. A total of 220 new one in. diameter bolt shear connectors were added to the bridge: 58 on the interior stringers and 52 on the exterior stringers.

2.2.2. Strengthening system design

The design of the strengthening system for the bridge was a two step processes. First, the live load and dead load stresses in the bridge stringers were computed. Following the

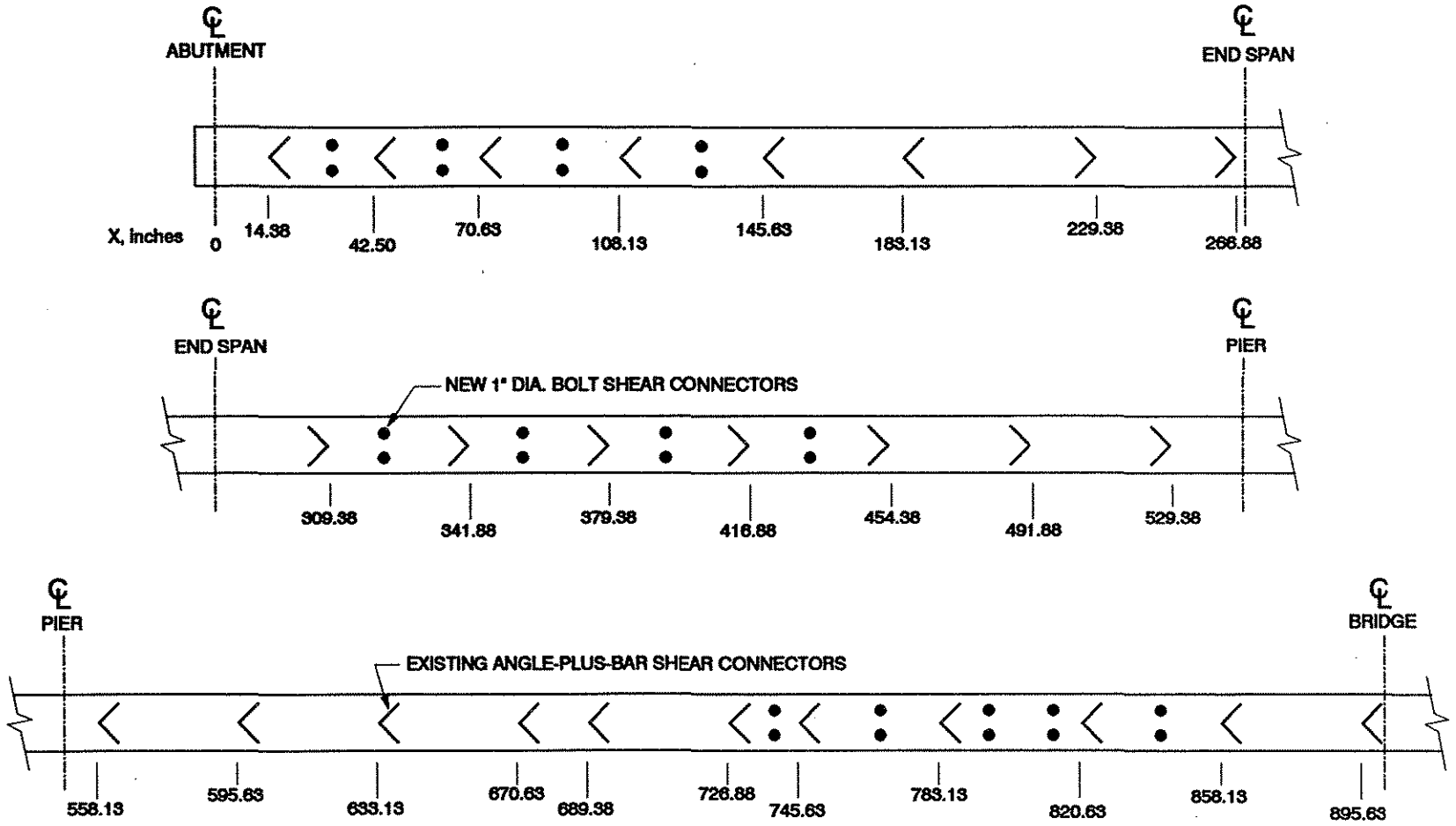

a. EXTERIOR STRINGER (52 bolts total)

Fig. 2.4. New bolt shear connector layout.

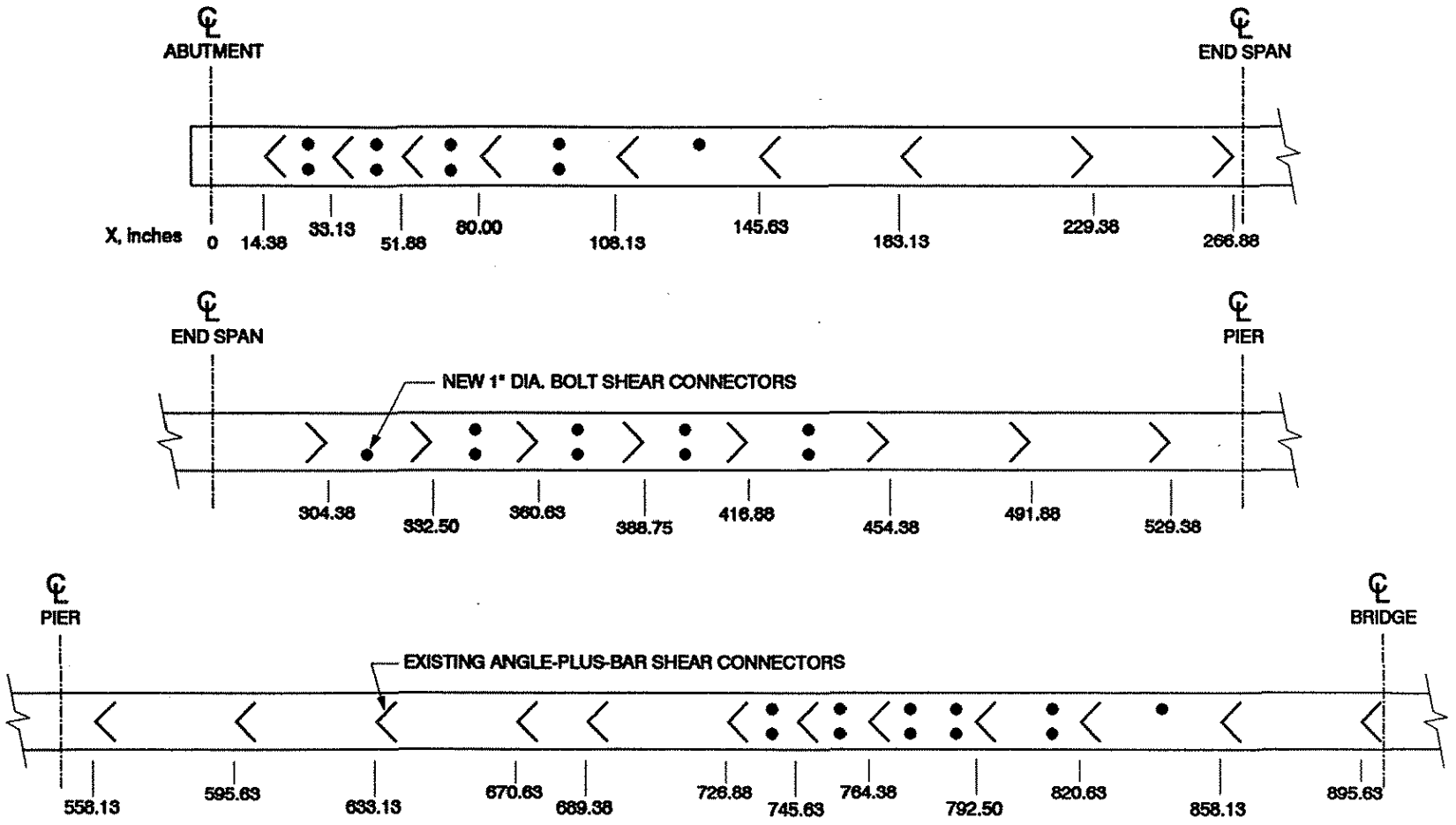

b. INTERIOR STRINGER (58 bolts total)

Fig. 2.4. Continued.

stress computation, it was possible to determine the forces required to reduce the overstresses at the critical locations. The computed forces were applied to the bridge by post-tensioning the positive moment regions of all the stringers (12 locations) and by trusses in the negative moment regions on the exterior stringers only (four locations). A layout of the post-tensioning system employed is shown in Fig. 2.5; photographs of the system are shown in Figs. 2.6. Figure 2.7 illustrates the superimposed truss system used at the pier locations on the exterior stringers. Dimensions of the trusses (one on each side of the exterior stringer web) are shown in Fig. 2.7a; a photo of the trusses in place is shown in Fig. 2.7b.

The moments and stresses in the stringers were computed using Iowa DOT standard procedures. Table 2.2 outlines the section properties assumed along the stringer length. The letters in the *Length* column correspond to the reference sections shown in Fig. 2.3. The bottom-flange stresses that resulted from these assumptions are shown in Figs. 2.8a-c and 2.9a-c for exterior and interior stringers, respectively. From Figs. 2.8a and 2.9a, it can be seen that the maximum positive moment region stress of 22.5 ksi occurs in the

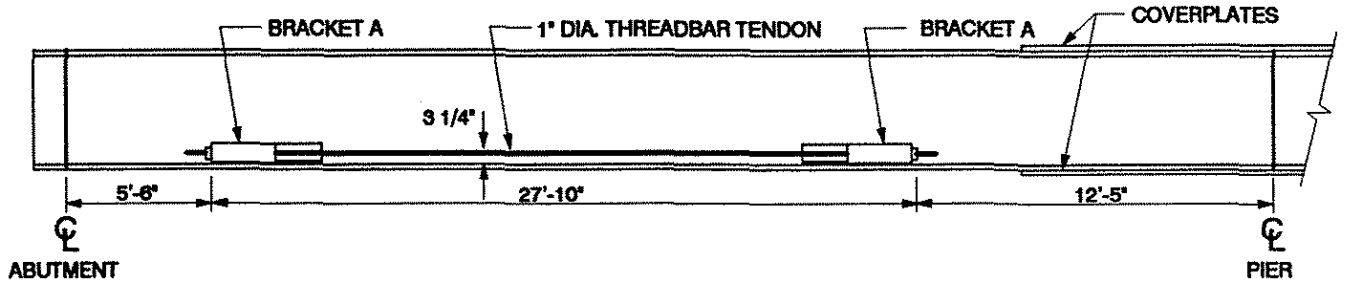

a. END SPAN

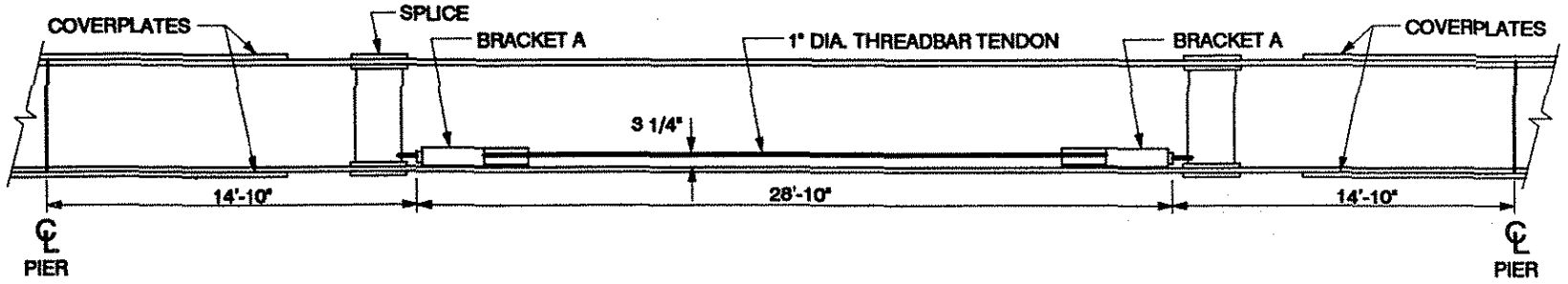

b. MIDDLE SPAN

Fig. 2.5. Post-tensioning layout.

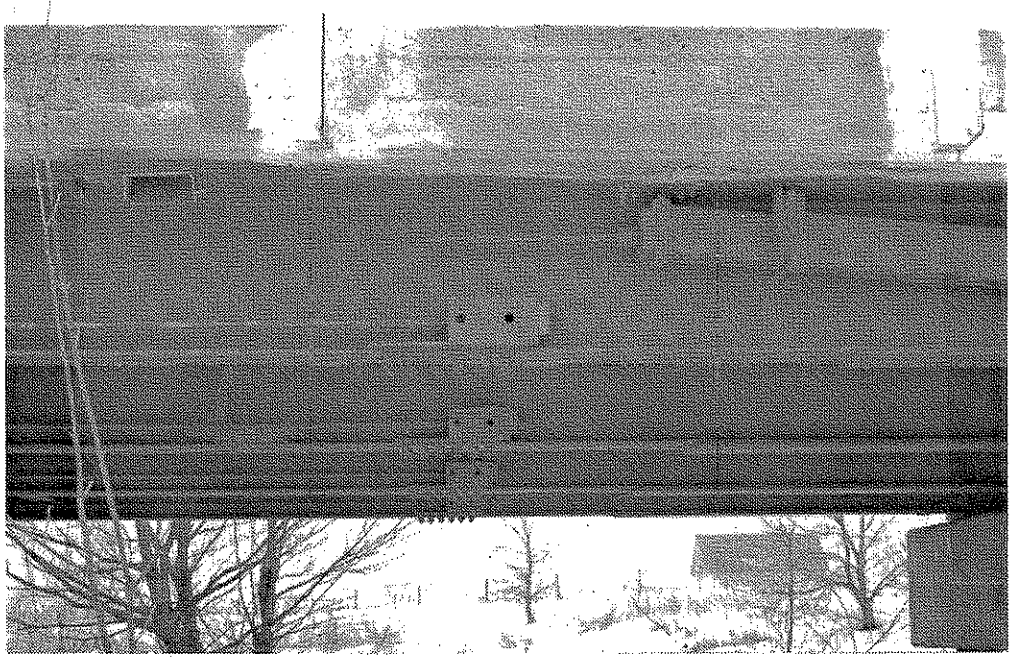

a. POST-TENSIONING BRACKET AND TRUSS BEARING

b. TRUSS STRENGTHENING SYSTEM

Fig. 2.6. Photographs of strengthening system in place.

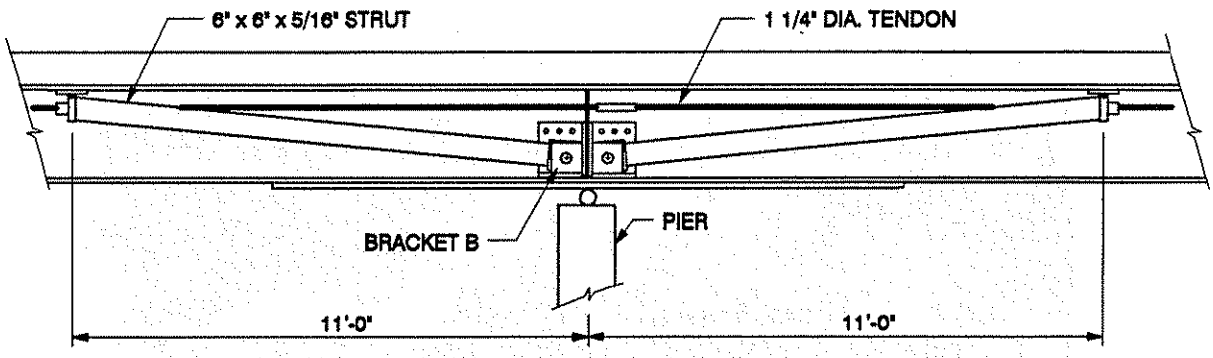

a. SUPERIMPOSED TRUSS

b. SUPERIMPOSED TRUSS PHOTOGRAPH

Fig. 2.7. Superimposed truss system.

Table 2.2. Bridge load-behavior assumptions.

Load	Length[1]	Assumed Effective Cross-Section
Dead (steel stringer and concrete deck)	A-G	wide-flange stringer
	G-K	coverplated wide-flange stringer
	K-P	wide-flange stringer
Long-Term Dead	A-D	composite deck and wide-flange stringer, n=27
	D-G	wide-flange stringer
	G-K	coverplated wide-flange stringer
	K-N	wide-flange stringer
	N-P	composite deck and wide-flange stringer, n=27
Live-positive moment envelope-(Iowa legal trucks and impact) and post-tensioning	A-G	composite deck (and curb for ext. stringer) and wide-flange stringer, n=9
	G-N	composite deck (and curb for ext. stringer) and coverplated wide-flange stringer, n=9
	N-P	composite deck (and curb for ext. stringer) and wide-flange stringer, n=9
Live-negative moment envelope-(Iowa legal trucks and impact) and post-tensioning	A-G	wide-flange stringer
	G-N	coverplated wide-flange stringer
	N-P	wide-flange stringer

[1] Lengths are defined by reference sections given in Fig. 2.3 and Table 2.1.

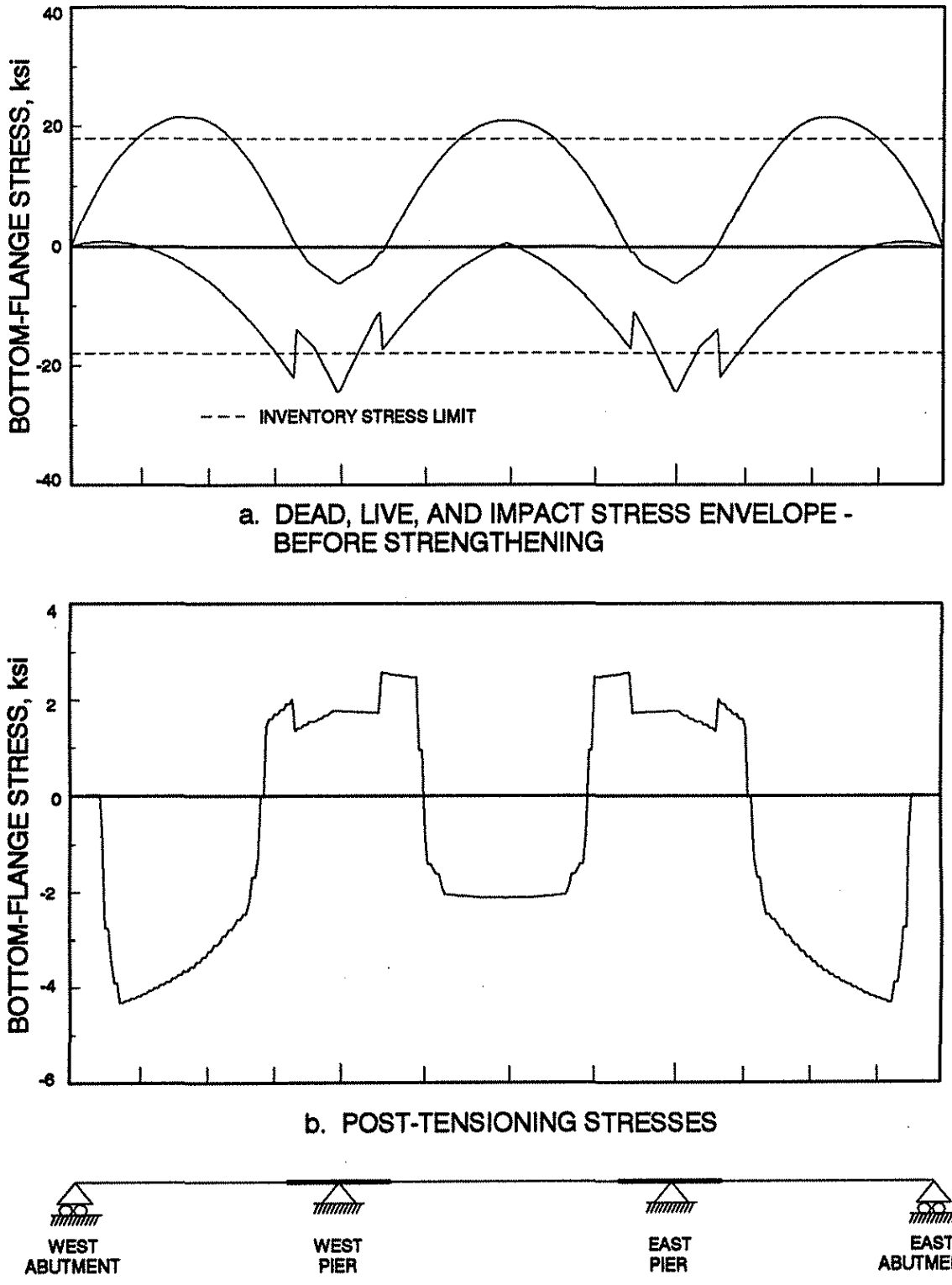

Fig. 2.8. Exterior stringer bottom-flange stress envelope.

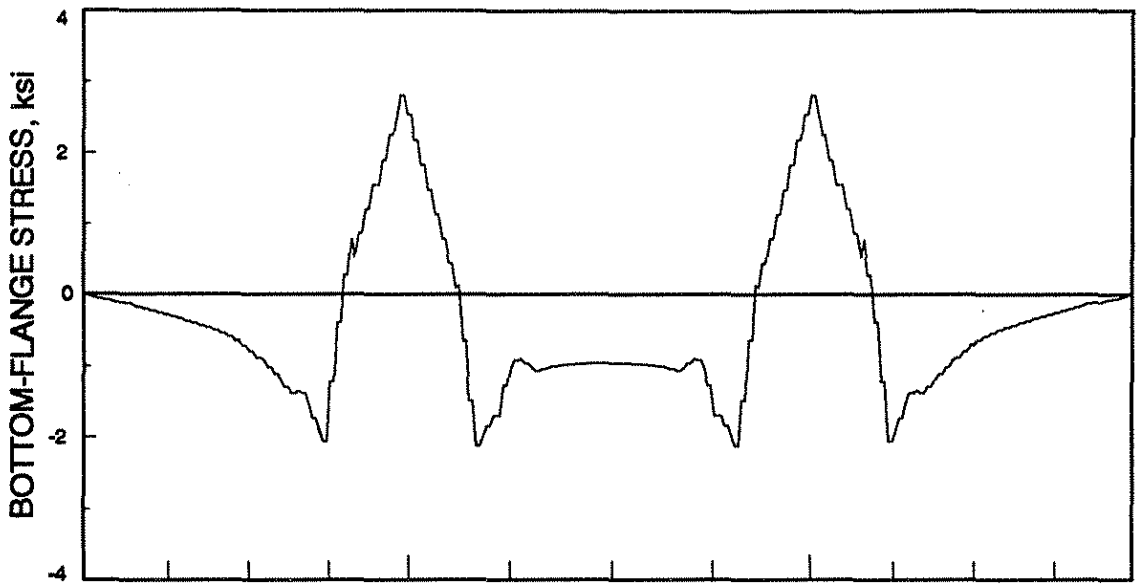

c. SUPERIMPOSED TRUSS STRESSES

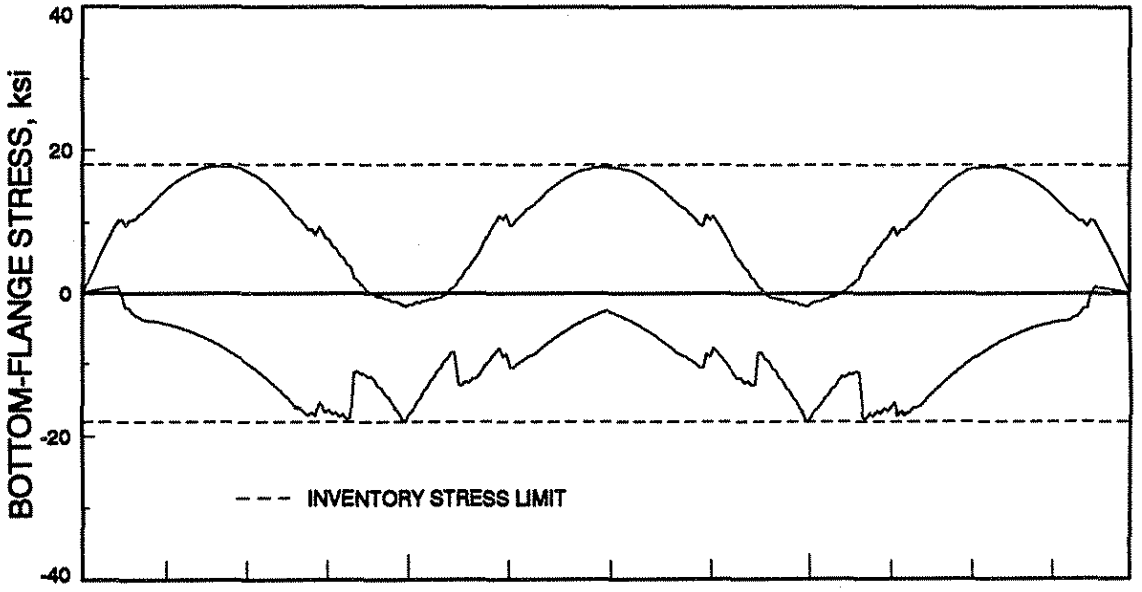

d. COMBINED STRESS ENVELOPE - AFTER STRENGTHENING

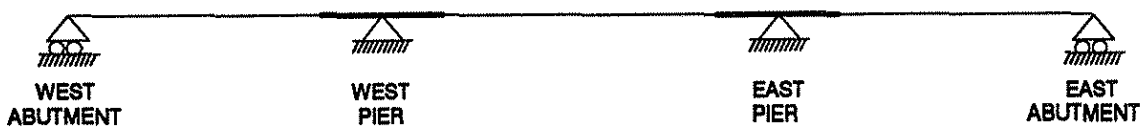

Fig. 2.8. continued.

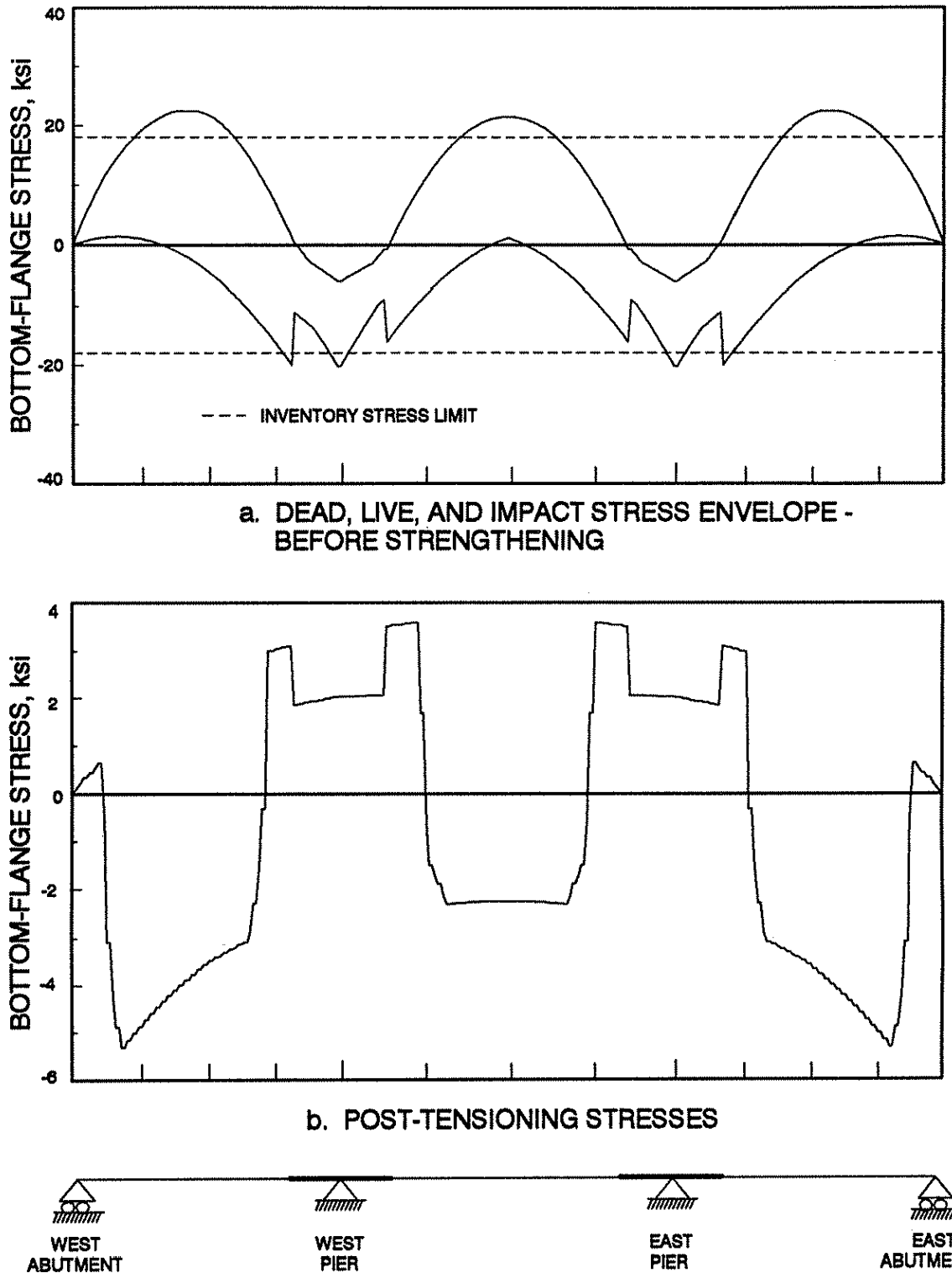

Fig. 2.9. Interior stringer bottom-flange stress envelope.

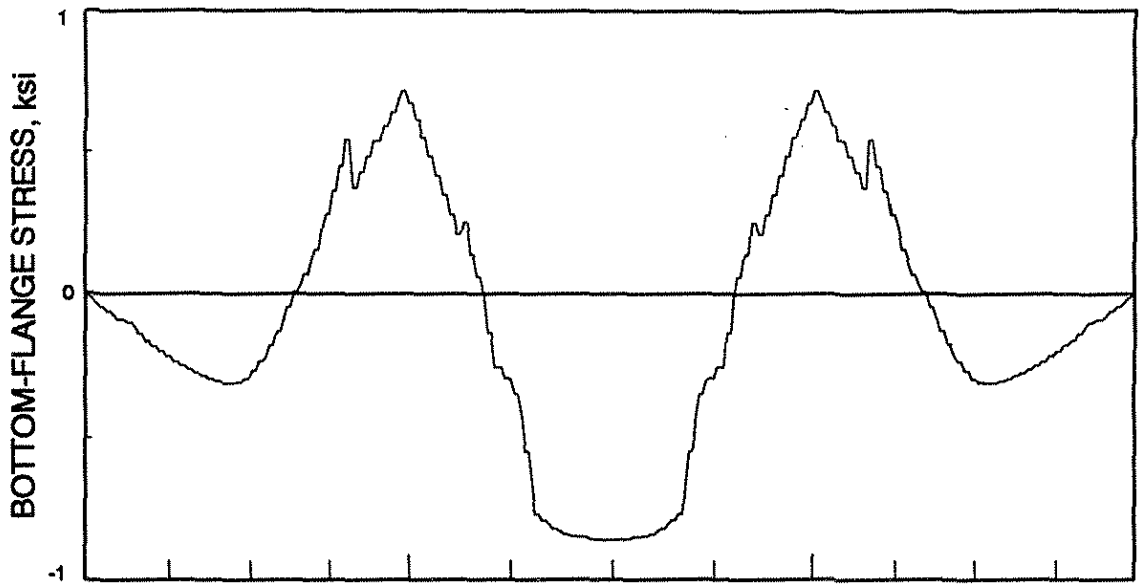

c. SUPERIMPOSED TRUSS STRESSES

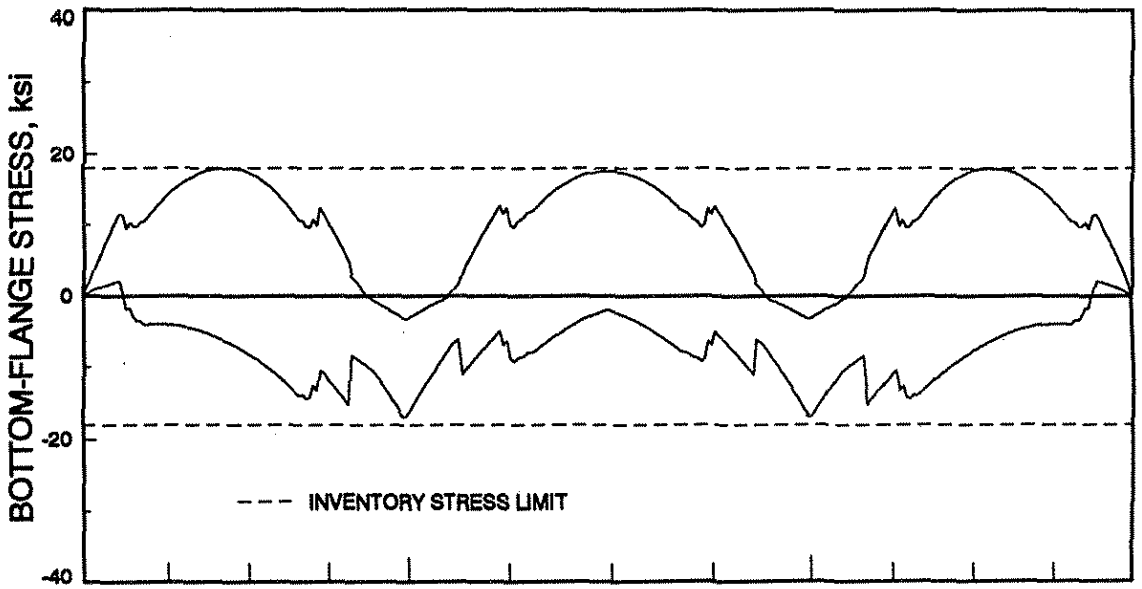

d. COMBINED STRESS ENVELOPE - AFTER STRENGTHENING

Fig. 2.9. continued.

interior stringers while the maximum negative moment region stress of -24.4 ksi occurs in the exterior stringers. These stresses are above the inventory stress level, i.e. above 18 ksi, hence it was necessary to provide a strengthening system to reduce these overstresses to the allowable values.

To design the strengthening system, finite element analyses were performed to calculate the required post-tensioning forces and truss forces. The finite element model is discussed in Sec. 4.1.

The bridge was analyzed using the finite element model considering unit loads applied at the locations shown in Fig. 2.10. For each of the cases illustrated in Fig. 2.10, a unit force was applied to the post-tensioning or truss tendons. Parameters such as location of post-tensioning brackets and truss bearing points were varied so that an optimum strengthening system was achieved. The analysis provided axial forces and moments across the bridge section as well as at different locations along each stringer for each of the above listed parameters.

To calculate the required strengthening forces for this particular bridge, a computer program was developed. The program is comprised of several routines and performs the steps listed:

1. The designer first selects first the strengthening scheme to be used,i.e, use post-tensioning alone or post-tensioning plus superimposed trusses, bracket positions, assumed strengthening forces, and assumed vertical force component of the truss system.
2. The designer inputs files containing the maximum moments obtained from the analysis of the stringers under vertical loads.

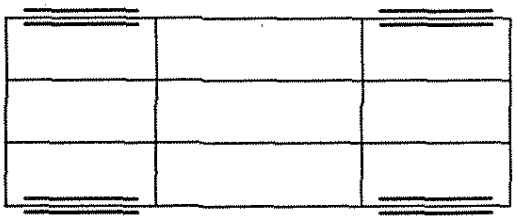

a. CASE 1

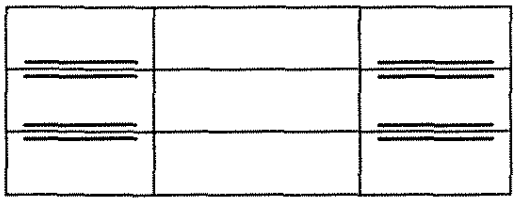

b. CASE 2

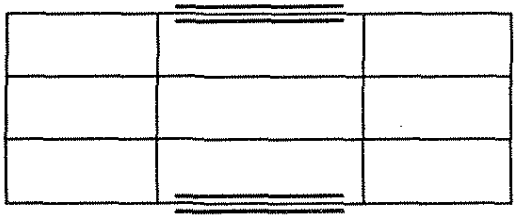

c. CASE 3

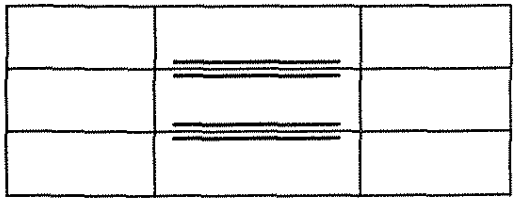

d. CASE 4

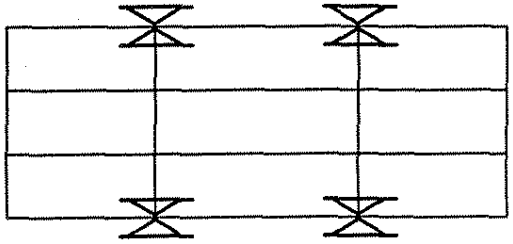

e. CASE 5

Fig. 2.10. Finite element model cases.

3. The designer provides files containing axial forces and moments on the stringers due to unit strengthening forces. These values are those obtained from the finite element analyses. The program selects the correct input according to the tendon length and the truss bearing points.
4. The designer inputs the section properties along the stringer length.
5. The program calculates the moments induced in the stringers due to the vertical loads and the strengthening forces are computed. The program magnifies the moments induced by the strengthening system and combines the magnified values with the vertical load moments. The final stress are then computed and compared with the inventory stresses. The program iterates until the optimum strengthening forces are determined.
6. The program plots the final stress envelopes along the bridge stringers. These are needed to determine if the desired stress reduction in the entire bridge structure was achieved.

An attempt was made to reduce the overstresses at the critical locations using post-tensioning only. However, it was determined that using this alternative did not reduce the overstresses at the pier locations to inventory level. Therefore, it was decided to add superimposed trusses on the exterior stringers at the pier locations to help reduce these overstresses.

The final strengthening forces will be discussed in Sec. 3.2. Figures 2.8d and 2.9d show the resulting bottom-flange stress envelopes. The stress envelopes do not exceed the 18 ksi inventory level at any section along the stringer.

3. *TESTS AND TEST PROCEDURES*

3.1. Instrumentation

Figure 3.1 shows the location of the strain gages on the bridge stringers. There were 56 strain gages located on the top surface of the bottom flange of the stringers oriented with their longitudinal axes parallel to the longitudinal axis of the bridge. All of the flange strain gages were located approximately 1 1/4 in. from the flange edge (see Fig. A.1 in Appendix A). Figure 3.1 also indicates that at six of the abutment locations, strain gages were placed on the bottom surface of the top flange as well as the top surface of the bottom flange. The strain gages near the abutments were positioned to provide an estimate of the end restraint at each end of the bridge.

Strain gages were also attached to the guardrails at ten locations along the bridge length. These gages are also shown on Fig. 3.1 and were oriented in the same direction as the flange gages. The guardrail instrumentation provided an indication of the contribution the guardrails make to the load carrying capacity of the bridge.

Weldable strain gages were used on the bridge. These gages were attached to the bridge by spot welding using a portable hand-probe spot welder. The main advantages of the weldable strain gages are that they can be installed while the bridge is open to traffic, they require only minimal surface preparation for installation, and because no curing time is required, they are usable immediately after installation.

Each of the tendons used in the strengthening system was instrumented with two conventional strain gages to monitor

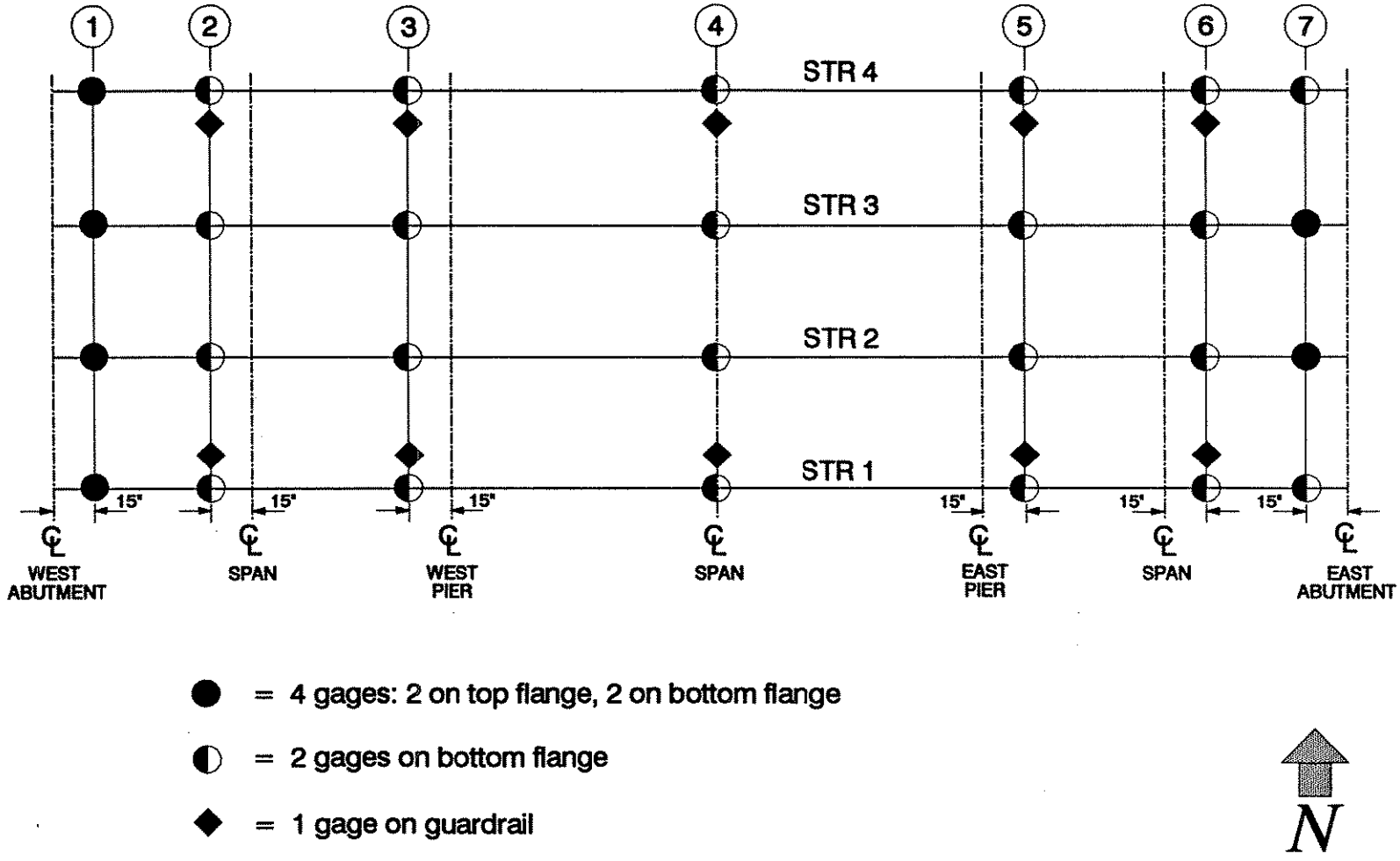

Fig. 3.1. Location of strain gages.

forces. These were mounted on the opposite sides of the tendon so tht the tendon force can be directely measured. Both the one in. dia. and the 1 1/4 in. dia. tendons were instrumented diametrically (see Fig. A.1 in Appendix A). The gages were installed in the laboratory before the tendons brought to the field.

All strain gages (weldable and conventional) were self temperature-compensated and were water-proofed with appropriate protective coatings. Three-wire leads were used to minimize the effect of the long lead wires (in excess of 150 ft in some instances) and temperature changes.

Eight of the 16 truss tubes were instrumented with three strain gages each. Two of the gages were placed on opposite faces (top and bottom) of the tube to determine if the tube was subjected to any flexural strains. The third gage was located on the outward face of the tube (see Fig. A.1 in Appendix A).

A total of 166 strain gages were monitored during the testing procedure. Twenty-four of the strain gages were on the truss tubes, 64 were on the tendons, ten were on the guardrails, and the remaining 68 were located on the bridge stringers. Because of the large number of instruments that needed to be read during the testing, it was necessary to use more than one data acquisition system (DAS). A HP 3852A DAS capable of monitoring 30 strain gages and a HP 3054 wired to monitor the remaining gages and vertical deflection instruments were utilized in the field.

Vertical displacements were measured at twelve locations using direct current displacement transducers (DCDT's). Figure 3.2 illustrates the locations of the vertical

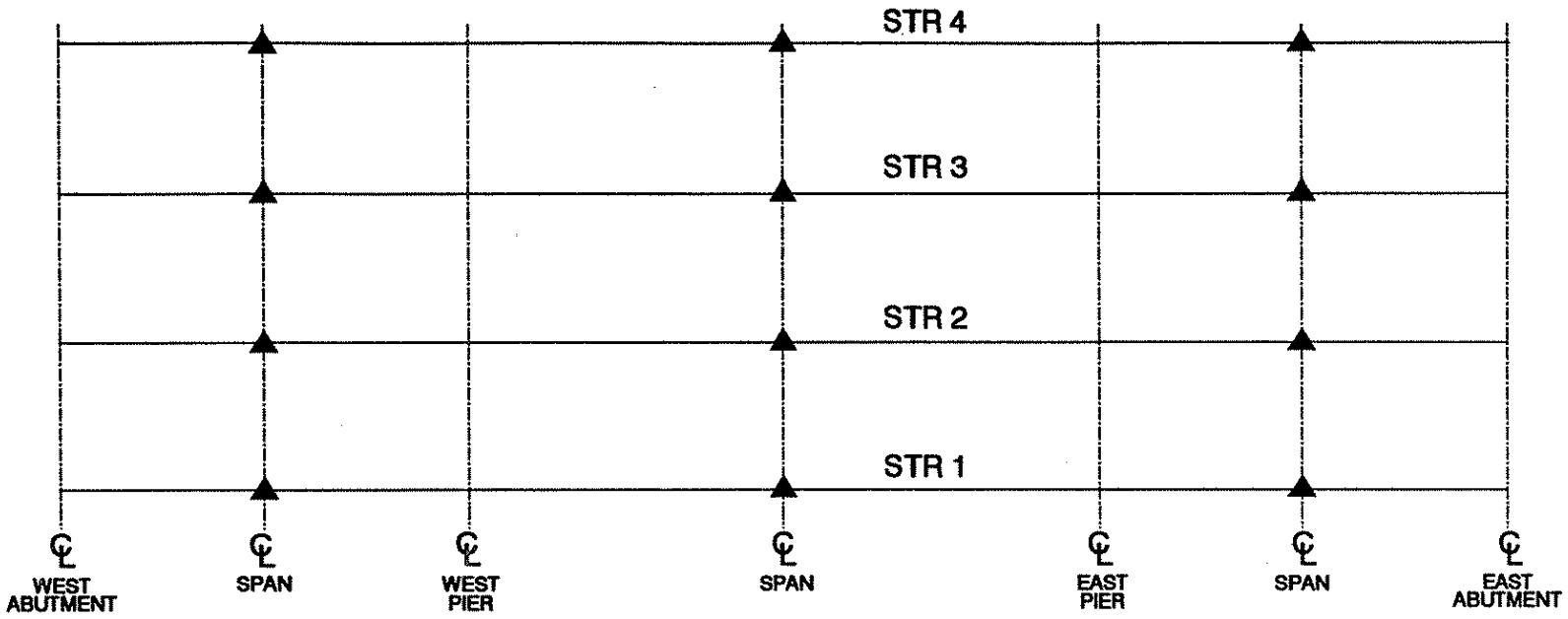

Fig. 3.2. Location of vertical displacement instrumentation.

displacement instrumentation. At each location, the DCDT's were supported by a telescoping pipe which was driven into the ground. For additional stability, the pipe stands were stayed with a system of cables.

Crack monitors were positioned at each abutment bearing to measure any longitudinal movement of the bridge during application of the strengthening stages. Crack monitors were not placed at the pier bearings because these bearings were constructed such that translation was not possible, only rotation.

For corrosion protection, all tendons were given a 3M Co. fusion-bonded powder epoxy-coating (thickness = eight mils ± two mils). Because the tendons were factory coated, scratches in the epoxy-coating which occurred during delivery or installation were recoated by hand using the same material.

Furthermore, the brackets used for the post-tensioning tendons and the truss tube support brackets were primed (using Iowa DOT approved red-oxide Type 2 primer) and painted (using an Iowa DOT Foliage Green finish coat) in the laboratory prior to field installation. All of the exposed bolts and nuts used for bracket installation and exposed portions of the double-nutted shear connectors were primed and painted prior to leaving the field. Where necessary the brackets were also "touched-up" using the same primer-painting procedure.

For installation of the truss tubes over the piers, it was necessary to remove the four diaphragms (two at each pier) at these locations. The unpainted areas exposed by the removal of these diaphragms were also primed and painted. It was also necessary to cut the bottom flanges of the diaphragms within each span for adequate clearance of the post-tensioning

tendons. The areas effected by the cutting torch were also primed and painted.

3.2. Field Tests

Field testing of the bridge consisted of determining the bridge strains and deflections when it was subjected to various loading conditions. The term "loading conditions" as used here refers to the vehicle load cases and the various stages of strengthening.

3.2.1. Load tests

The trucks (configuration and weights) used to load test the bridge are shown in Fig. 3.3. The center of gravity of the truck's wheel loads was calculated for each truck, and this point was positioned at the load points shown in Fig. 3.4. Note, there are 28 load points (Lanes 1, 2, and 3 with the truck heading east and Lane 4 with the truck heading west). The load points shown in Fig. 3.4 correspond to the one-quarter and center span points of the west and middle span and the center span points of the east span. Single truck load cases have been numbered using an " X.Y" notation. The first number in this notation, X, indicates the lane in which the truck was located. The second number, Y, is the particular point along the bridge. Thus, load point 3.5 indicates the truck is in Lane 3 at location 5. Load positioned at one of the 28 points shown in Fig. 3.4 will be referred to as a load case. The systematic nature of the load points used made it possible to examine the symmetry of the bridge.

In addition to the single truck loadings, several pattern load cases were investigated by positioning two trucks on the bridge. A total of twelve pattern load cases were employed;

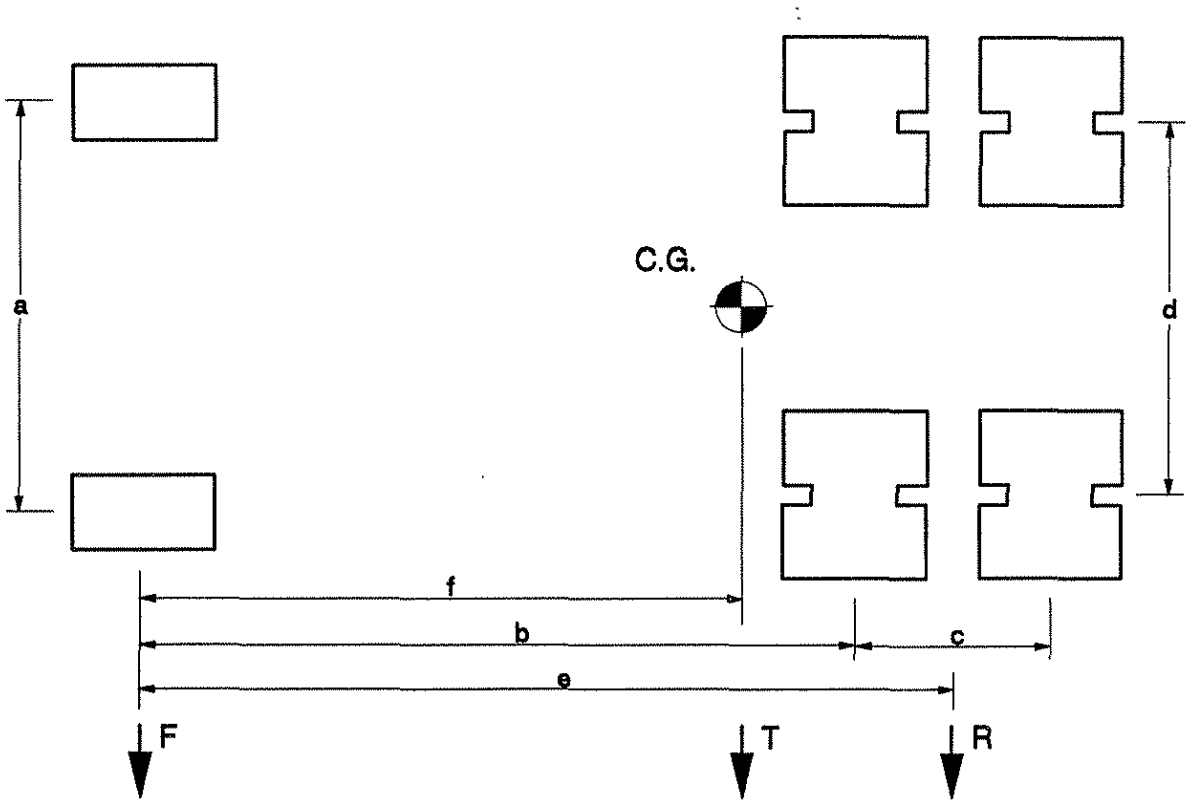

Trk	a (in.)	b (in.)	c (in.)	d (in.)	e (in.)	f (in.)	R (lbs)	F (lbs)	T (lbs)
1	83.5	179	53.5	72	206	152.1	39,460	14,240	53,700
2	80.5	180	50.5	72	206	142.2	34,400	15,640	50,040

Fig. 3.3. Wheel configuration and weight distribution of test vehicles.

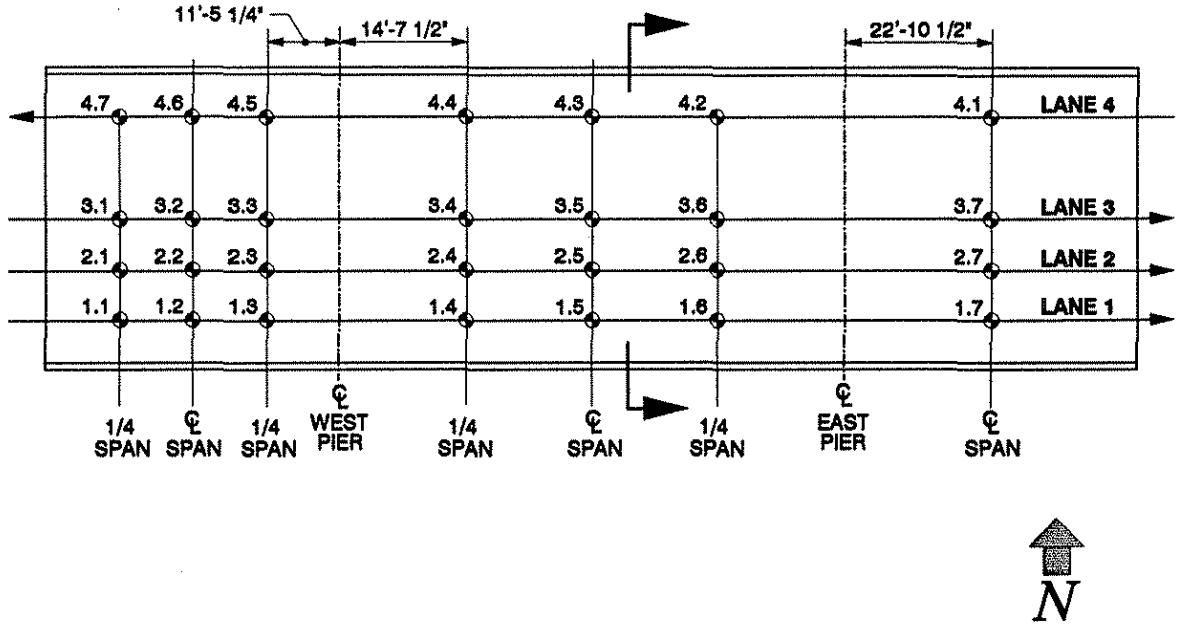

a. PLAN VIEW

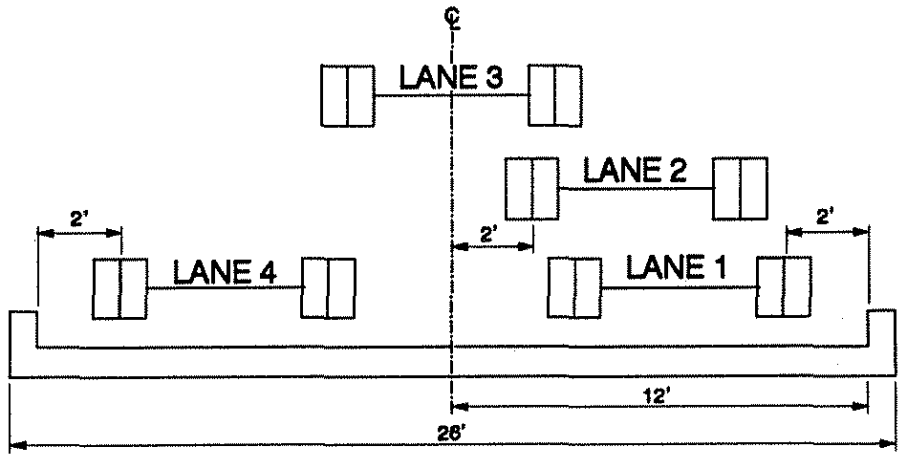

b. SECTION VIEW

Fig. 3.4. Location of test vehicles.

these pattern loading cases are given in Table 3.1. Thus, the bridge was subjected to a total of 40 load cases. The load points in this table are shown in Fig. 3.4. For example, in load case PL 5 (Pattern Load Case 5) the trucks were positioned at points 2.2 and 2.7 which will tend to maximize the positive moment in the end spans. The term "tend to maximize" is used because the trucks do not coincide with the influence line ordinates which produce maximum positive moments in these spans. Figure 3.5 shows a typical load case with the vehicles positioned on the bridge.

3.2.2. Superimposed truss stages

To obtain load distribution data and to learn more about the bridge behavior due to truss system forces, the bridge was subjected to various stages of truss loading. Four stages of truss loading were selected for investigation; these are shown in Fig. 3.6.

For truss Stages 1 and 2 (Figs. 3.6a and 3.6b) the load was applied in increments of 15 kips, 30 kips, 45 kips, 60 kips, and 80 kips. At each load increment, strain and deflection readings were taken. Because the bridge was not load tested during these stages, the tendon nuts did not need to be seated at each of these increments. For Stages 3 and 4 shown in Figs. 3.6c and 3.6d, respectively, readings were only taken when the tendon force was 80 kips.

After the truss system was completely activated (Stage 4 of Fig. 3.6) Truck 2 was positioned on the bridge to determine the effectiveness of the trusses. Midspan load points of lanes 1 and 3 (see Fig. 3.4) (points 1.2, 1.5, 1.7, 3.2, 3.5, and 3.7) were selected as representative load cases.

Table 3.1. Pattern loading vertical load points.

Load Case	Vertical Load Points *																										
	Lane 1							Lane 2							Lane 3							Lane 4						
	1	2	3	4	5	6	7	1	2	3	4	5	6	7	1	2	3	4	5	6	7	1	2	3	4	5	6	7
PL 1		●			●																							
PL 2		●					◐																					
PL 3					●		◐																					
PL 4									●			●																
PL 5									●					●														
PL 6												●		●														
PL 7																●			●									
PL 8																●					●							
PL 9																			●		●							
PL 10																						●		●				
PL 11																						●					●	
PL 12																								●			●	

● = Loaded location.

* See Fig. 3.4 for location of load points.

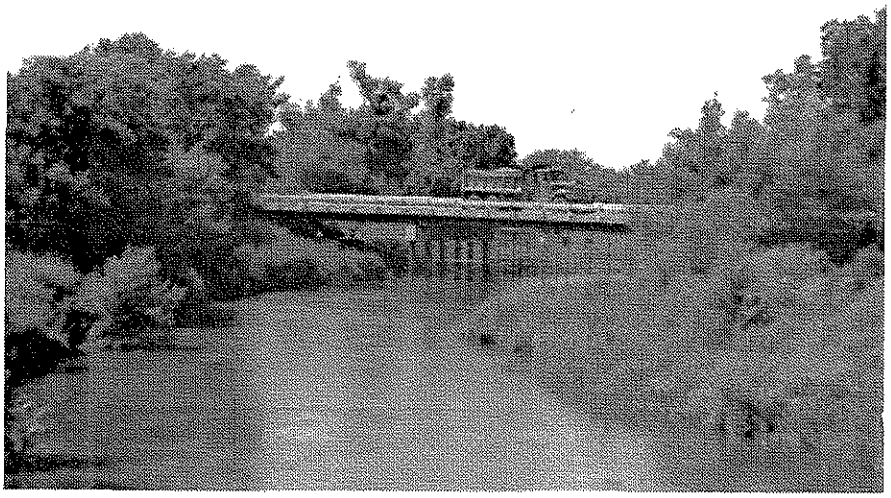

a. SINGLE TRUCK LOAD CASE

b. PATTERN LOAD CASE

Fig. 3.5. Photographs of field test vehicles on bridge.

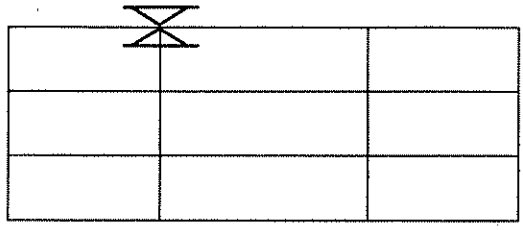

a. STAGE A

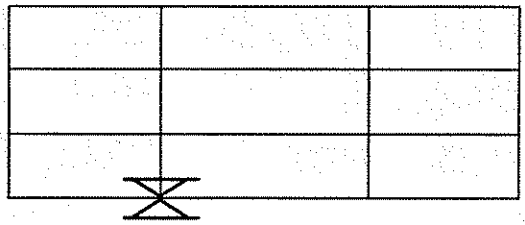

b. STAGE B

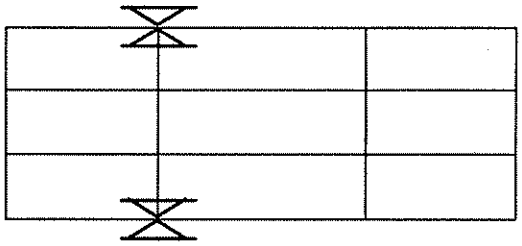

c. STAGE C

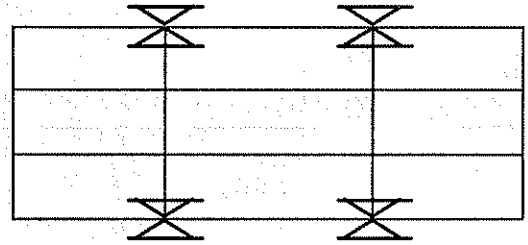

d. STAGE D

Fig. 3.6. Preliminary truss testing stages.

3.2.3. Bridge strengthening

Post-tensioning forces were applied to the tendons on the stringers and trusses using four 120-kip capacity, six-in. stroke, hollow-core-hydraulic cylinders, which were 6 1/4 in. in diameter. The diameter of the cylinders controlled the position of the tendons relative to the stringer bottom flange. There was a hydraulic pump available for each of the hydraulic cylinders so that the applied load could be accurately controlled. Because each stringer and truss had two tendons and there were only four hydraulic cylinders available, only two stringers or trusses could be post-tensioned at a time.

The eight stages required to strengthen the bridge are illustrated in Fig. 3.7. Review of the strengthening stages reveals the following:

1. The truss system was activated prior to post- tensioning.
2. Exterior stringers were post-tensioned prior to interior stringers.
3. Transverse symmetry of the applied forces was maintained during the strengthening process.
4. End spans were completely post-tensioned prior to post-tensioning the middle span.

The theoretical forces required to strengthen the bridge in each stage are shown in Fig. 3.8. Notice that lateral and longitudinal distribution occurred when post-tensioning forces were applied to the positive moment regions.

The field testing procedure used to obtain data for the vehicle load testing (see Fig. 3.4) and the various strengthening stages (see Figs. 3.6 and 3.7) was as follows:

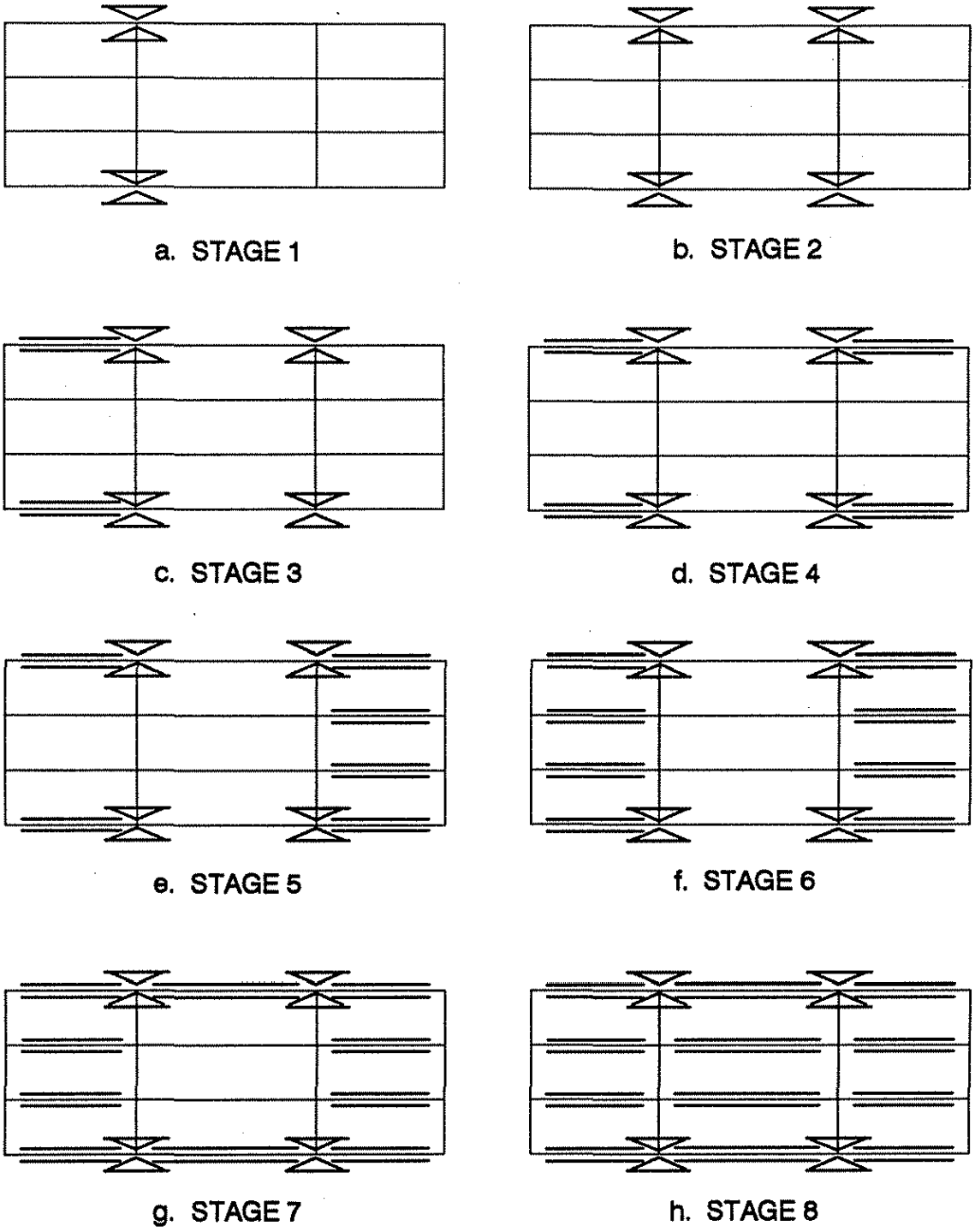

Fig. 3.7. Order strengthening system was applied to bridge.

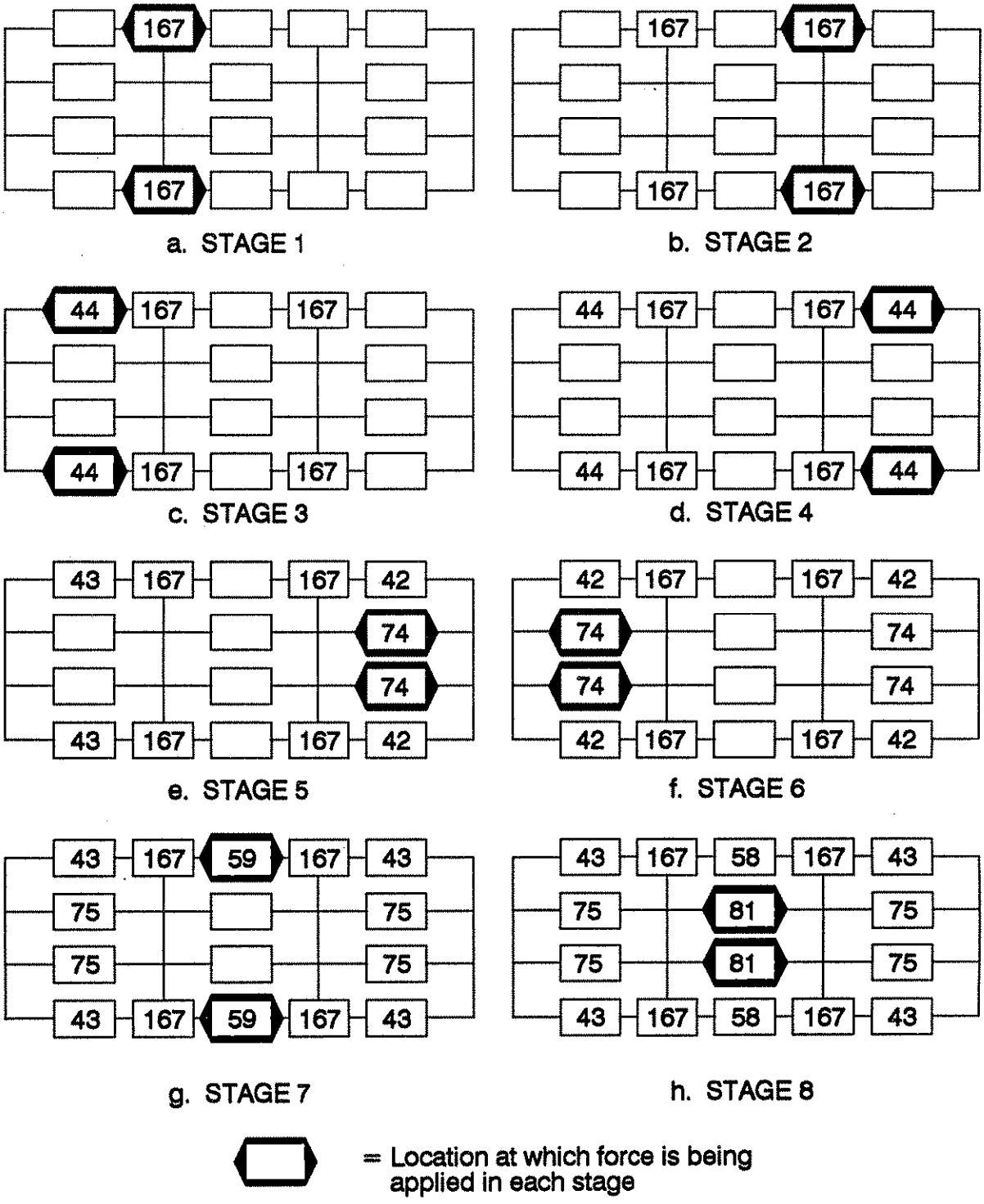

Fig. 3.8. Theoretical strengthening force (kips) required per stage.

1. Record "zero" strain and "zero" deflection readings.
2. Apply loading (one truck, post-tensioning, truss loading, truck plus strengthened bridge, etc.) at predetermined locations.
3. Record strain, post-tensioning force, and deflection readings as in step 1; note any changes in the bridge behavior.
4. Repeat steps 1 through 3 for all loading conditions.

The testing program listed above was implemented on June 14 and 15, 1993. On June 14th data for all 40 of the vehicle load cases (single truck and pattern loading) were taken for the unstrengthened bridge. Also on the first day Stages 1 and 2 of the strengthening system (trusses) were applied to the bridge. As mentioned in Sec. 3.2.2 the bridge was then subjected to truck loading at six locations.

On the second day of testing (June 15) the remaining stages of the strengthening system were applied (Stages 3 through 8). Upon completion of the post-tensioning (trusses and stringers), the strengthened bridge was loaded again with Truck 1 at the same 28 load points; data were taken after each load case. The final loading applied to the bridge was the 12 pattern load cases described in Table 3.1. Data were obtained after each of these load cases also. In all of these pattern load cases, Truck 1 was always the lead vehicle. After completion of the testing, the bridge was left in the strengthened condition.

4. DEVELOPMENT OF A STRENGTHENING DESIGN METHODOLOGY

The analysis of continuous-span bridges under the effect of vertical loads is addressed in the AASHTO Standard Specifications for Highway Bridges [21]. Wheel load fractions are provided to aid the designer in determining the percentage of the vertical loads distributed to each of the bridge stringers.

The analysis of continuous-span bridges strengthened using post-tensioning and superimposed trusses presents a significantly more involved analysis problem. Strengthening forces acting on the bridge in this case include axial forces and concentrated moments induced by the tendons at the various bracket locations, as well as vertical forces at the bearing points of the superimposed trusses. Due to the lateral stiffness of the deck and the diaphragms, a significant portion of the axial forces and moments from a strengthened stringer is transferred to other stringers. Longitudinal continuity of the stringers and the deck results in force and moment transfer from one span to the others. To date, no data are available for determining the distribution of the previously described strengthening forces and moments throughout a given continuous-span bridge.

This chapter describes the design methodology developed for the strengthening of three-span, four-stringer, continuous-span composite bridges. This strengthening system includes the post-tensioning of steel stringers in the positive moment regions, as well as the option of adding superimposed trusses to the exterior stringers at the piers. A more detailed description of the development of the design methodology is given in Chp. 4 of Ref. 3.

4.1. Finite Element Model

The authors utilized the finite element method for the development of the proposed design methodology. Several finite element packages are available at ISU, for instance, ABAQUS, ANSYS, NASTRAN and SAP. The ANSYS program was selected for the use in this investigation, primarily because of its very convenient preprocessing (i.e., input data generation) and postprocessing (i.e., retrieving results). The program contains over 90 different types of finite elements that can be used to analyze different structures.

4.1.1. Preprocessing and postprocessing programs

One of the main advantages of the ANSYS programs is the integration of the three phases of finite element analysis - preprocessing, solution, and postprocessing. However, to expedite generation of the finite element meshes and to retrieve particular results, the authors found it necessary to develop additional preprocessing and postprocessing programs. These programs were developed in "PC TURBO PASCAL".

The function of the preprocessing program was to read in the basic bridge parameters and to develop a command file which is subsequently used by ANSYS to create the finite element model. This preprocessor made it possible to create models of several bridges in a minimum amount of time.

The postprocessor developed was used to sort through the ANSYS results to retrieve the nodal forces that are needed to compute the resultant axial forces and moments on the composite sections of the stringers. These resultants are used later in determining the distribution fractions which describe the distribution of axial forces and moments throughout the bridge.

4.1.2. ANSYS finite element model

The basic finite element model used in this work is shown in Fig. 4.1. The model consisted of plate elements idealizing the bridge deck, bridge curbs and post-tensioning brackets while 3-D beam elements were used to model the stringers and the diaphragms.

The shear connection between the steel stringers and the concrete deck is achieved through angle-plus-bar shear connectors (see Fig. 4.2). The locations of the shear connectors for the bridge are presented in Fig. 2.4. In practice, the angle-plus-bar shear connectors allow no vertical movement between the concrete and the steel surfaces, as well as provide restraint in the longitudinal direction. Rotations are essentially the same in the concrete and the top flange of the stringers. Only a small horizontal movement occurs between the concrete and the steel at the shear connectors; the movement (slip) depends on the stiffness of the shear connector. The stiffness of the shear connectors has been determined through shear tests in the laboratory; force-displacement relationships for the angle-plus-bar shear connectors are presented in Refs. 6 and 22.

In order to model the shear connectors accurately, slip elements were used to model the link between the stringer nodes and the deck nodes. Constraint equations were utilitzed to couple the rotations and the vertical displacement of the deck and the stringers. Beam elements were used to connect the two nodes; their stiffnesses were computed to give a stiffness equivalent to that of the actual shear connectors (see Fig. 4.3).

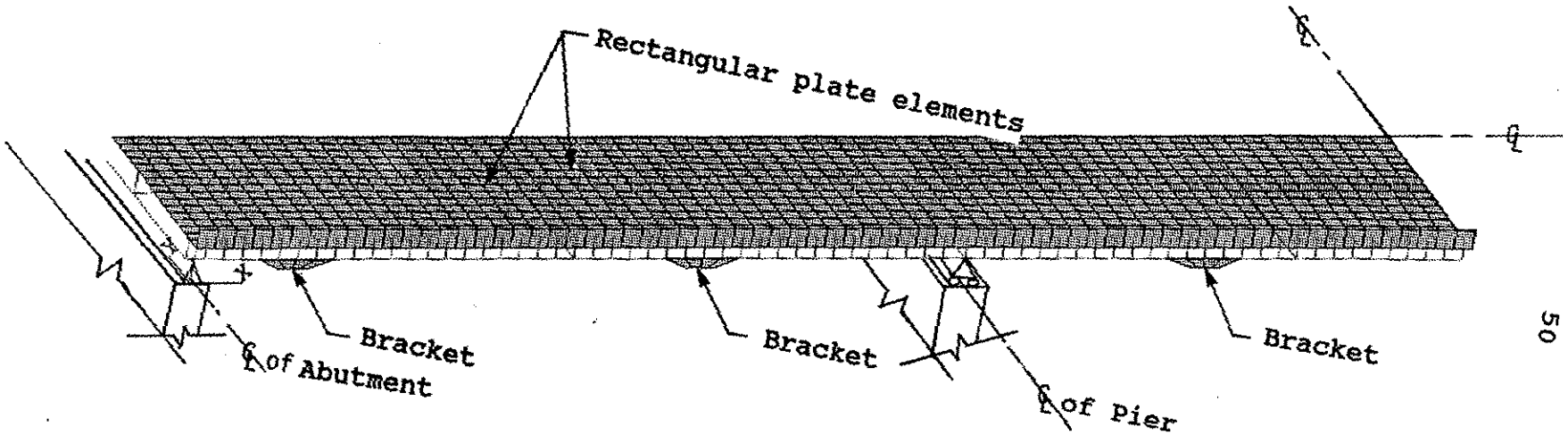

Fig. 4.1. Finite element model of continuous-span composite bridge.

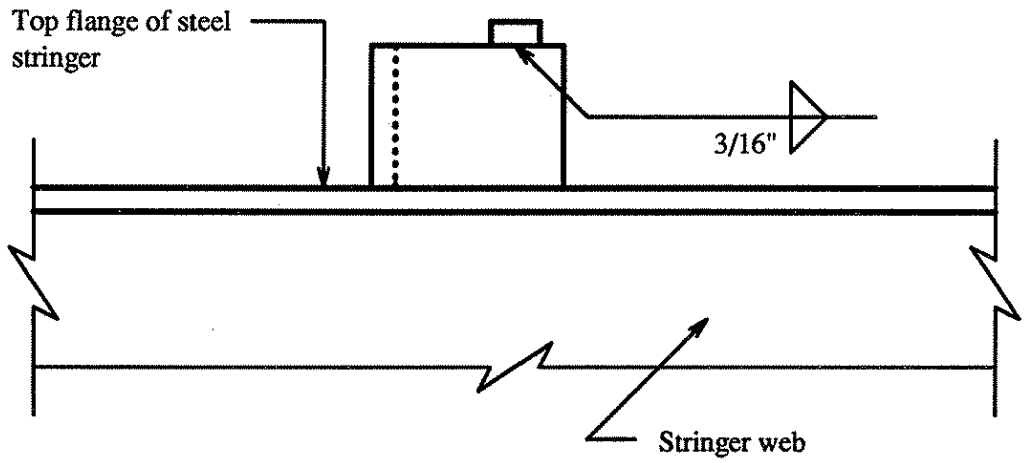

a. ELEVATION

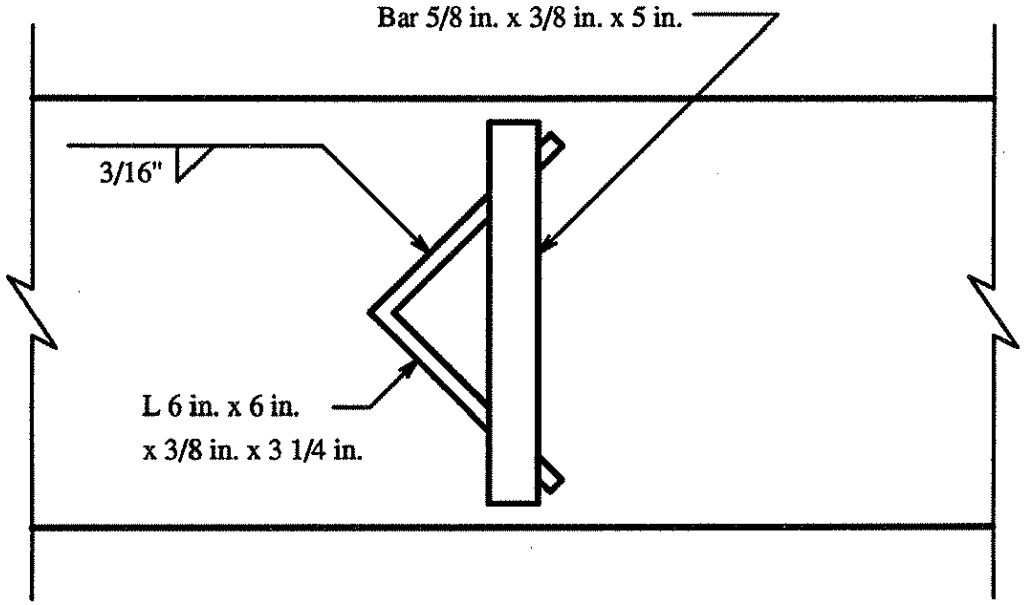

b. PLAN

Fig. 4.2. Details of angle-plus-bar shear connector.

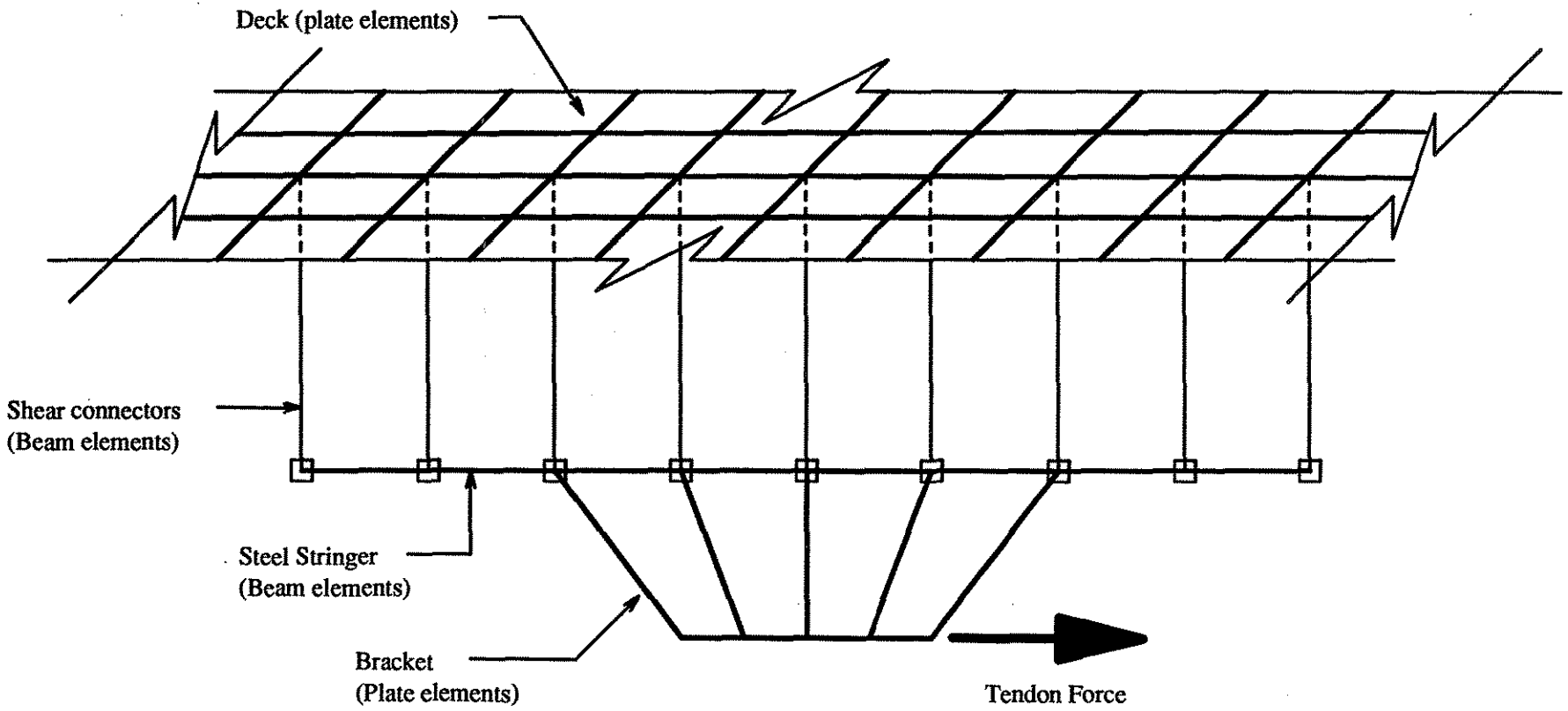

Fig. 4.3. Modeling of shear connectors and post-tensioning brackets.

The diaphragms were modeled as 3-D beam elements connecting the bridge stringers. Due to differences in the vertical level of the diaphragm centerlines and the steel stringer centerlines, rigid links were used to connect the diaphragm nodes to the steel stringer nodes.

Two models were investigated to determine the most suitable idealization for the connection between the post-tensioning forces and the stringers. In the first attempt, a tendon force was modeled as a concentrated force together with a concentrated moment at the bracket location. This model produced stress concentrations at the bracket locations. To eliminate this problem, plate elements were used to model the brackets thus distributing the force and moment along the actual bracket length (see Fig. 4.3). This removed the stress concentrations, and made it possible to obtain the desired stress reductions at the critical sections without obtaining overstresses at the bracket locations.

An analysis was performed to investigate the effect of the stiffness of the tendons and superimposed trusses on the analysis results. It was found to be insignificant due to the large stiffness of the stringers compared to that of both the post-tensioning tendons and the superimposed trusses.

Two alternatives were investigated to model the deck in the negative moment regions, i.e., between the dead load inflection points. The previously strengthened continuous span bridge [1] was used in this investigation. First, all plate elements representing the bridge deck in these regions were removed from the finite element model. In the second idealization, all plate elements modeling the entire deck were assumed to be uncracked. Results obtained by these alternatives were compared to field data. From the comparison, it was determined that the second idealization

yielded results closer to the experimental results. Therefore, it was decided to use the later idealization - no deck cracking - throughout the remainder of finite element analysis. This modeling can be explained by the fact that although the deck is cracked, it can still transfer longitudinal forces transversely. Moreover, the existence of the reinforcing steel helps the lateral transfer of forces through the deck.

4.2. Force and Moment Fractions

4.2.1. Definition of force and moment fractions

To simplify the determination of the distribution of axial forces and moments in the bridge stringers, force and moment diagrams have been idealized into a number of straight line segments as shown in Fig. 4.4; the straight line segments are defined by a number of critical points on the actual force and moment diagrams. The idealized diagrams represent the actual forces and moments on the stringers fairly accurately.

The next step in calculating the distribution fractions was to relate the axial force and bending moment at each of the chosen critical sections to the axial force and total moment at that section. Figure 4.5 illustrates the axial force and moment diagrams obtained from the finite element analysis for the total bridge section as well as for the individual stringers due to post-tensioning forces in the end-span exterior stringers, i.e., strengthening scheme [A]. The force (or moment) fractions at each point are defined as the ratio of the force (or moment) on the composite section of the exterior stringer to the force (or moment) on the composite bridge at that location. As shown in Fig. 4.5, a representative sample, there are four critical locations for

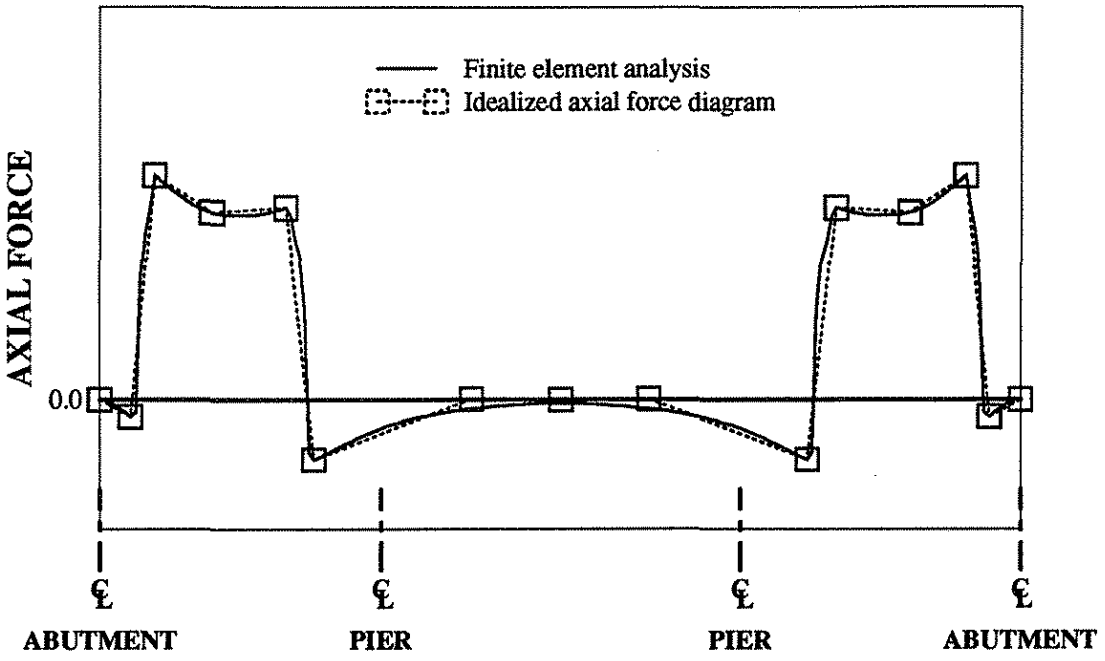

a. AXIAL FORCE ON EXTERIOR STRINGER

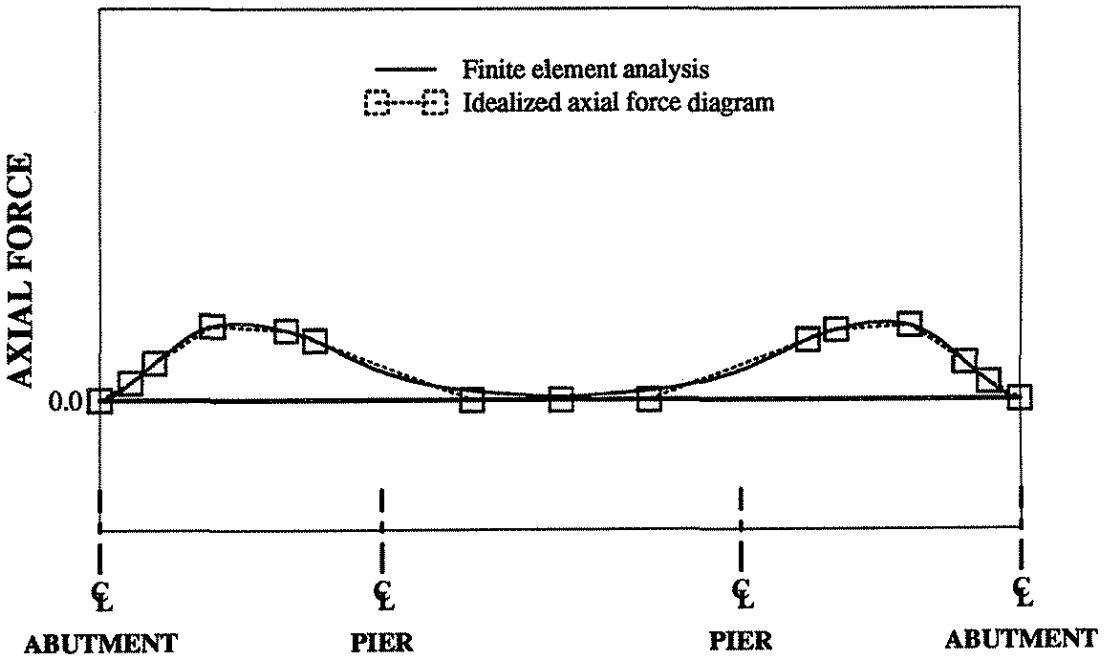

b. AXIAL FORCE ON INTERIOR STRINGER

Fig. 4.4. Idealization of axial force and moment diagrams on the stringers due to the strengthening system: Strengthening scheme [A].

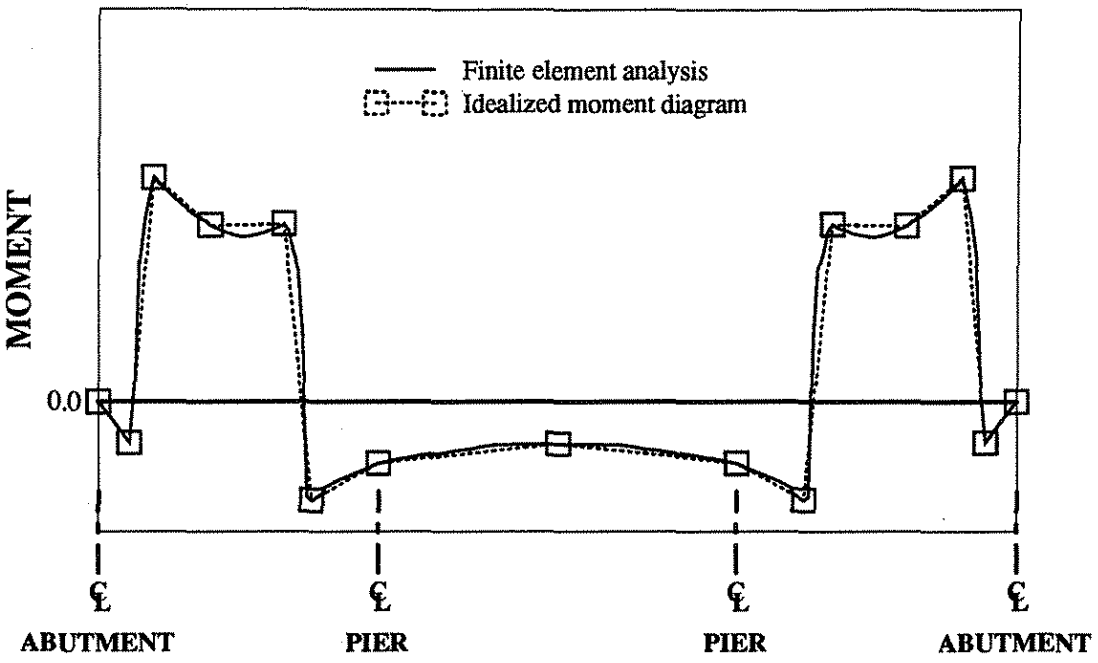

c. MOMENT ON EXTERIOR STRINGER

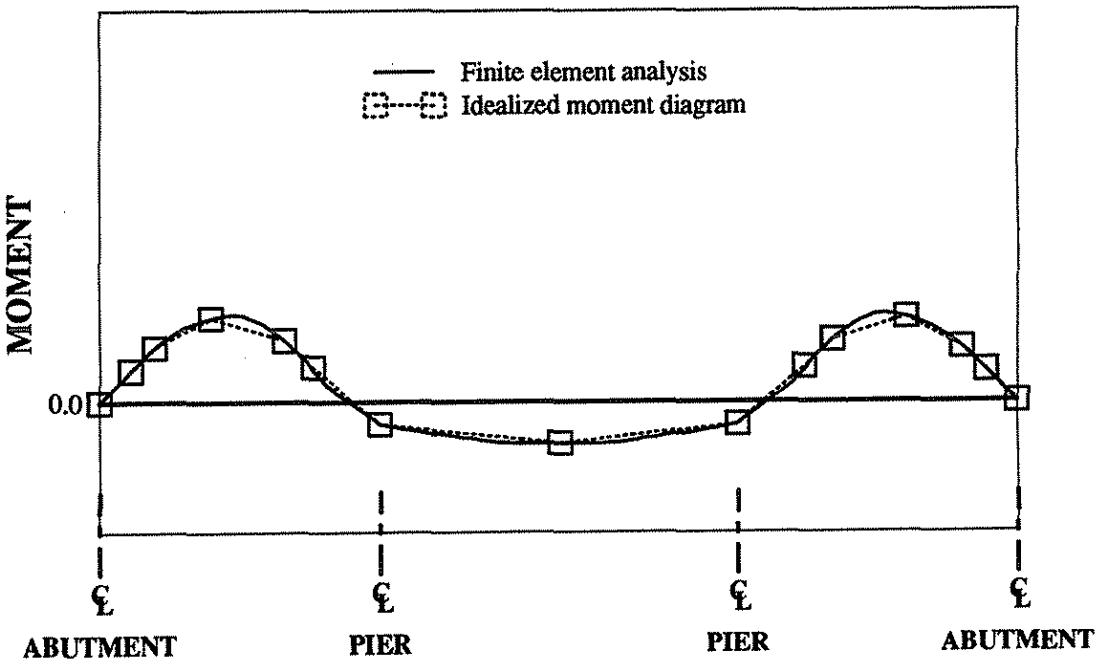

d. MOMENT ON INTERIOR STRINGER

Fig. 4.4. Continued.

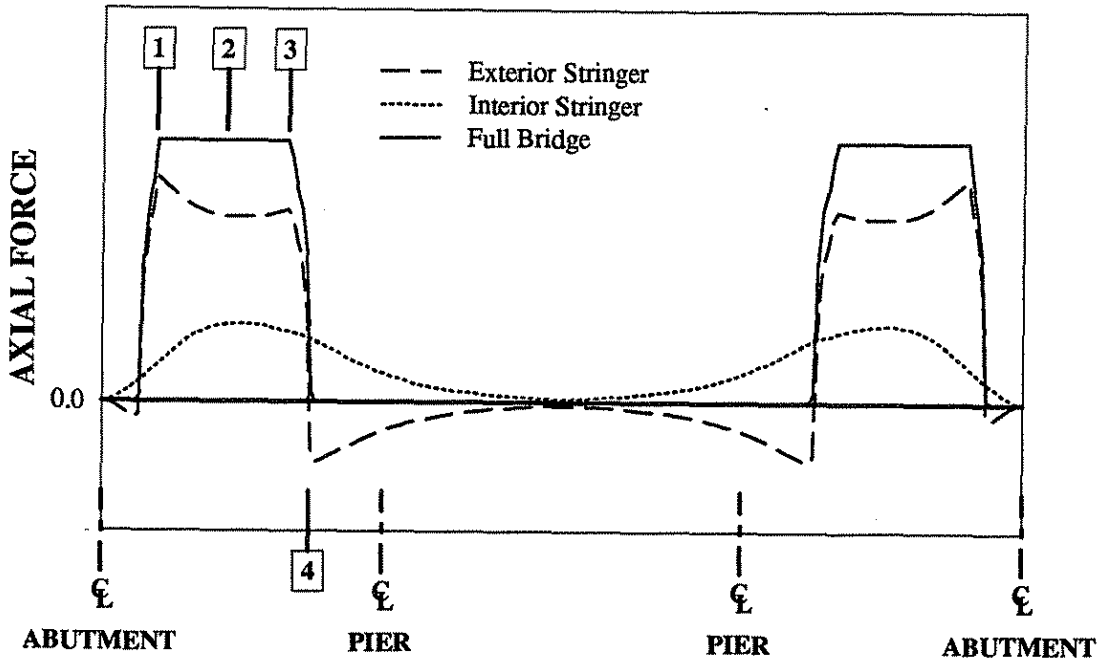

a. AXIAL FORCE DIAGRAM

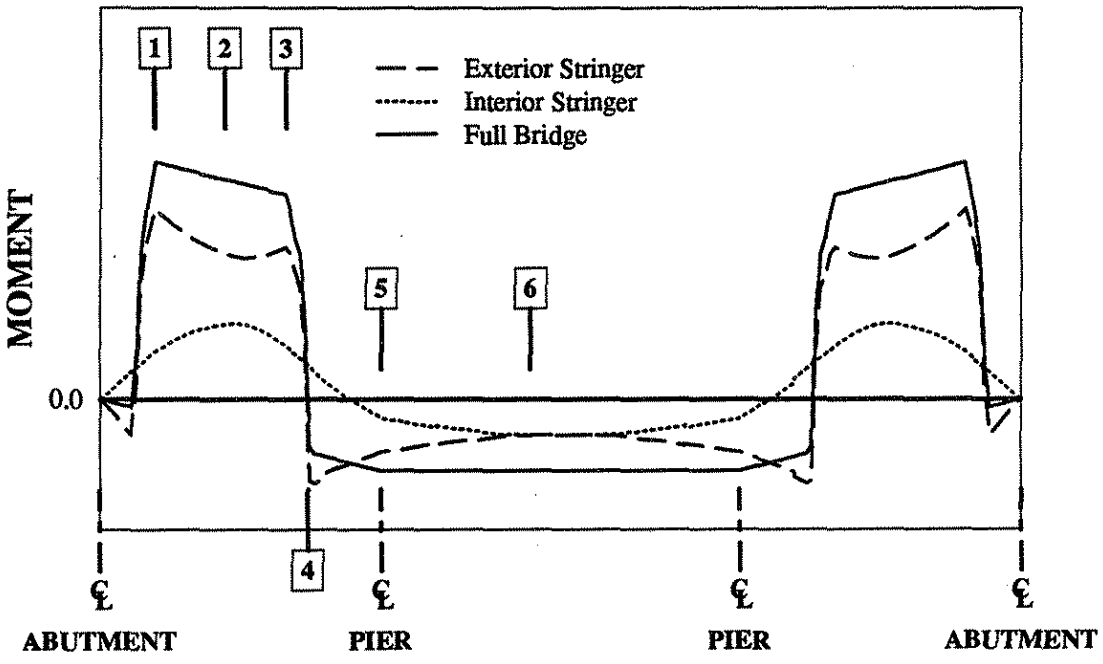

b. BENDING MOMENT DIAGRAM

Fig. 4.5. Location of distribution fractions: Strengthening scheme [A].

axial force fractions and six critical locations for moment fractions for strengthening scheme [A]. The critical distribution fraction locations for all strengthening schemes [A] through [E] are presented in Appendix A of Ref. 25. It should be noted that no vertical scale is provided in this figure because the force and moment distribution fractions are independent of the magnitude of the strengthening force and the axial forces and moments developed in the stringers. The development of formulas for the force and moment fractions at the different locations is presented in Sec. 4.2.2.

A comparison was made between the axial forces and moment diagrams obtained by analyzing the total bridge section using finite element analysis, and the diagrams obtained by analyzing the bridge as a continuous beam with variable moments of inertia. Figure 4.6 is a representative sample which illustrates this comparison in the case of strengthening scheme [B], i.e., post-tensioning the center spans of the exterior stringers. Similar to Fig. 4.5, no vertical scale is provided; however, at most locations the difference in moments is less than 7%. Thus, it was determined that there was no significance between the two analyses; it was decided to use the beam assumption since it was considerably simpler and required less computational time.

The design methodology is therefore based on solving the bridge as a continuous beam with variable moments of inertia. The axial forces and moment in each stringer are then calculated using the force and moment fraction formulas developed in Sec. 4.2.2. By applying these fractions to the forces and moments obtained from the continuous beam analysis, one can calculate the axial forces and moments throughout the bridge.

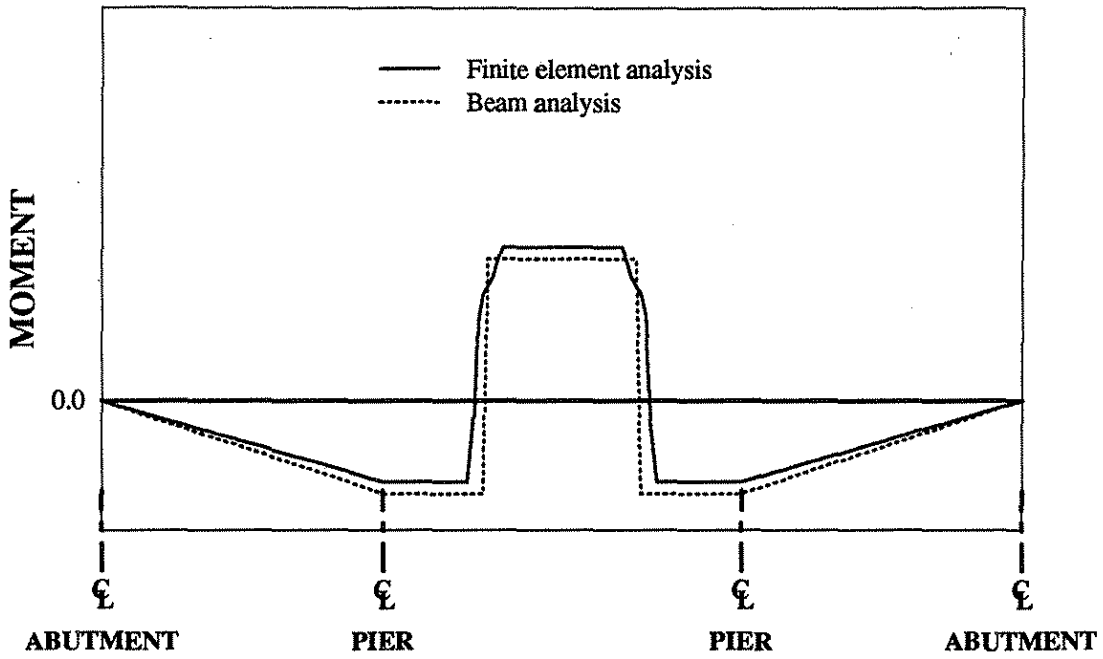

Fig. 4.6. Total moments on the bridge section: Strengthening scheme C.

4.2.2. Development of force and moment fraction formulas

Initially, a large number of bridges was analyzed using the ANSYS finite element model. These included both standard Iowa DOT bridges and nonstandard bridges. When developing regression formulas for the force and moment fractions, it was found more practical to develop the formulas only for the standard bridges; this limitation resulted in formulas which are both more accurate and simpler. The bridges for which the formulas were developed are the standard Iowa DOT V12 and V14 series [23,24]. The models were analyzed with the individual stringer spans strengthened separately as shown in Fig. 4.6. Axial forces and moments were computed assuming unit tendon forces in each of the individual tendons.

Due to practical considerations, it is recommended to place the tendons above the bottom flange of the steel stringers as mentioned in Sec. 3.2.2 of Ref. 25. All bridges were analyzed with the tendons positioned 3 1/2 in. above the top surface of the bottom flange. The effect of changing the elevation of the tendons above the top surface of the bottom flange in the range of 3 in. to 5 in. was investigated. The results revealed that this change in elevation has a minimal effect on the force and moment fractions. Thus, the force and moment fractions determined in this investigation
are valid for elevations above the bottom flange in this range.

In order to obtain accurate yet relatively simple expressions for the force and moment fractions at the various locations on the stringers, a sensitivity study was conducted to determine the most significant parameters. The parameters investigated included bridge length, bridge skew, end-span to centerspan length ratio, deck thickness, stringer spacing, stringer moments of inertia (composite and noncomposite) and

the ratio of the post-tensioned portion of the span to the span length for the various strengthening schemes.

The statistical analysis software package, SAS, was used for the regression analysis. A program was prepared on SAS to perform a regression analysis using the force and moment fractions obtained from the finite element analyses considering the effects of the various parameters and combinations thereof to determine the parameters that had the most significant effect on each force or moment fraction. A SAS routine, "PROC.REG", was used to perform several iterations of the regression analysis. In each iteration, the routine excluded the least significant parameters. After performing several tests on the various parameters and combinations thereof, the parameters significantly affecting the largest number of fractions were determined and used in the final regression analysis. From the analysis, it was determined that the three most significant variables are the deck thickness to stringer spacing ratio, the total bridge length to stringer spacing ratio, and the ratio of the post-tensioned portion of the span to the span length for the various strengthening schemes.

It should be noted that some of the variables excluded from the regression analysis (ratio of exterior to interior stringer moments of inertia, ratio of end-span length to centerspan length, etc.) are not excluded because their effect is insignificant, but rather because the variation of these variables within the limits of the standard Iowa bridges is small and therefore insignificant. Also, since these variables are closely related to other variables used in the regression formulas (e.g. composite section moments of inertia of the stringers are closely related to deck thickness and

stringer spacing), their effect was implicitly taken into account in the regression formulas.

In developing the formulas, the authors chose to put the variables in the form of dimensionless parameters, as shown in Appendix A of Ref. 25. Using this approach, the values of the parameters were kept between the limits of zero and one, which results in well conditioned equations that are more convenient for the user to apply.

The terms used in the equations were limited to the parameters, the parameters squared, the products of the parameters, the reciprocals of the parameters, the reciprocals of the parameters squared, or the reciprocals of the products of the parameters. Higher powers were not used in the formulas for two reasons: sufficient accuracy was obtained with the squared terms, and it was desired to keep the formulas as simple as possible.

The formulas developed for the force and moment fractions are given in Appendix A of Ref. 25. In developing each formula, the authors attempted to minimize the number of terms, while obtaining good accuracy (generally, coefficients of determination, $R^2 >> 90\%$). In a few formulas, this was not possible, especially in case of the fractions with very low average values. Nevertheless, the error was small enough in these formulas so that the effect on the force or moment fractions at that section is generally very small. The range of error is generally less in the moment fractions than in the force fractions. This further minimizes error as moment fractions have a greater effect on the final stringer stresses.

Limits have been provided for the variables, and for the force and moment fractions computed using the regression formulas. Variables and the computed force and moment fractions of the Iowa standard V12 and V14 series bridges are well within the established limits. For bridges with lengths, widths, etc. that vary significantly from those of the standard bridges, the formulas do not give accurate force and moment fractions. In these cases, it is recommended that a finite element analysis be performed to determine the axial forces and moments in the bridge stringers.

As previously described, several approximations have been made to provide the designer with a simplified procedure for determining the response of the bridge to the strengthening system, and for designing the required strengthening system. Potential sources of error in the design methodology developed are summarized below:

- The assumption that the moments in the bridge are equal to those obtained from the analysis of the bridge as a series of continuous stringers with equivalent moments of inertia.
- Idealizing the axial force and bending moment diagrams as diagrams composed of straight line segments.
- Errors in the force and moment fractions obtained using the regression formulas.
- Post-tensioning losses such as:
  - Steel relaxation.
  - Concrete creep.
  - Temperature differential between the tendons and the bridge.
  - Anchor seating.

Due to the complexity of the design procedure, and the large number of formulas, it is difficult to account for the errors in the regression formulas using the error limits corresponding to each formula. The authors therefore developed a simplified approach to account for these errors. The recommended procedure accounts for the losses and errors by increasing all strengthening forces by a conservative percentage; an 8% increase is recommended. The designer needs to check that the stringer stresses based on the original strengthening forces and the increased strengthening forces are within the allowable limits.

4.3. Flexural Strength Model

The design methodology developed in Sec.4.2 is based on the working stress design method. The distribution fraction formulas developed were obtained from the results of elastic analyses of several hundred composite bridges. These distribution fractions obviously can not be used to predict the behavior of the bridge at ultimate load.

Several laboratory tests have been conducted to investigate the behavior of post-tensioned bridge stringers at failure. A review of this work, conducted in the ISU Structural Research Laboratory, is described in Sec. 5.4 of Ref. 7.

In this section, a procedure is suggested for predicting the ultimate strength of bridge stringers strengthened by post-tensioning and/or superimposed trusses. Using a theoretical analysis, it was determined that increasing the vertical loads on the bridge caused a significantly larger percentage increase in the stresses in bridge stringers, than

in the post-tensioning tendons or superimposed trusses. This is mainly due to the relatively small stiffnesses of the post-tensioning tendons and the trusses compared to the stiffness of the stringers. It is therefore assumed that failure would occur due to the formation of plastic hinges in the bridge stringers, rather than due to the collapse of the strengthening system.

The suggested pattern of failure is shown in Fig. 4.7a. The following principles and assumptions are recommended for use in predicting the approximate flexural strength of bridge stringers:

1. The failure pattern shown in Fig. 4.7a may be used. Plastic hinges are assumed to form at three locations:
   - At the maximum positive momentlocation in the end span (assumed to be at a distance of 40% of the span length from the support).
   - At the maximum positive moment location in the centerspan (assumed to be at midspan).
   - At the maximum negative moment location (i.e., at the centerline of the pier).
2. The deflection of the positive moment locations at which plastic hinges occur may be assumed to be (L/80), where L is the span length, L1 or L2.
3. The effective flange width can be determined according to the AASHTO rules for load factor design [21, Sec. 10.38].
4. The compressive force in the slab can be determined according to AASHTO rules, which account for slab reinforcing (unlike service load design), relative capacity of concrete slab vs. steel beam, and partial or full shear connection [21, Sec. 10.50].
5. The tendon strain can be obtained from the idealized stringer configuration shown in Fig.4.7a as follows:

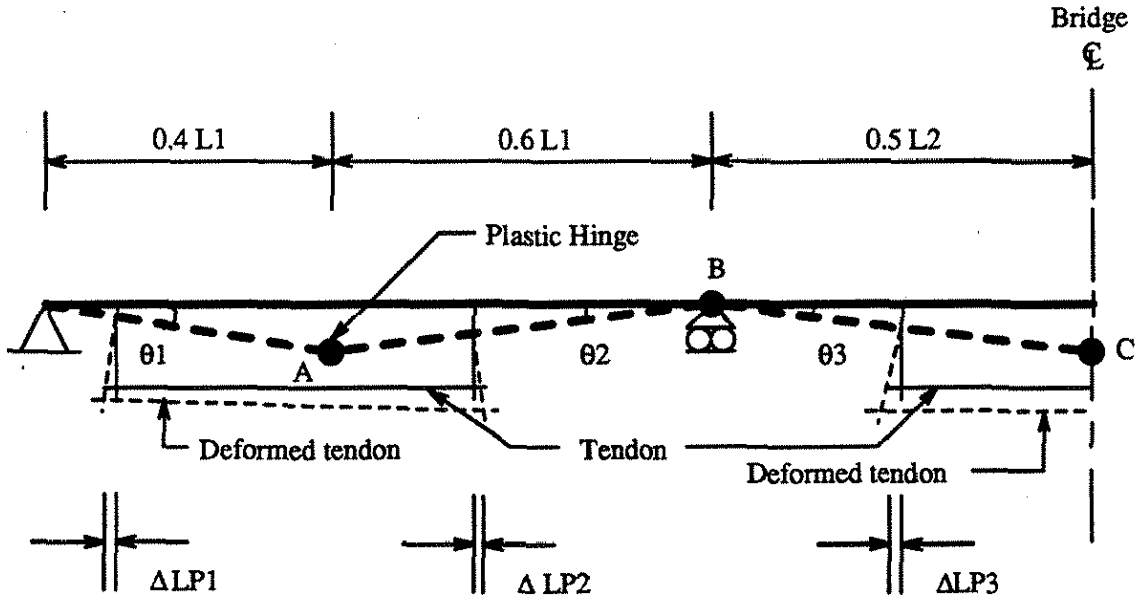

a. FAILURE PATTERN

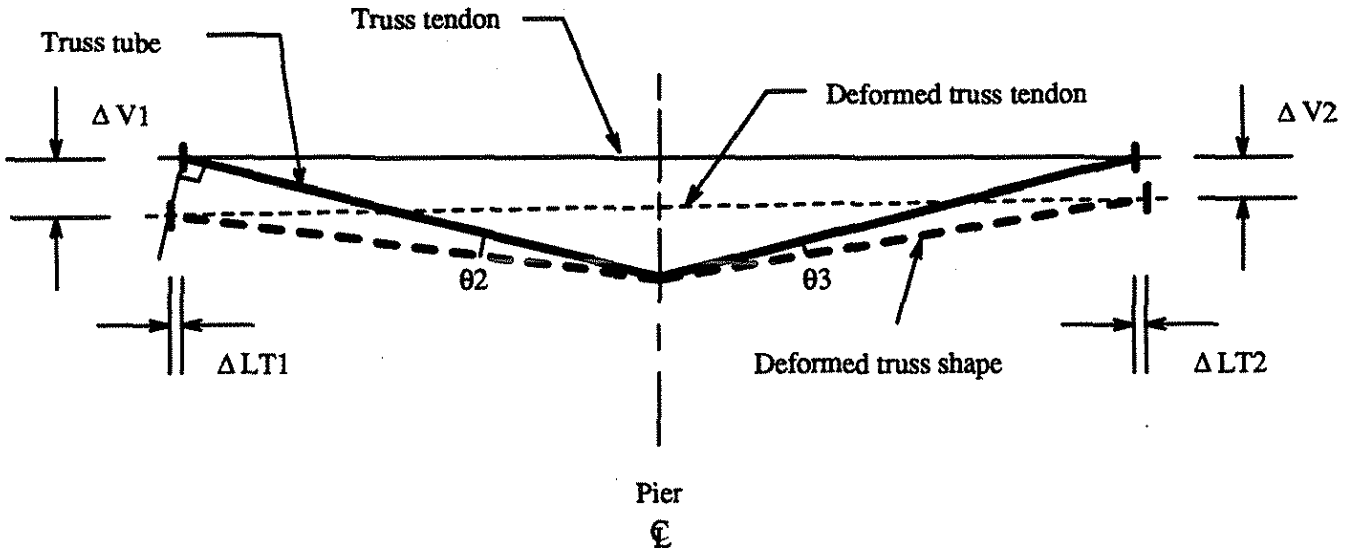

b. DEFORMATION OF SUPERIMPOSED TRUSS

Fig. 4.7. Idealization of bridge stringer at ultimate load.

Endspan tendon elongation = $\Delta LP1 + \Delta LP2$

Centerspan tendon elongation = $2 \times \Delta LP3$

In the idealized stringer, the tendon is permitted to rise and the change in elevation is accounted for in the computation. If the tendons are restricted from rising, the configuration in Fig. 4.7a must be modified to correctly represent the actual condition.

6. The superimposed truss tendon strain can be obtained from the idealized truss configuration shown in Fig. 4.7b as follows:

   $\Delta LT1 = \Delta V1 \times \tan(\theta 2)$

   $\Delta LT2 = \Delta V2 \times \tan(\theta 3)$

   Truss tendon elongation = $\Delta LT1 + \Delta LT2$.

7. Tendon force can be computed from an idealized stress-strain curve for the tendon steel.
8. The increase in the truss tendon force can be used to compute the increase in the truss vertical forces acting on the bridge exterior stringer.
9. Shear connector capacities can be computed from the formulas given in Sec. 10.38 of Ref. 21. For angle-plus-bar shear connectors, the capacity can be based on a modified channel formula as noted in Ref. 6.
10. The distribution of forces in the bridge stringers at failure has not been addressed in this study. It is left for the designer either to obtain these distribution fractions by performing a nonlinear finite element analysis, or to use engineering judgement to make reasonable assumptions for the distribution fractions.

5. TEST RESULTS

A detailed description of the bridge that was strengthened and tested as well as the finite element analysis that was used to design the strengthening system was presented in Chp. 2. The field instrumentation and a description of the various bridge loadings were described in Chp. 3. In Chp. 4, the procedure for developing the strengthening design methodology was presented.

This chapter has been subdivided into several sections. Results of vehicle load testing the unstrengthened bridge are presented in Sec. 5.1. The truss strengthening data including vehicle loading are presented in Sec. 5.2. Section 5.3 addresses the results obtained during the complete strengthening process utilizing post-tensioning plus superimposed trusses (see Fig. 3.7). Results of the strengthened bridge load testing and comparisons with the unstrengthened load testing are presented in Sec. 5.4. Finally, the contribution of the guardrails to the load carrying capacity of the bridge is analyzed in Sec. 5.5.

Note, when data are presented as "before strengthening" it should be understood that the additional shear connectors were in place when this data were collected. Time limitations did not permit instrumentation and load testing of the bridge *prior* to adding the shear connectors. Also, because all testing was done in the elastic range, the contribution of the additional shear connectors would have been difficult to measure.

5.1. Unstrengthened Bridge Load Testing

The truck loading data are presented here for the single truck load cases on the unstrengthened bridge. Section 5.4 will provide results for the same load cases and pattern load cases for the strengthened bridge and will present comparisons between the two tests.

As mentioned earlier in Sec. 3.2.1, load testing of the bridge was performed before and after the strengthening system was activated. An evaluation of the effectiveness of the strengthening system was made from the data obtained during these tests. See Figs. 3.3 and 3.4 for details of the vehicle configuration and load points.

Figures 5.1 through 5.3 show the behavior of the unstrengthened bridge when subjected to vertical loads. Figure 5.1 shows bridge behavior in the west span region due to truck loads in the same region. Figures 5.2 illustrates middle span behavior due to loads in the middle span and Fig. 5.3 shows east span behavior for the truck loads in the east span. Although longitudinal distribution of the vertical loads was exhibited, these results are not presented here.

In Fig. 5.1, load cases 1.2 and 4.6 are compared to determine if symmetrical distribution of the load occurs at each section. The plots should be approximately mirror images of each other. The only difference between the loads is that Lane 4 and Lane 1 are in the opposite direction. Therefore, for load point 1.2, the rear axles are slightly west of midspan and for load point 4.6 the rear axles are slightly east of midspan. This small difference in load position is ignored for comparison purposes. The comparison of the experimental data for these two load cases is very good. Lane

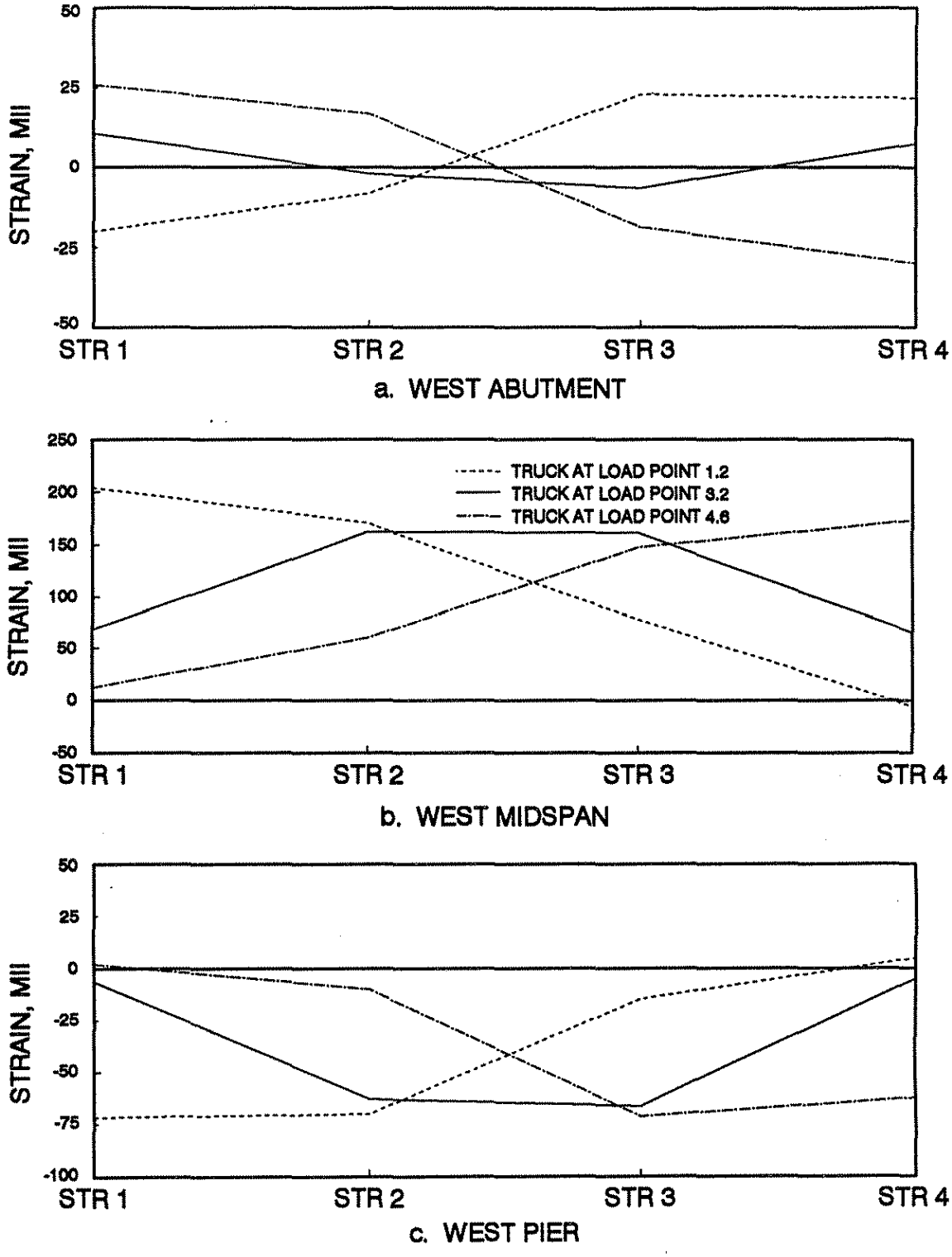

Fig. 5.1. Bottom-flange strains, truck in west span, no strengthening.

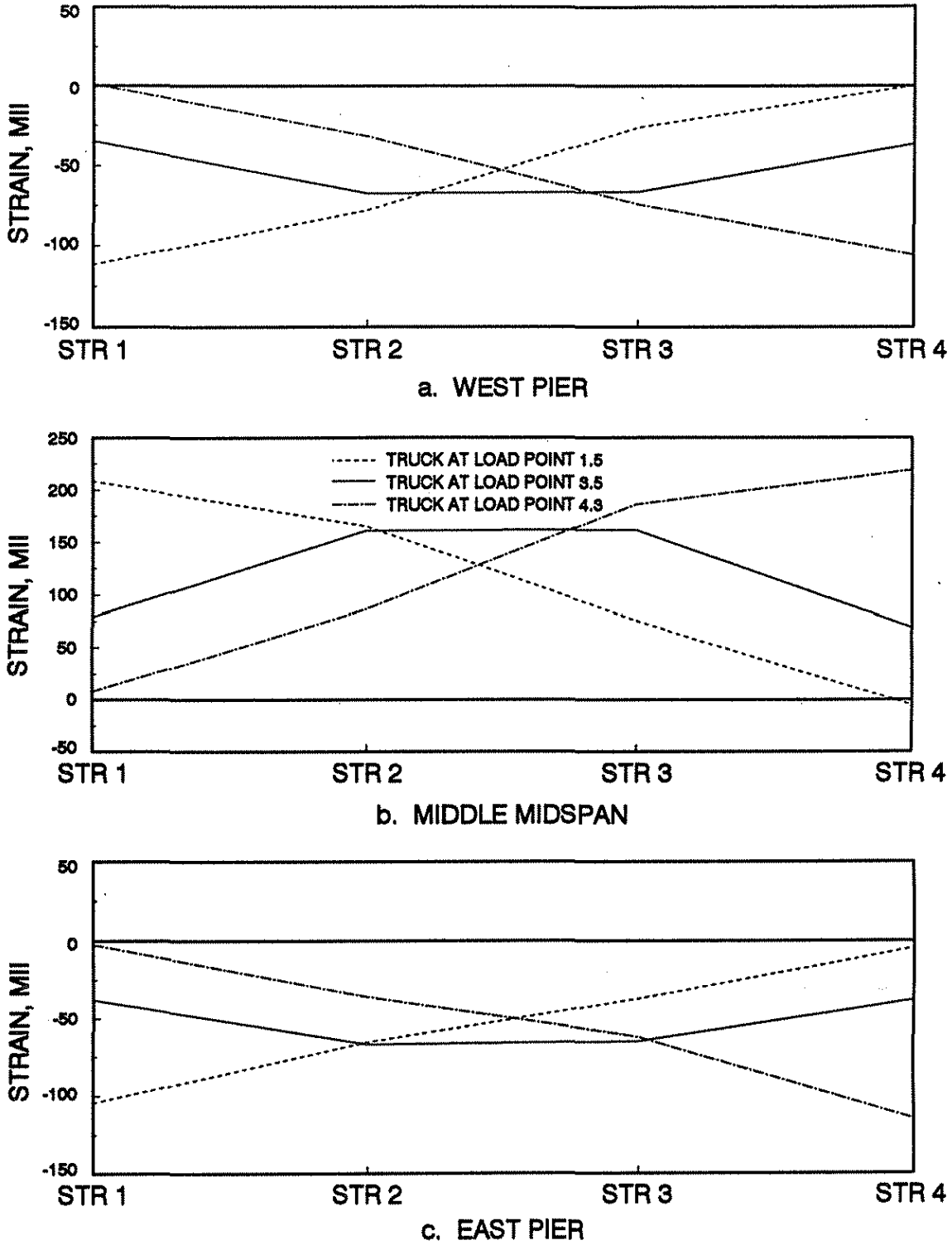

Fig. 5.2. Bottom-flange strains, truck in middle span, no strengthening.

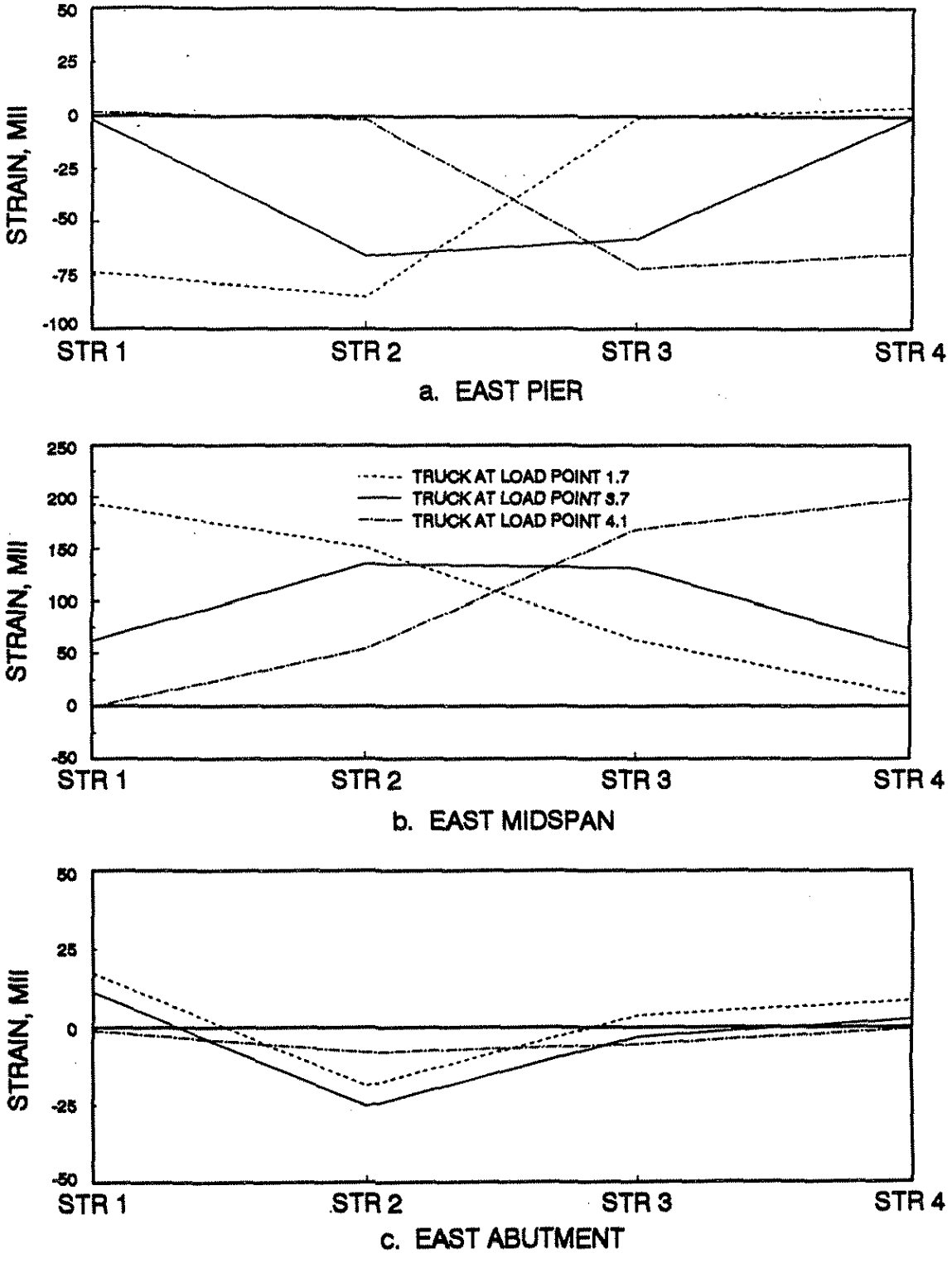

Fig. 5.3. Bottom-flange strains, truck in east span, no strengthening.

3 loading, which is symmetric relative to the bridge width, results in symmetric strains across the bridge section. The two end spans also yield symmetric results if the restraint differences at each end of the bridge are considered. A more complete discussion of end restraint will be presented later in this report.

The figures show that transverse symmetry is exhibited for all locations with the exception of the east abutment (Fig. 5.3c). This lack of symmetry at the east abutment can be attributed to differences in end restraint between the individual stringers at the east abutment (i.e., east abutment end restraint is not symmetrical). Figs. 5.1a and 5.3c reveal the presence of partial end restraint at these locations, with the west abutment strains indicating more end restraint than at the east abutment. Comparison of Figs. 5.1b and 5.3b indicates symmetry in the end spans.

5.2. Superimposed Trusses

To determine the effect of the superimposed trusses on the bridge behavior, tests were performed with only the truss strengthening system in place. The four truss stages described earlier (see Fig. 3.6) with truck loading at six locations were used to evaluate the effectiveness of the truss system.

For convenience, later in this report the following truss numbering sequence will be used (see Fig. 2.1):

Truss 1 - west pier, stringer 4
Truss 2 - west pier, stringer 1
Truss 3 - east pier, stringer 4
Truss 4 - east pier, stringer 1

Note that each of the four trusses are comprised of two individual trusses, one on each side of the stringer web.

5.2.1. Strengthening forces

Forces were applied to the truss tendons in four stages as shown in Fig. 5.4. Truss Stages C and D of Fig. 5.4 are Stages 1 and 2, respectively, of the strengthening scheme discussed in Sec. 5.3 of this report.

After force was applied (and locked in place) to all four of the truss locations, the bridge was tested positioning Truck 1 at six load positions. As shown in Fig. 5.4, the applied truss forces varied between 156 kips and 161 kips, with an average value of 158.5 kips. This average force is 5.1% less than the force required theoretically (see Fig. 3.8).

5.2.2. Deflection data

Deflection data were obtained at various increments as force was applied to the truss strengthening system. Figure 5.5 illustrates a typical response exhibited during the jacking process for truss Stage A (see Fig. 3.6). In this figure, the tendon force is the total force for both tendons at each truss location (i.e., one tendon on each side of the web). Figure 5.5a illustrates the response of the end spans as the force is applied to Truss 1. A maximum upward displacement of 0.0193 in. occurred in the west span when a strengthening force of 159 kips was applied. The east span displaced downward 0.0086 in. under the same force. These linear results are consistent with the response at each location.

The transverse distribution caused by the truss system is shown in Fig. 5.5b. For truss Stage A (159 kips), the upward displacement of the adjacent stringer in the west span was

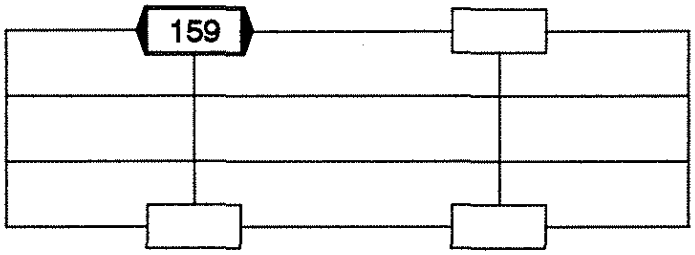

a. STAGE A

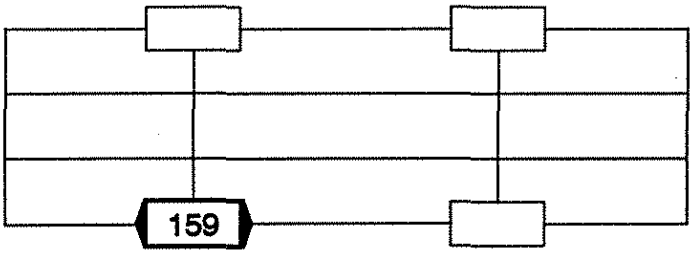

b. STAGE B

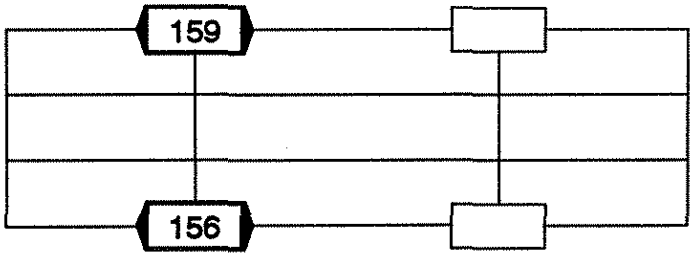

c. STAGE C

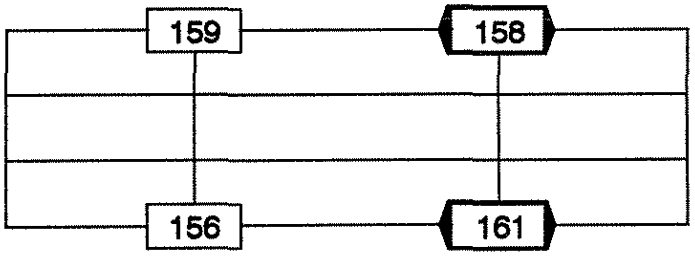

d. STAGE D

Fig. 5.4. Force (kips) applied per truss stage.

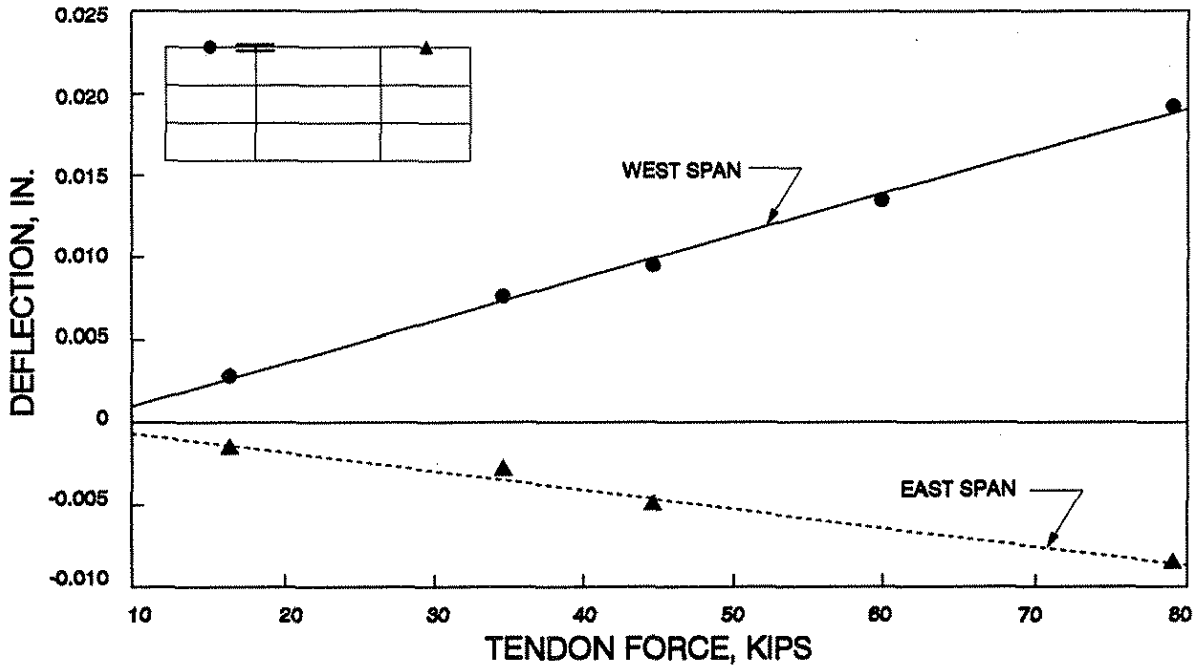

a. STRINGER 4

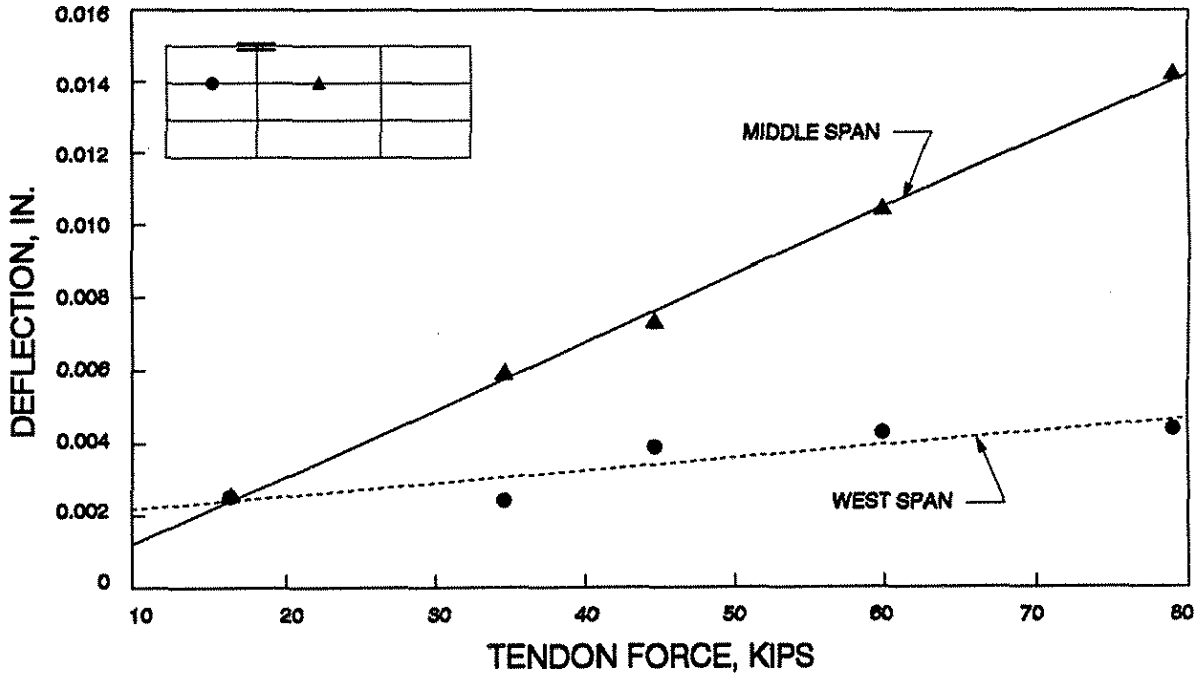

b. STRINGER 3

Fig. 5.5. Deflection response to truss strengthening.

0.0044 in., or approximately 23% of the exterior stringer deflection in the west span.

It can also be seen in Fig. 5.5b that the middle span deflected more than the exterior span for a given truss force. The difference in deflection can be attributed to the larger span length of the middle span.

5.2.3. Truck loading strain data

Figures 5.6 and 5.7 illustrate the increase in bridge stiffness caused by the truss system. The term stiffness is used here to describe the reaction of the bridge when subjected to vertical loading. An increase in stiffness caused by the strengthening system would be indicated by a decrease in stringer strain or deflection when subjected to vertical loading.

Note that Figs. 5.6 and 5.7 represent only the live load stringer strains at these locations and do not include the strain caused by the truss strengthening. Because Truck 1 was not available at the time of these tests, Truck 2 was used for the truss strengthening load tests. Truck 1 was 3660 lb. heavier than Truck 2 (a 6.8% difference), so direct correlation is not impossible.

The load point locations and positions along the stringers presented in Figs. 5.6 and 5.7 were selected because the strains at these locations were a maximum for the given load position. For example, load point 1.2 produces maximum positive strains in the west span; the curves shown in Fig. 5.6a are west midspan strains caused by load case 1.2. The remaining curves in Figs. 5.6 and 5.7 were similarly constructed.

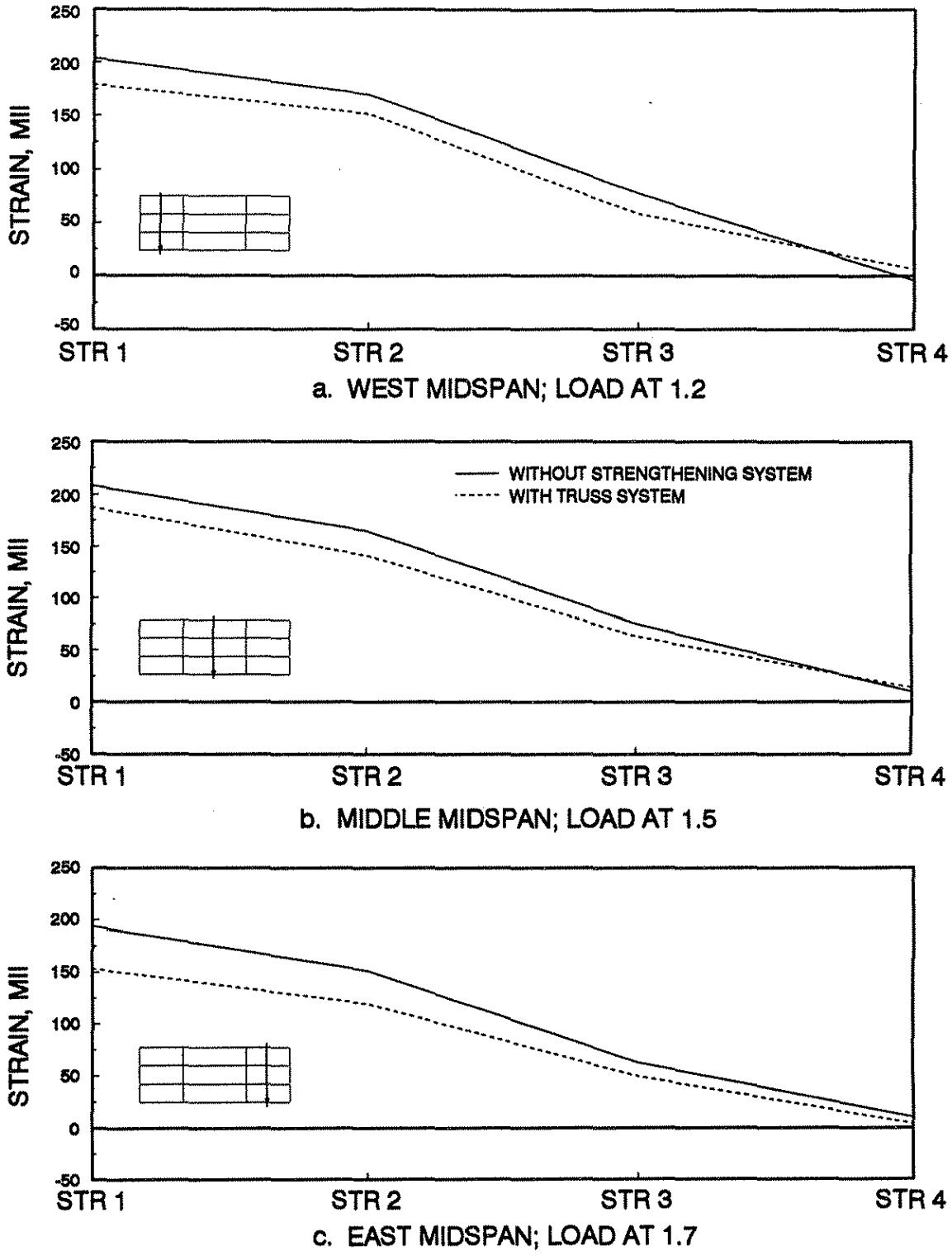

Fig. 5.6. Effect of truss system on midspan live load strains, Lane 1 loading.

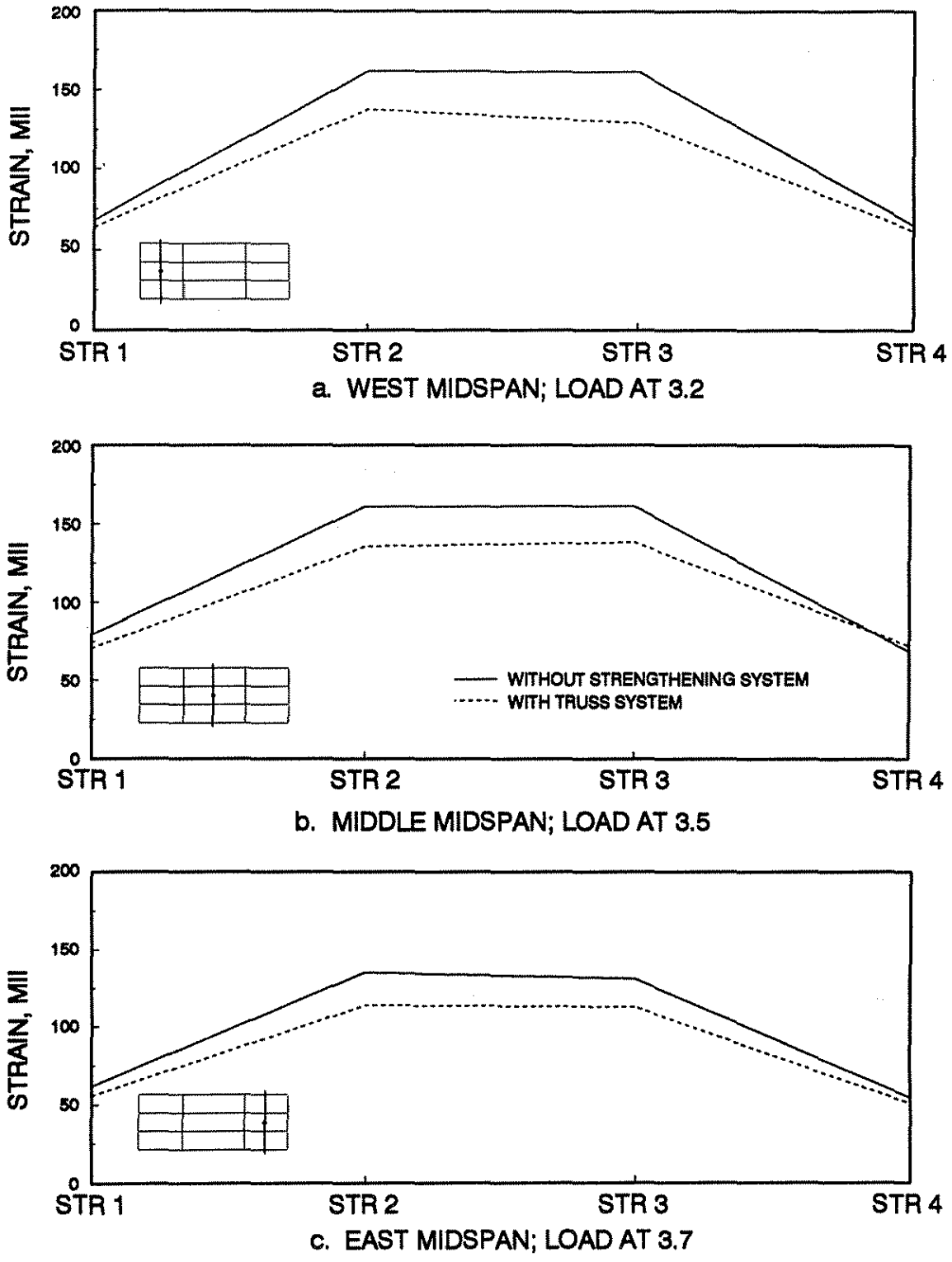

Fig. 5.7. Effect of truss system on midspan live load strains, Lane 3 loading.

Straight lines have been used to connect the data points so trends in the data can be more easily reviewed. This does not suggest that the actual strain distribution between the data points is linear.

Decreases in stringer 1 midspan strains, with the addition of the trusses, for Lane 1 loading (Fig. 5.6) ranged from 9.9% to 20.8%; the average decrease was 14.3%. Similarly, decreases in interior stringer midspan strains for Lane 3 loading (Fig. 5.7) ranged from 14.3% to 19.7%; the average decrease was 15.7%. Data for stringer 1 in Fig. 5.6 and stringers 2 and 3 in Fig. 5.7 were closest to the load and therefore, experience the greatest benefit. For Lane 3 loading, the average decrease in midspan strains experienced in the exterior stringers was 5.6% (see Fig. 5.7). Figure 5.7 also verifies the transverse distribution of the truss force to the interior stringers.

From previous research, HR-287, it has been shown that post-tensioning alone does not significantly increase the stiffness of a continuous span bridge [4]. This is because post-tensioning adds very little material to the member cross section. Therefore, the increase in the moment of inertia is negligible.

The decrease in stringer strains at the pier locations was not as significant as at midspan. Figures 5.8a and 5.8b are plotted for the west pier when the load is at the midspan of the west and middle spans, respectively. Similar plots are shown in Figs. 5.8c and 5.8d for the east pier. The exterior stringer strains in Figs. 5.8a and 5.8d increased slightly. Note that for both of these cases the vehicle is positioned in an end span. No increase occurred when the vehicle was located in the middle span. The authors believe that a

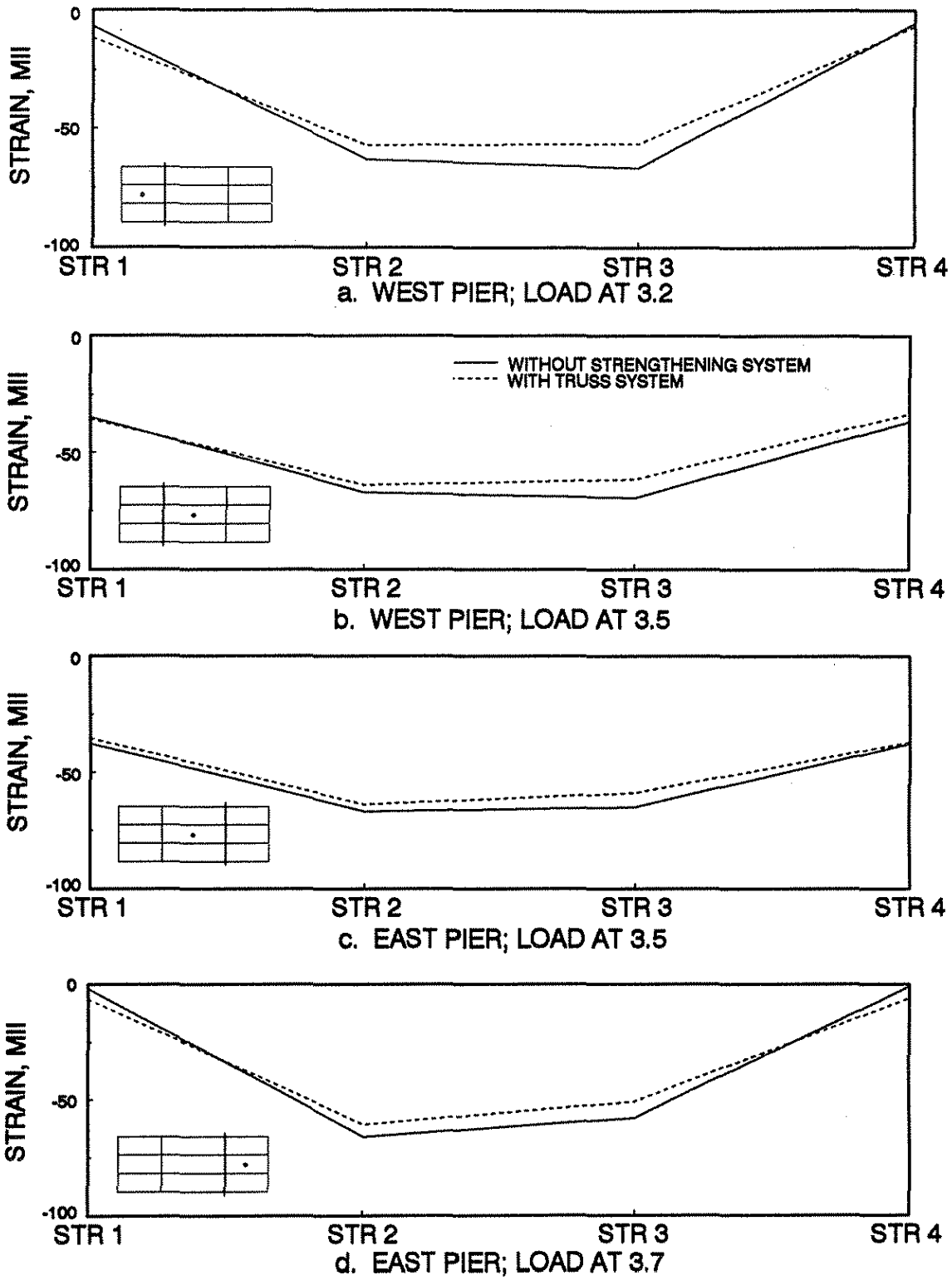

Fig. 5.8. Effect of truss system on pier live load strains, Lane 3 loading.

combination of the exterior stringer truss system loads and partial end restraint caused these increases.

The truss system increased the stiffness of the bridge. The tubes provided an additional support at the bearing location on the top flanges of the exterior stringers. The trusses also provide an additional "load path" for live load on the bridge, thus increasing the redundancy of the original bridge.

5.3. Strengthening Stages

The various stages used to strengthen the bridge were presented in Fig. 3.8. As previously mentioned, several stages were necessary because of the limited strengthening equipment available. In this section, the response of the bridge to the strengthening system will be presented.

5.3.1. Strengthening forces

The forces that were applied in each stage of the strengthening process are shown in Fig. 5.9 and are indicated by the highlighted boxes for each stage. The other numbers reflect changes in force that occurred because of subsequent strengthening stages. A summary of these force changes is shown in Fig. 5.10. Figure 5.10d shows that the percent change in force ranged from -3.5% to +3.8%.

As previously noted, the theoretical strengthening forces were calculated using a finite element model (Chp. 4). The forces applied in the field were slightly different than the required theoretical forces. These differences are shown in Fig. 5.11a and 5.11b. All of the truss forces applied were less than theoretically required and all but two of the post-tensioning forces were greater than theoretically required.

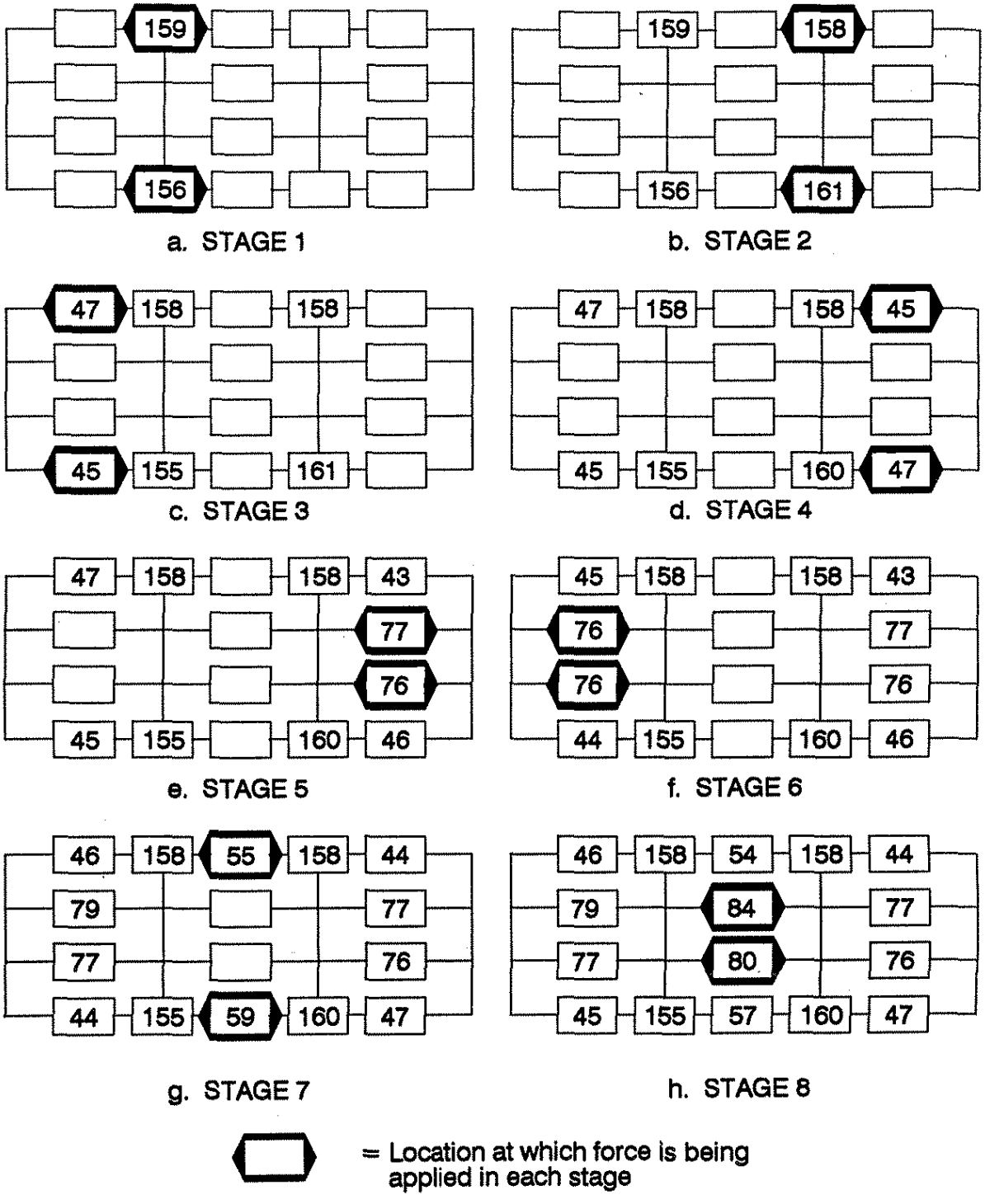

Fig. 5.9. Actaul force (kips) applied per stage.

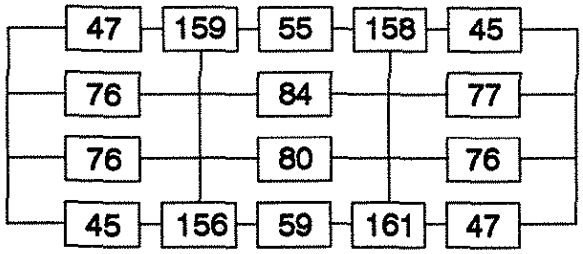

a. INITIAL FORCE APPLIED

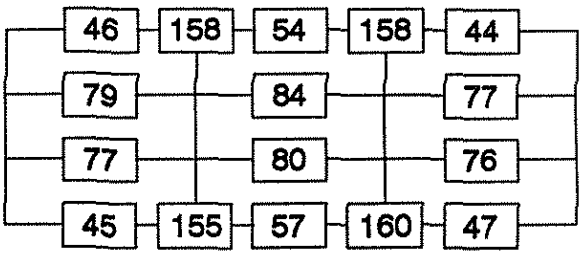

b. FINAL FORCE

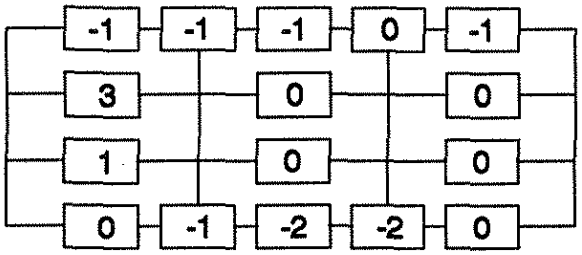

c. CHANGE IN INDIVIDUAL FORCE DUE TO APPLICATION OF ADDITIONAL FORCE

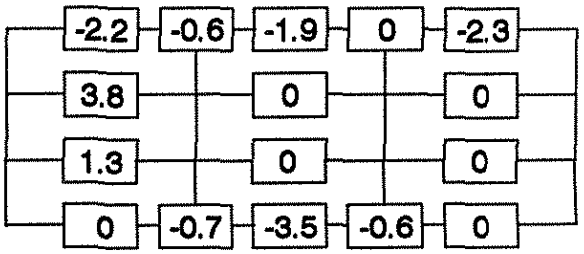

d. PERCENT CHANGE

Fig. 5.10. Change in forces due to various stages.

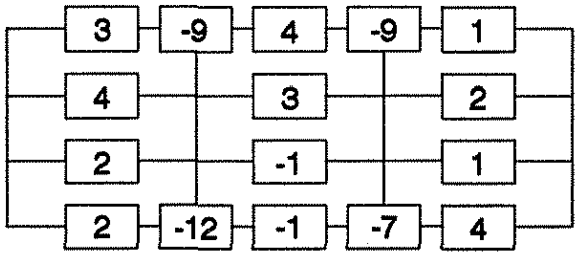

a. DIFFERENCE BETWEEN THEORETICAL FORCE REQUIRED AND ACTUAL FORCE APPLIED

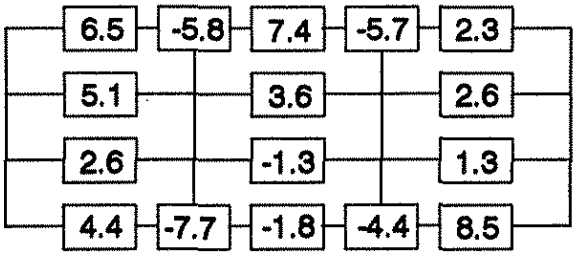

b. PERCENT DIFFERENCE

Fig. 5.11. Actual force applied versus theoretical force required.

Because the trusses and post-tensioning are complimentary, the desired stress reduction was obtained.

5.3.2. Deflection data

As was previously mentioned, the electronic instrumentation consisted of 166 strain gages and 12 DCDT's. Two DAS's were required to monitor all of the instrumentation. Unfortunately, on the second day of the test, there were problems with one of the DAS's. Thus, deflection data were obtained for only one location in the bridge; the midpoint of stringer 4 in the west span. Therefore, only that location will be discussed in this section.

A plot of cumulative deflection for the west span of stringer 4 during the eight stages of strengthening is shown in Fig. 5.12. These values are referenced from the unstrengthened position of the bridge with a positive deflection change being upward. Stages 3 and 6 of the strengthening scheme caused the greatest upward deflection change as noted in the figure. The change in deflection during Stage 6 is significantly larger than that caused by Stage 3. This is due to the fact that the post-tensioning force applied to the interior stringers during Stage 6 is greater than the force applied to the exterior stringers during Stage 3. Transverse distribution of post-tensioning forces also accounts for part of the difference.

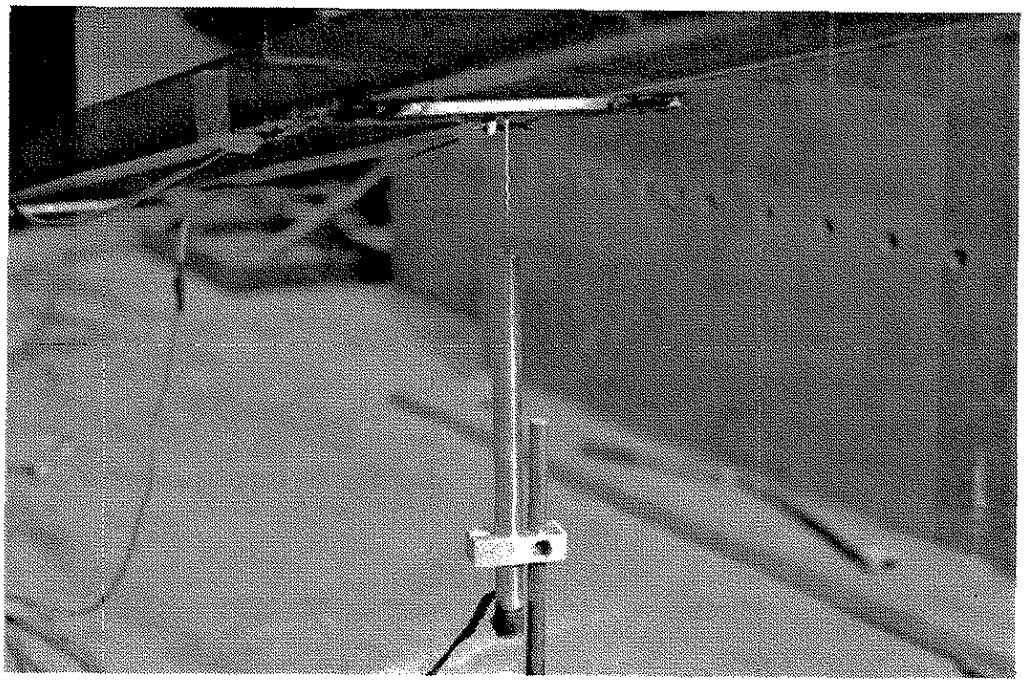

a. PHOTOGRAPH OF DEFLECTION INSTRUMENTATION

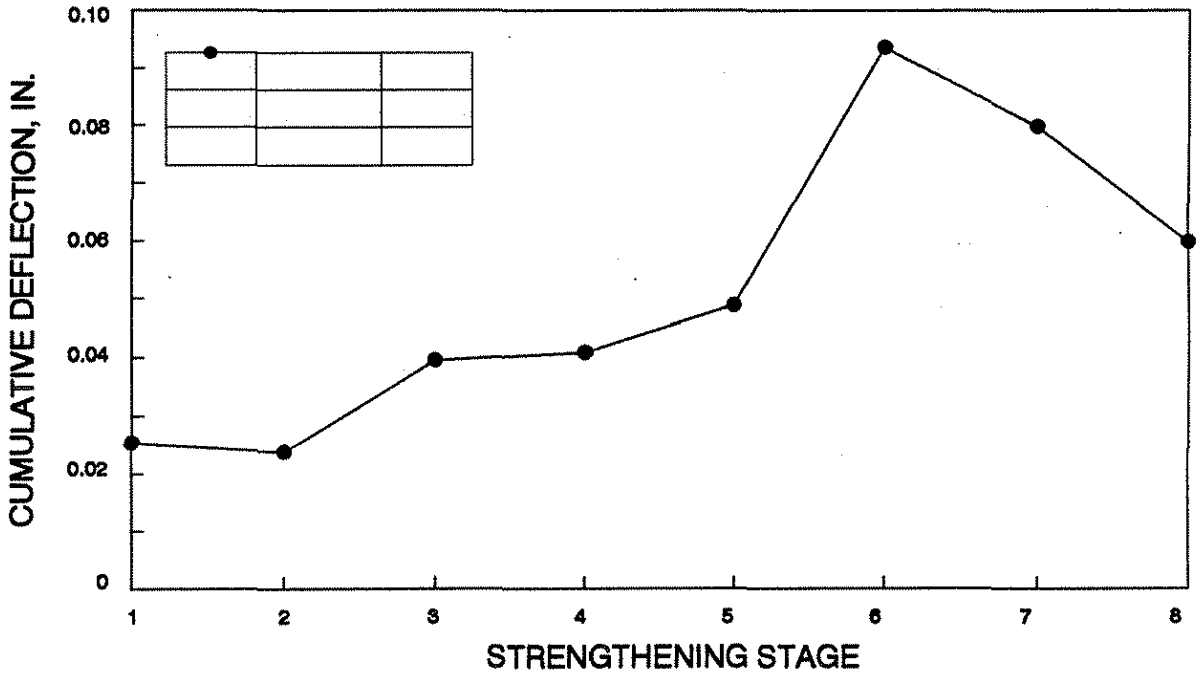

b. EFFECT OF STRENGTHENING STAGES ON DEFLECTION

Fig. 5.12. Variation in stringer deflection as strengthening stages are applied.

Qualitatively, one would expect downward deflection for Stages 2, 7, and 8 of the strengthening procedure. The deflections caused by Stages 7 and 8 should be larger in magnitude than the deflection caused by Stage 2 because of the location of the strengthening force. The remaining stages (Stages 1, 3, 4, 5, and 6) should each cause an upward (positive) deflection at this location. One would also expect Stages 3 and 6 to cause the largest upward deflections. Review of Fig. 5.12 verifies these qualitative predictions.

5.3.3. Strengthening strains

Based on the finite element model developed, the strain profile was predicted for the interior and exterior stringers as each symmetric strengthening stage was activated. Because the bridge was modeled using 1/4 symmetry only symmetric results could be predicted. The predicted theoretical strain profiles and experimental strains in the the exterior and interior stringers are presented in Figs. 5.13 through 5.17 for Stages 2, 4, 6, 7, and 8, respectively. Note that different vertical scales have been used for each figure.

Each field strain shown in the figures was calculated by averaging four strain gage readings associated with the pairs of interior and exterior stringers, respectively. In other words, the four strains from the two exterior stringers werea veraged as well as the four strains for the interior stringers.

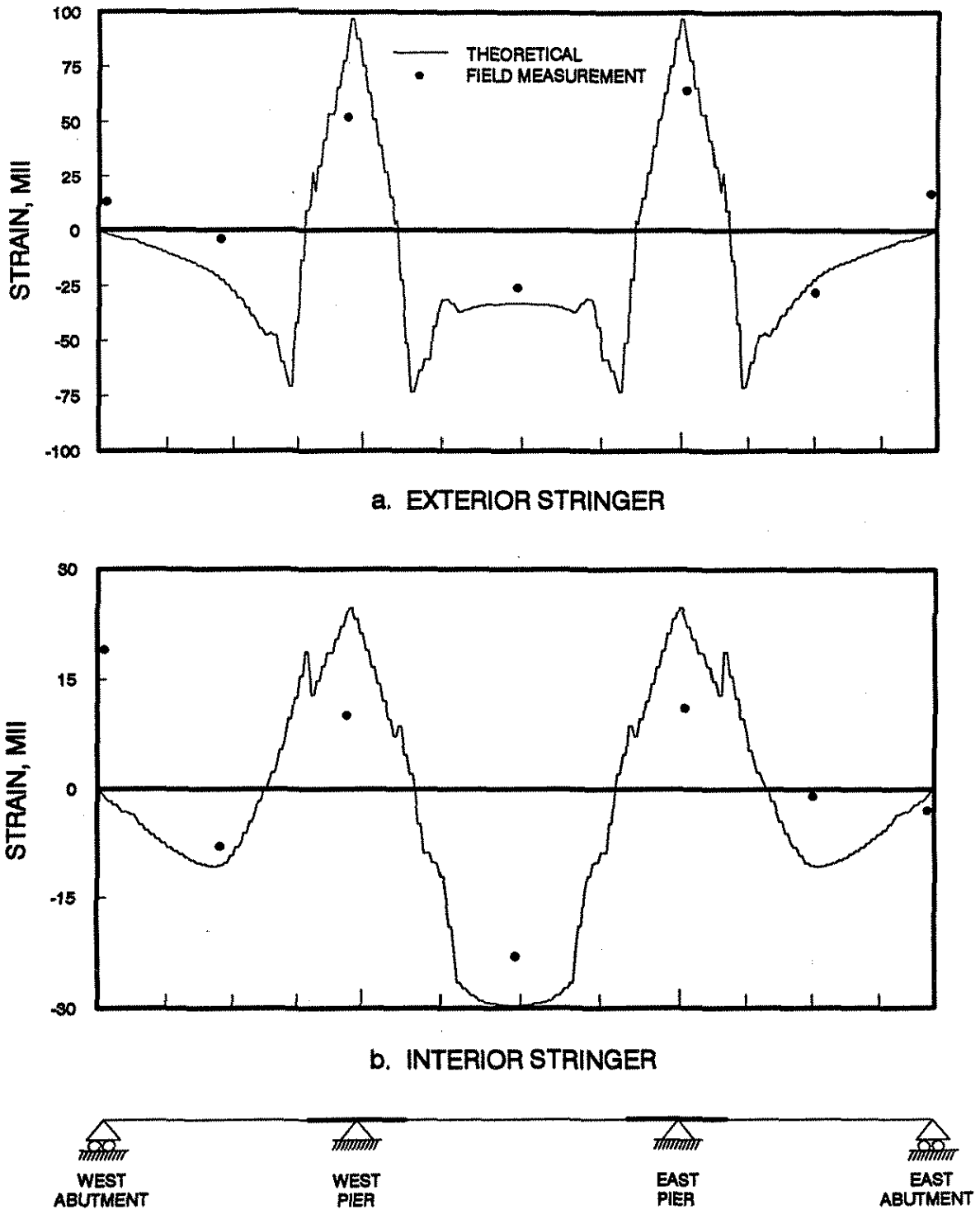

Fig. 5.13. Bottom-flange stringer strains: Stage 2 strengthening.

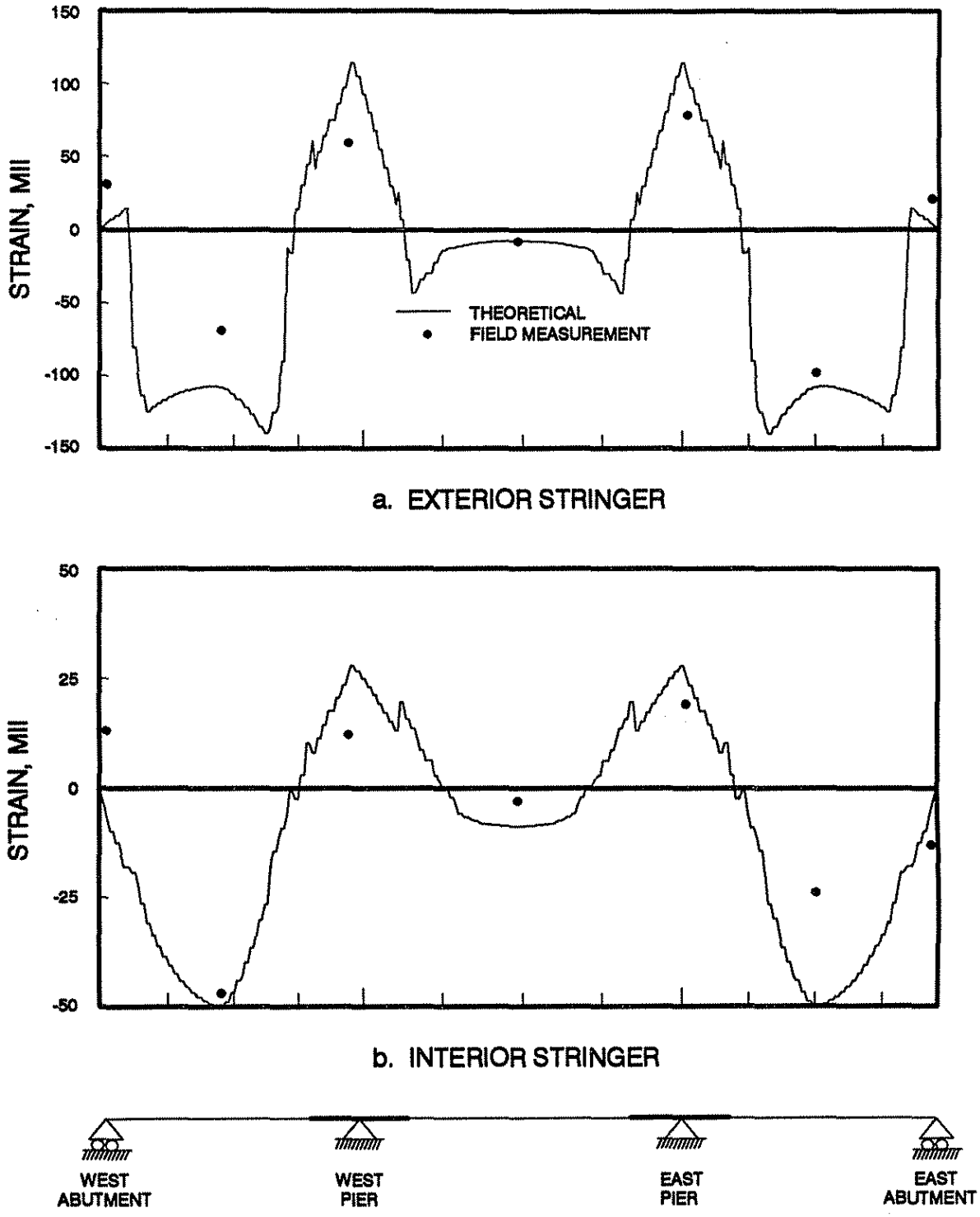

Fig. 5.14. Bottom-flange stringer strains: Stage 4 strengthening.

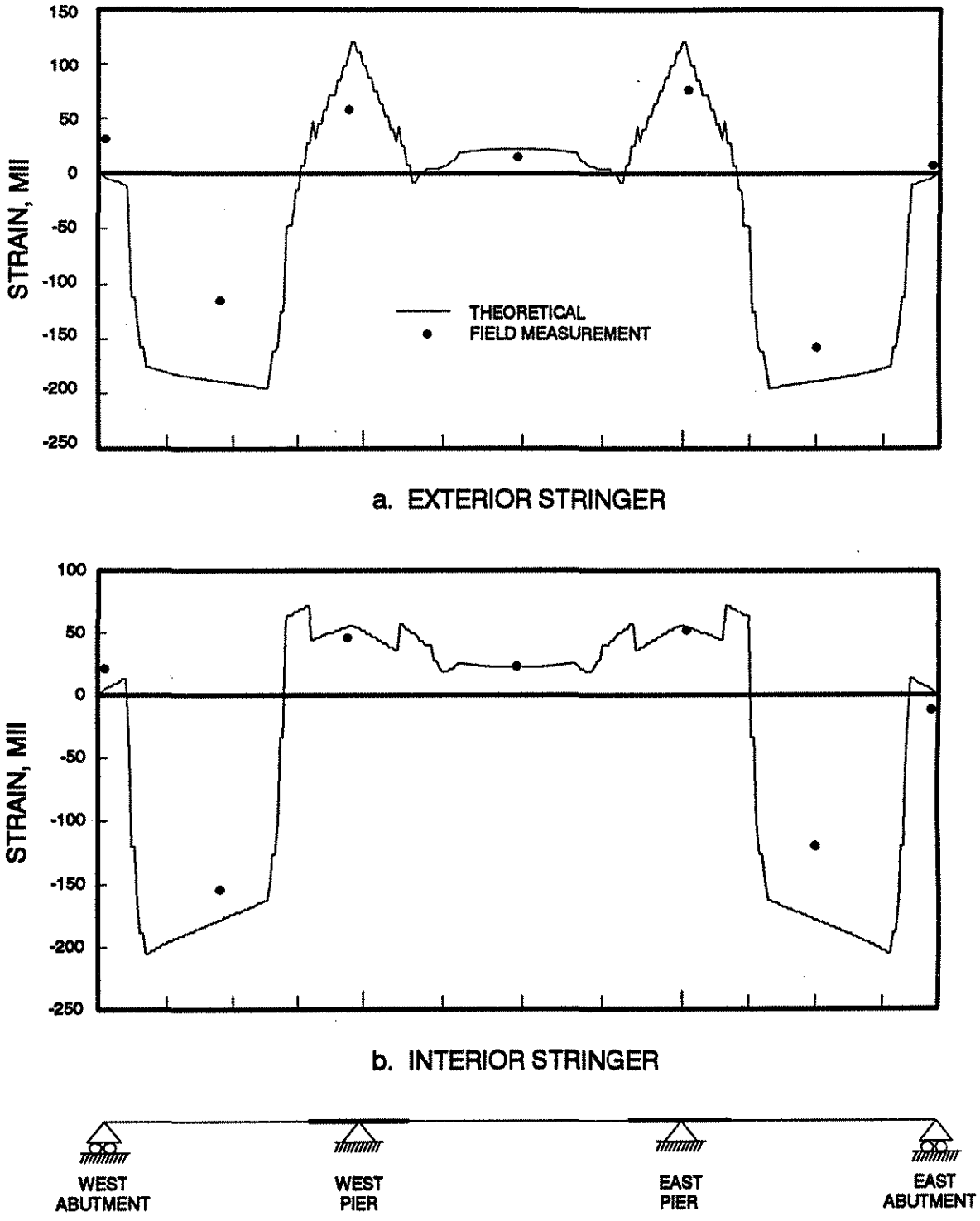

Fig. 5.15. Bottom-flange stringer strains: Stage 6 strengthening.

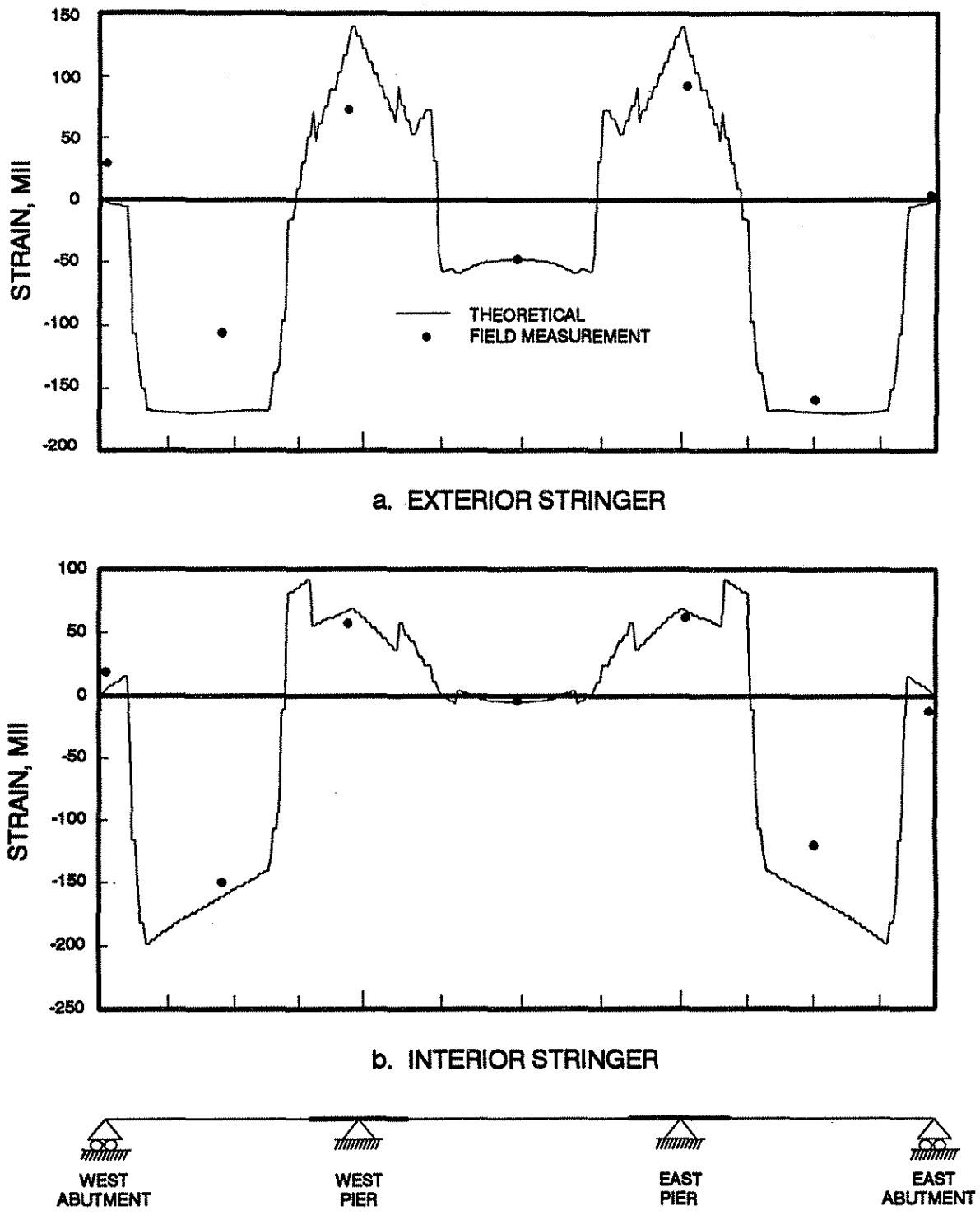

Fig. 5.16. Bottom-flange stringer strains: Stage 7 strengthening.

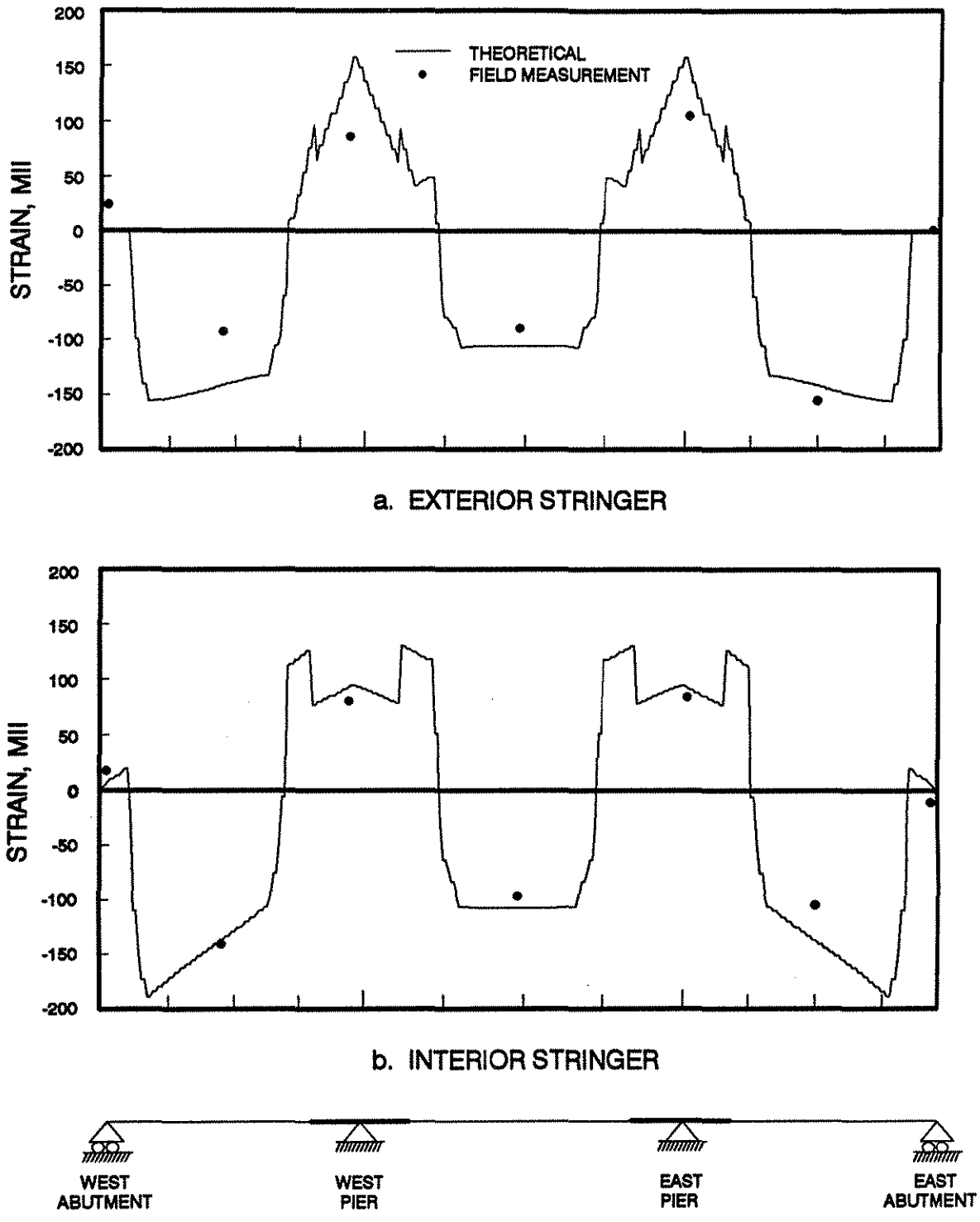

Fig. 5.17. Bottom-flange stringer strains: Stage 8 strengthening.

The theoretical strains assume roller supports at the abutments as indicated by the zero strains shown at the west and east abutments in all of the theoretical curves. The figures indicate that field strains occurred at the abutments during strengthening. Note from Fig. 3.1 that these strains are measured 15 in. from the centerline of the abutments. Also, inherent end restraint due to continuity between the deck and the abutment (probably due to the deck reinforcement continuing into the wing walls) will account for some of the restraint.

Further review of the figures indicates that the west abutment strains were larger than the east abutment strains. This result is consistent for both interior and exterior stringers throughout all strengthening stages. Although the abutment bearings were cleaned and treated with a silicone spray *prior* to testing, it is possible that some of the bearing pads were not moving freely. Crack monitors were attached at each abutment bearing location and monitored during the strengthening process. Data from the crack monitors indicated that the bearing pads did slide relative to one another. Therefore, most of the strain at the abutments is the result of rotational restraint.

Figure 5.13 shows the strains with the truss system completely activated (Stages 1 and 2). The purpose of the superimposed trusses was to apply upward forces that induce moments to oppose the moments induced by live load. Therefore, negative (compressive) bottom-flange strains due to live load should be opposed by a positive (tensile) strain from the trusses. The magnitude of the desired positive

strain from the trusses was determined using the finite element model discussed earlier; 87 MII (micro-in. per in.) on the exterior stringers and 24 MII on the interior stringers. However, the average strain achieved by the truss system was 58 MII and 11 MII for the exterior and interior stringers, respectively. Therefore, the actual strain applied on the exterior stringer was 67% of the predicted value. A small part of this difference is the result of the predicted strains being calculated at the stringer extreme fibers and the field strains being measured on the top surface of the stringer flange.

The superimposed truss system also introduced beneficial strains in the positive moment regions due to longitudinal distribution. The experimental results for these midspan regions agree well with the predicted values at all but two locations; the west span in Fig. 5.13a and the east span in Fig. 5.13b. These experimental data are questionable. Review of the figures shows that the strain at these two locations was always significantly below the predicted values.

Figure 5.17 displays the final strain profiles for the completely strengthened bridge. The midspan strains were, on the average, 88.4% of the predicted values. Bottom-flange strains at the piers were 76.8% of the predicted values. Considering interior stringers only, this value is 88.5%. Part of these discrepancies at the piers can be attributed to the way that the finite element model simulated the truss uplift points on the bridge. The model assumed a concentrated force acting at the contact point, when in fact the force was distributed over an area of eight in. x eight in. (i.e., the area of the 1/2 in. bearing plate). This assumption thus overestimates the analytical strains in the vicinity of the pier. Probably most of the differences between the

theoretical and experimental strains was due to the guardrails and end restraint. Neither of these contributions could be taken into account in the theoretical model. Guardrail strains are discussed in more detail in Sec. 5.5.

5.4. Strengthened Bridge Load Tests

The strengthened bridge load test data are presented in this section. Comparisons will be made between strain data for the strengthened and unstrengthened bridge. These comparison will be made for the single vehicle load tests (Sec. 5.4.1) and the pattern load tests (Sec. 5.4.2). Section 5.4.3 summarizes the tendon force changes caused by vertical loading.

5.4.1. Single vehicle loading

The effect of vehicle loading on the stringer strains for the strengthened bridge is shown in Figs. 5.18 and 5.19. These are live load strains for the strengthened and unstrengthened condition. The open circles represent bad data, however, they have been plotted to represent the expected strain for each load case. The basis for plotting these data points is previous research work (HR-308) performed by the authors [1]. Recall that similar strain plots were presented in Figs. 5.1 through 5.3 for the truss strengthened condition.

In general, the unstrengthened strains changed a small amount when the bridge was strengthened. This behavior is different than what was observed for the truss strengthened bridge shown in Figs. 5.1 through 5.3. Utilizing superposition would indicate that post-tensioning decreased the stiffness of the bridge. This is not the case, previous research (HR-308) indicates that post-tensioning provides a

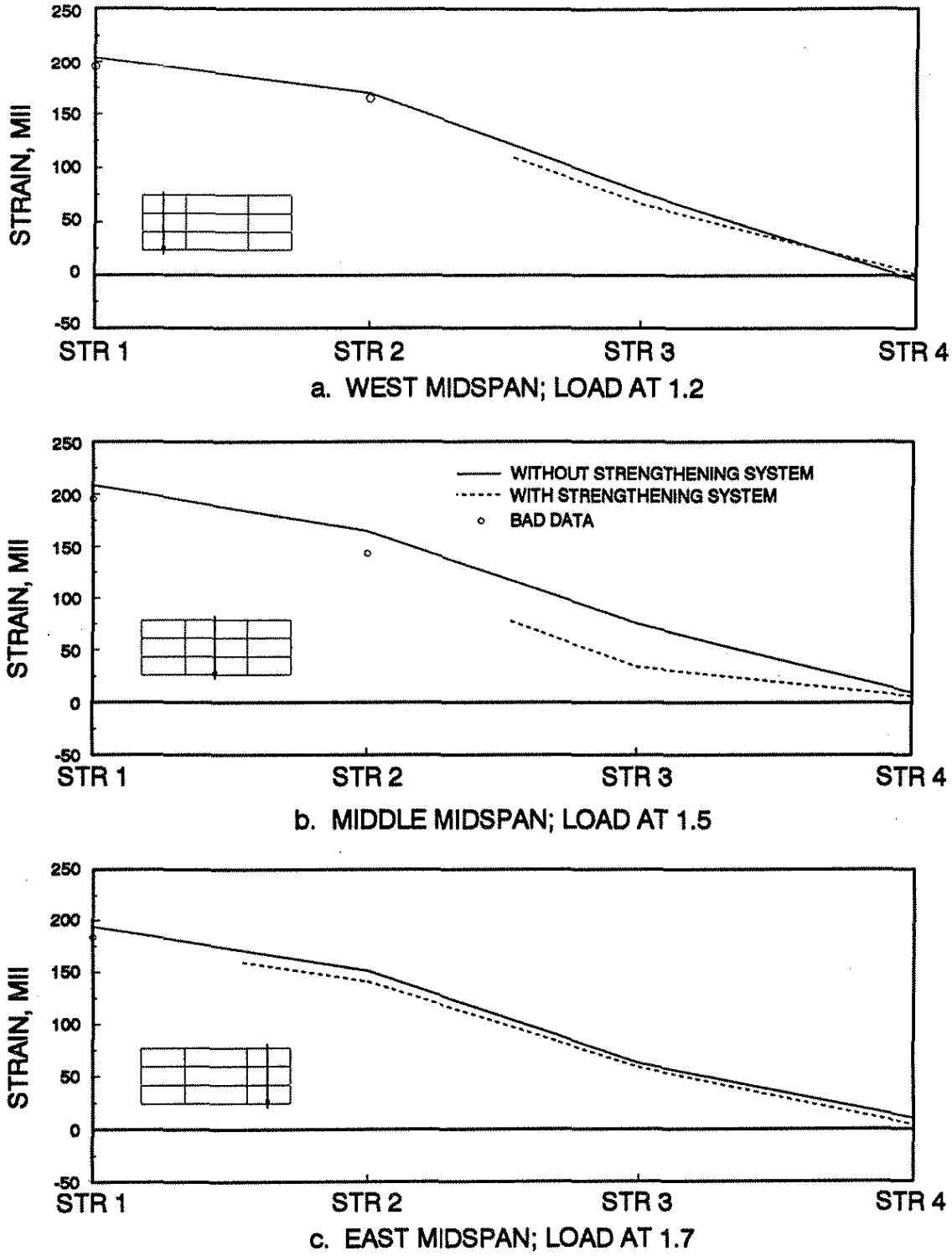

Fig. 5.18. Effect of strengthening on bottom-flange live load strains, Lane 1 loading.

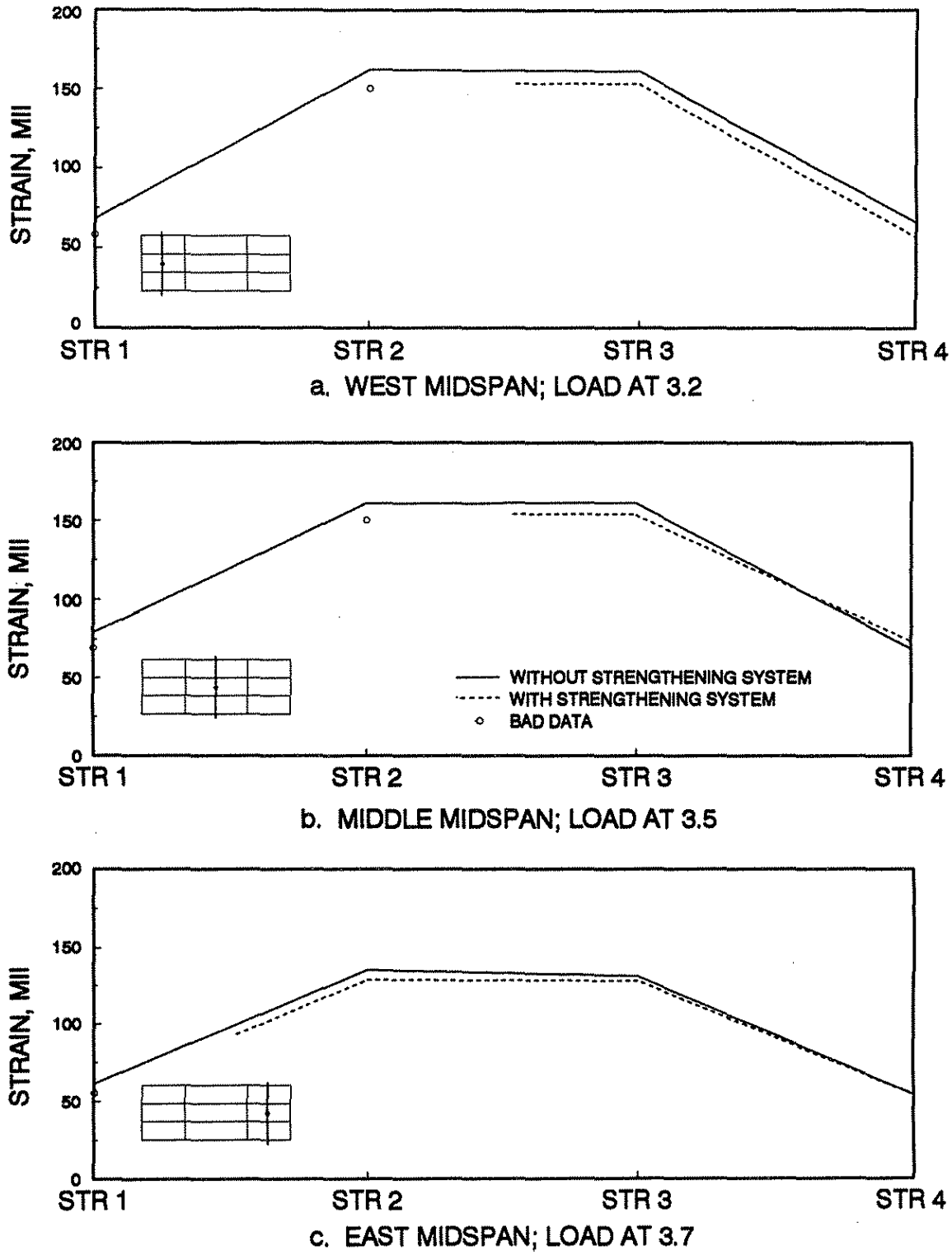

Fig. 5.19. Effect of strengthening on bottom-flange live load strains, Lane 3 loading.

slight increase in stiffness [1]. The discrepancy is a result of the trusses and post-tensioning tendons sharing the vertical load in the fully strengthened condition and only the trusses taking the vertical load for the truss strengthened condition. The effect of vertical loading on the strengthening tendons is discussed further in Sec. 5.4.3 of this report.

The effect of the strengthening system is illustrated more clearly by the strain plots for live load plus strengthening. Figure 5.20 shows these combined stringer strains for Lane 1 loading for the unstrengthened and strengthened cases as well as for the truss system only. Similar plots are shown for Lane 3 loading in Fig. 5.21. These data show the significant decrease in the strain due to the strengthening system.

5.4.2. Pattern loading

As mentioned in Sec. 3.2.1, pattern loading tests were performed before and after strengthening. Table 3.1 shows the location of the individual vehicles for each pattern loading case. The pattern loading cases were selected to maximize strains at various instrumented locations. Only representativecases of the twenty-four pattern loading cases (12 before and 12 after strengthening) are presented to show the bridge response.

Figures 5.22 through 5.24 show the interior and exterior stringer strain distribution before and after strengthening for PL 7, 8, and 9, respectively. The strains are for live load only. All three of these loading conditions are symmetric about the longitudinal centerline of the bridge (see Fig. 3.4). These strains represent averaged values for stringers 1 and 4 and stringers 2 and 3, respectively; the

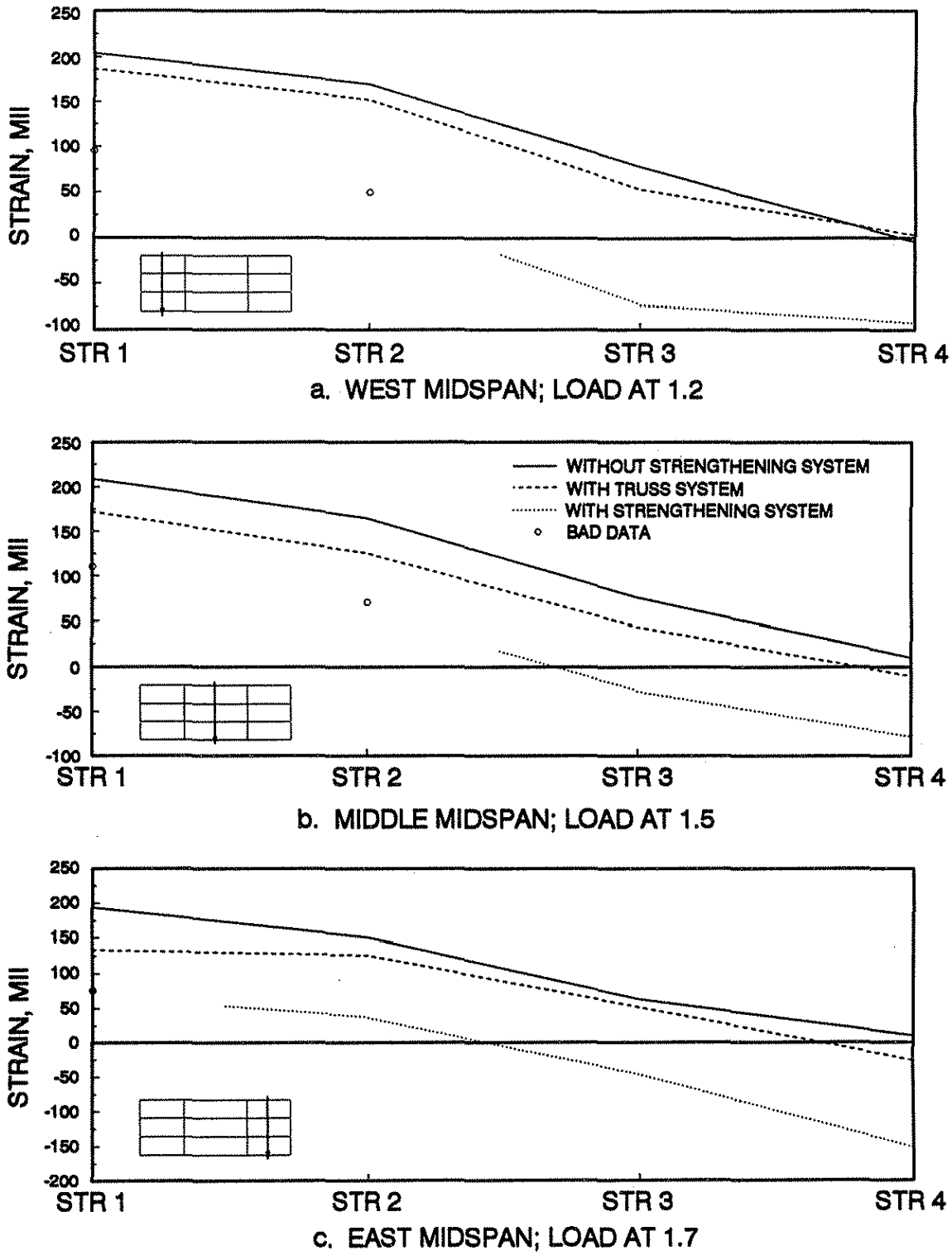

Fig. 5.20. Live load plus strengthening bottom-flange strains, Lane 1 loading.

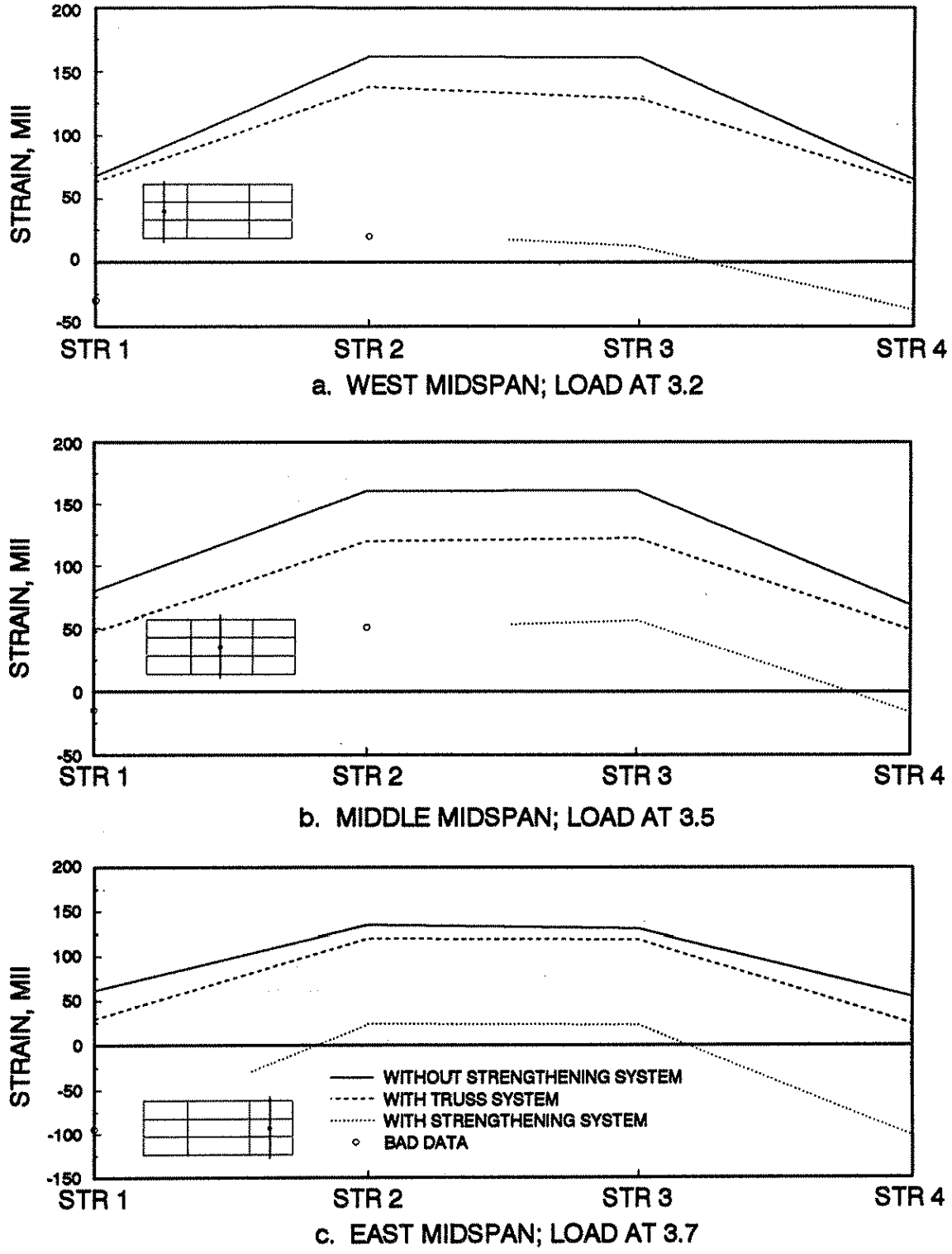

Fig. 5.21. Live load plus strengthening bottom-flange strains, Lane 3 loading.

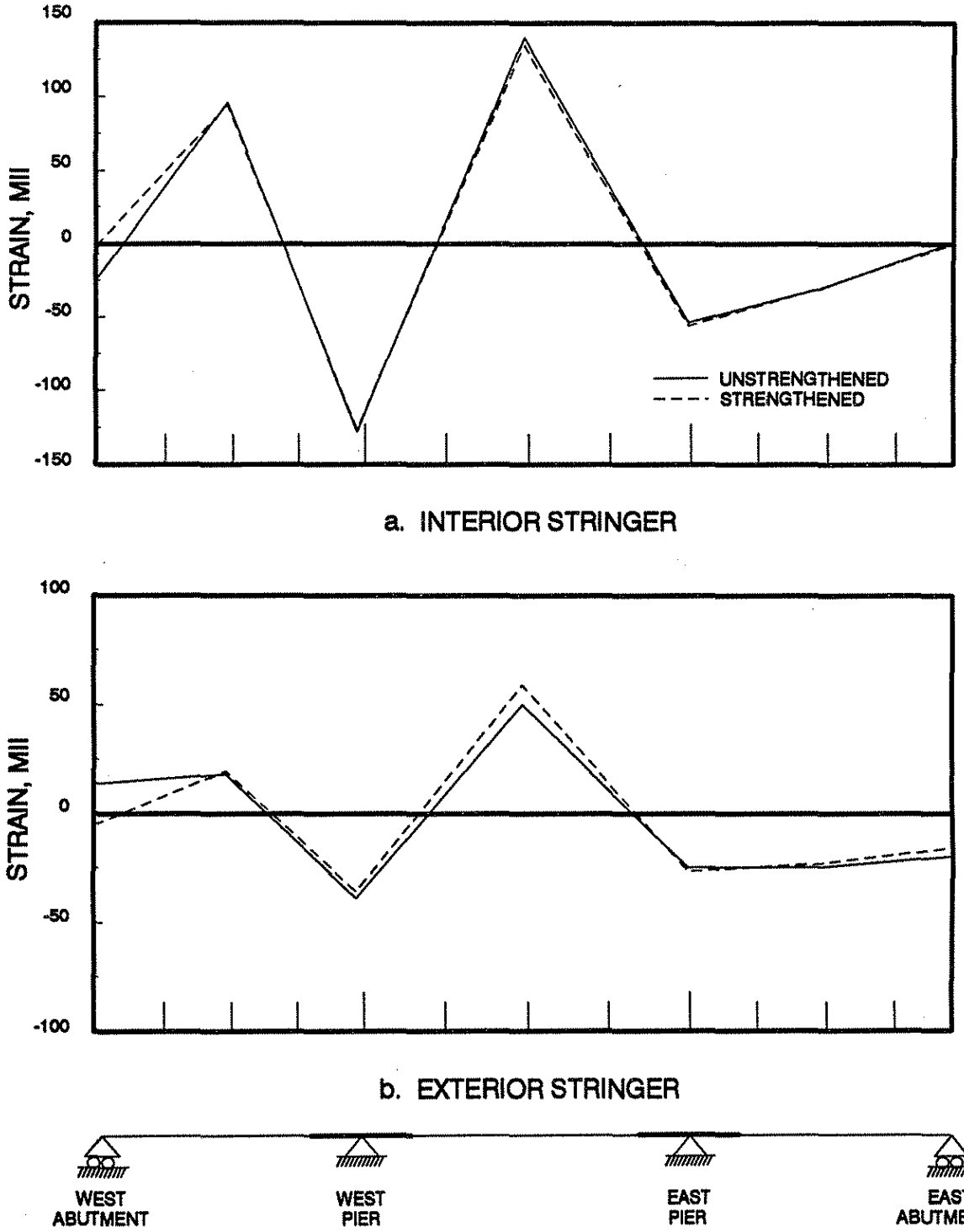

Fig. 5.22. Bottom-flange live load strain distribution, PL 7 loading.

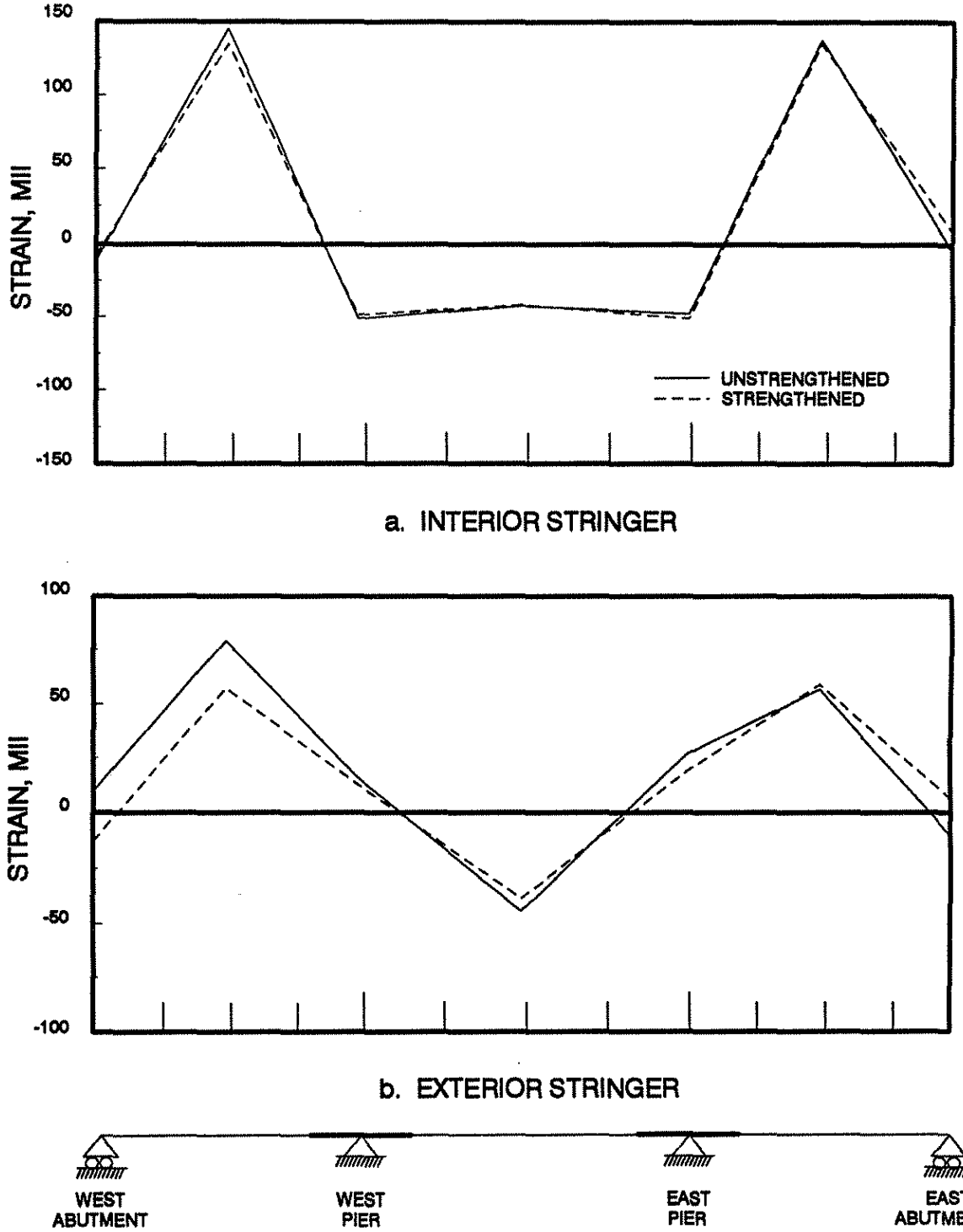

Fig. 5.23. Bottom-flange live load strain distribution, PL 8 loading.

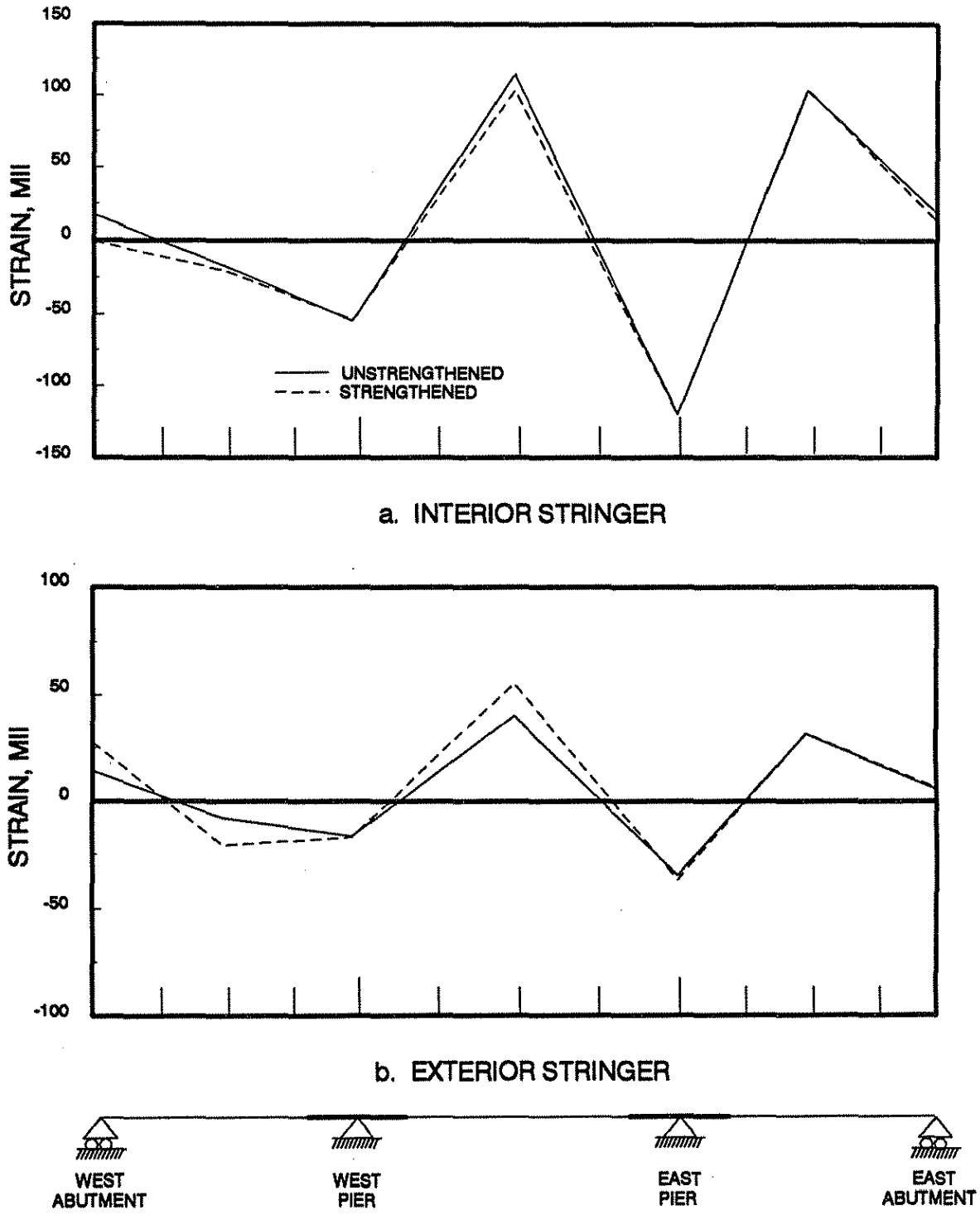

Fig. 5.24. Bottom-flange live load strain distribution, PL 9 loading.

correlation between these strains for the symmetric load cases was excellent.

To compare transverse symmetry about the center span of the bridge, unstrengthened strains for the interior stringer for PL 7 and PL 9 are considered. Results for PL 7 and PL 9 are shown in Figs. 5.22 and 5.24, respectively. The strains at the west pier for PL 7 were -128 MII and the corresponding strains at the east pier for PL 9 were -120 MII (only a 6% difference). Pattern Load 8 results are shown in Fig. 5.23. Note that the west and east span strains vary by only 5% for the unstrengthened condition.

Further study of Figs. 5.22 through 5.24 reveals that in all cases the exterior stringer strain at the abutment were larger after strengthening than before strengthening possibly due to end restraint. Because the superimposed trusses acted only on the exterior stringers, the increased end restraint could have resulted from the application of the truss system.

5.4.3. Tendon force changes

The changes and percent changes in the tendon forces (for both the superimposed trusses and positive moment region post-tensioning) due to the application of vertical load are shown in Figs. 5.25 through 5.29. The lanes and load points selected for the load testing sequence do not necessarily represent the locations that would maximize these changes as the truck wheel line was not always located directly above one of the stringers. Therefore, the changes in tendon forces shown may not be the maximum values that could occur.

Figures 5.25a and 5.25b show the percent change in tendon force for an interior and exterior middle span post-tensioning tendon for each single vehicle load case. To simplify interpretation of the data, Lane 4 load points are presented

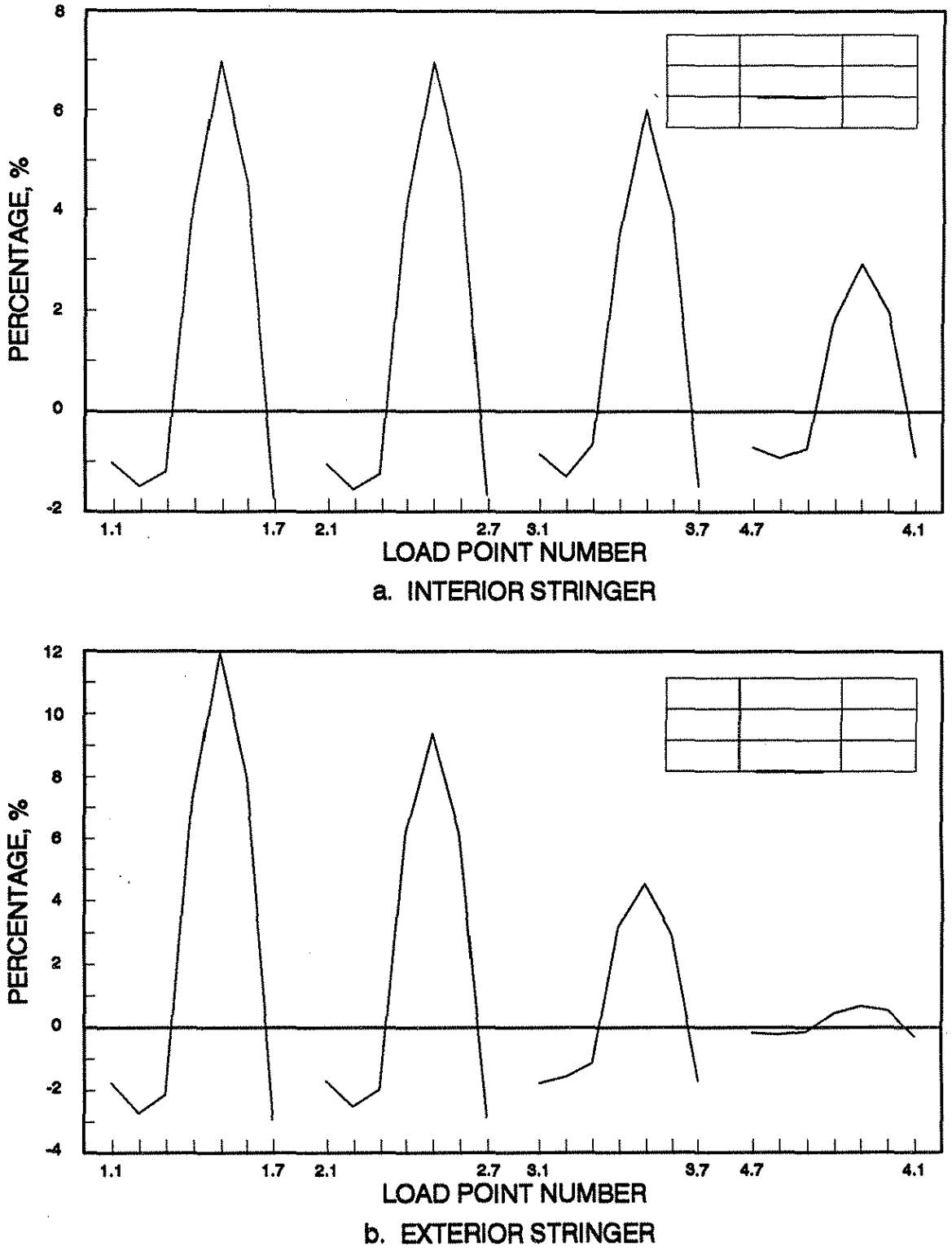

Fig. 5.25. Percent change in middle span tendon forces due to vertical loading.

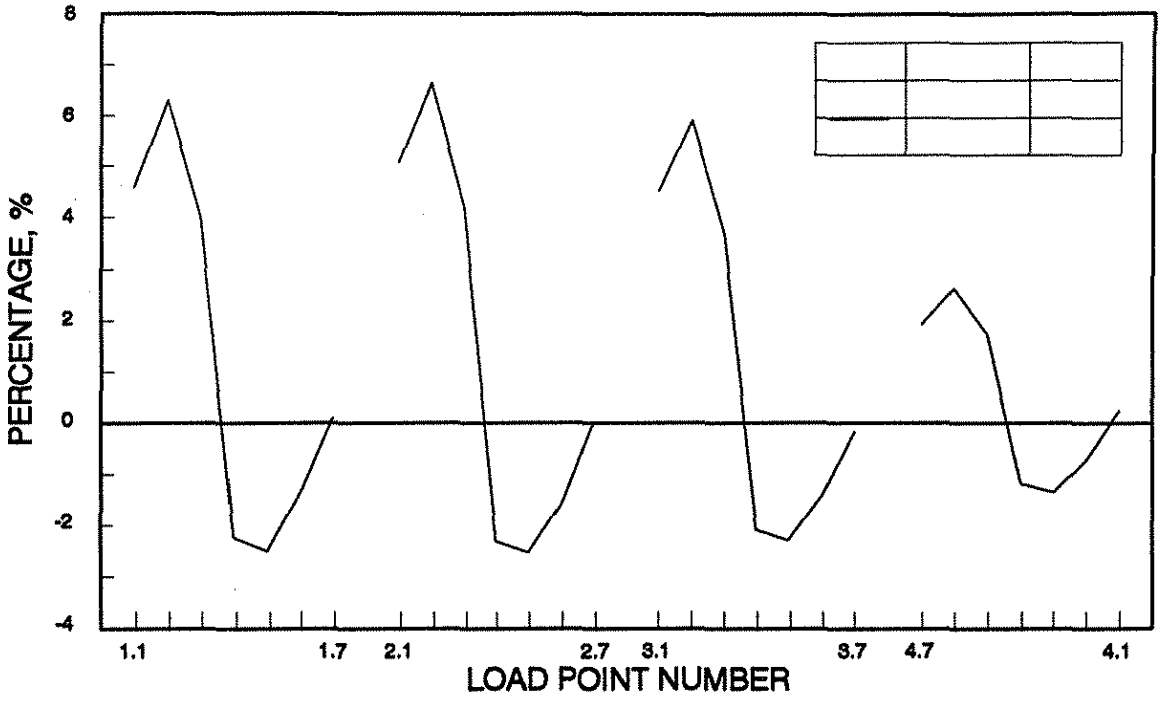

a. INTERIOR STRINGER

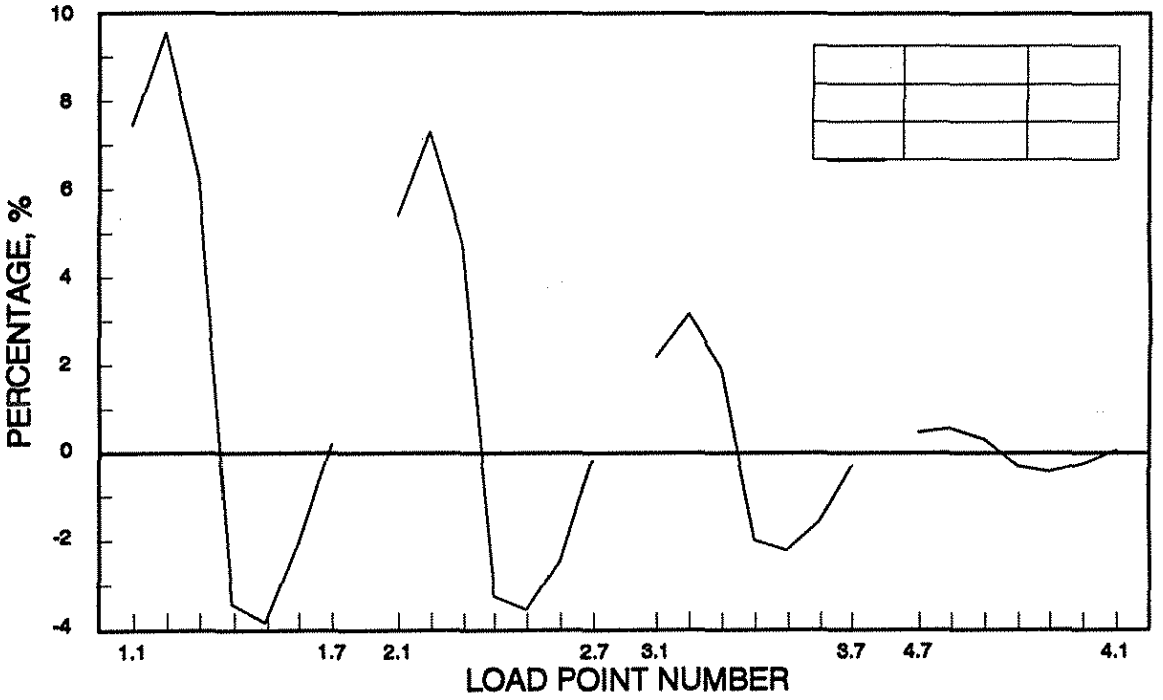

b. EXTERIOR STRINGER

Fig. 5.26. Percent change in west span tendon forces due to vertical loading.

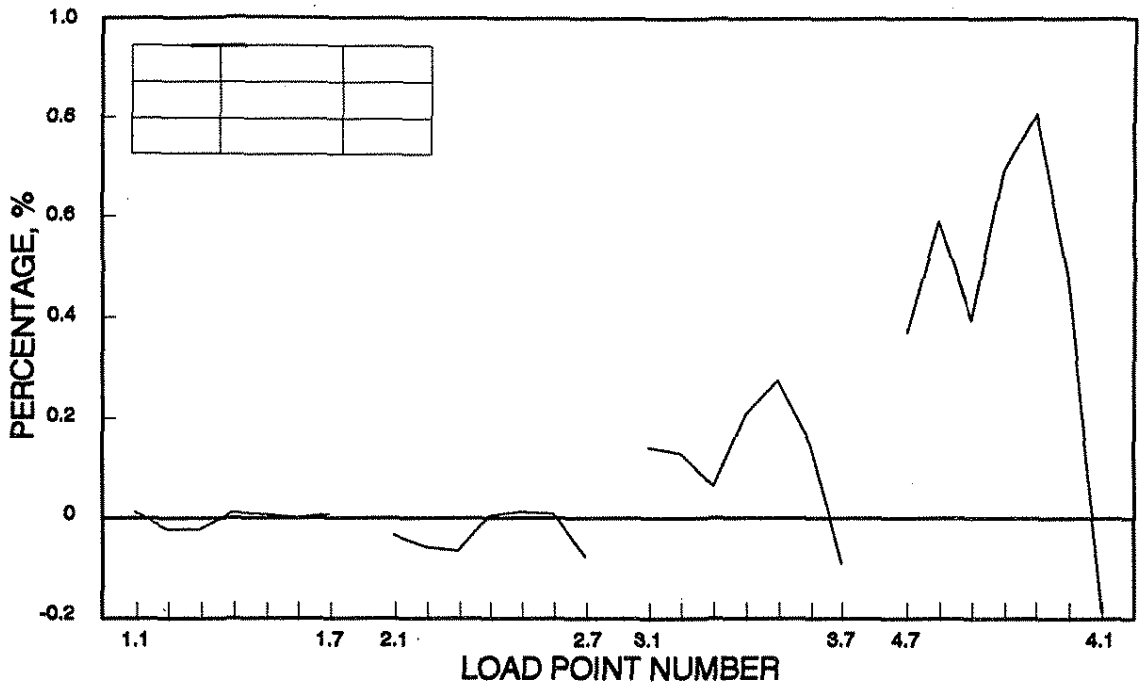

a. TRUSS 1

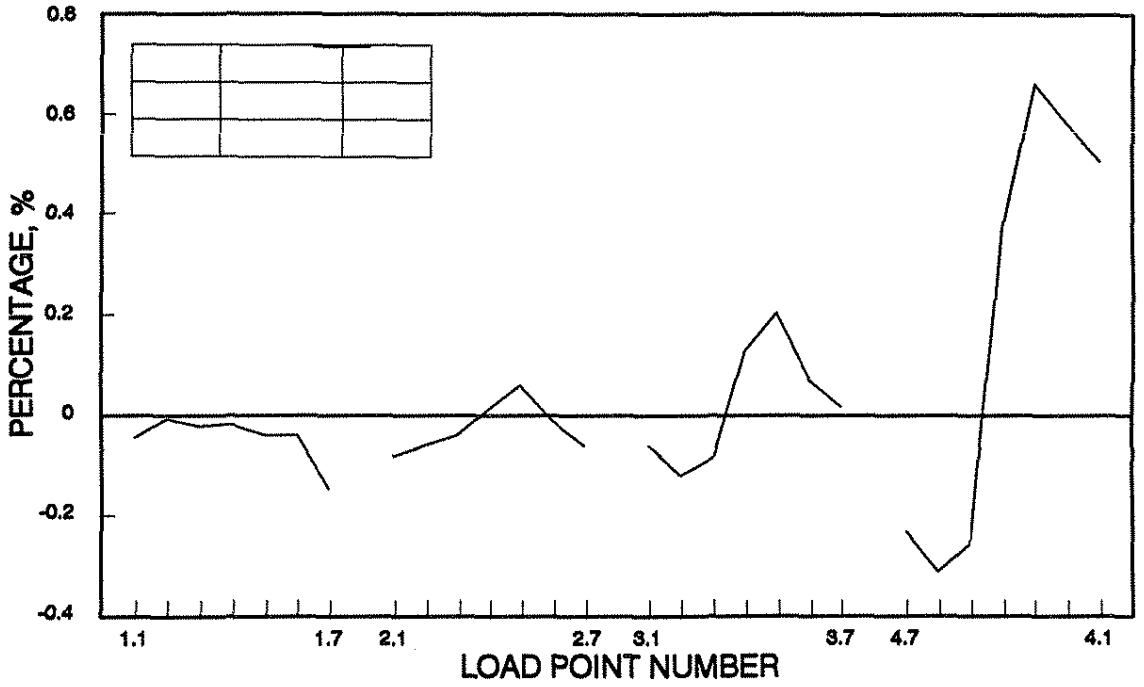

b. TRUSS 3

Fig. 5.27. Percent change in north truss tendon forces due to vertical loading.

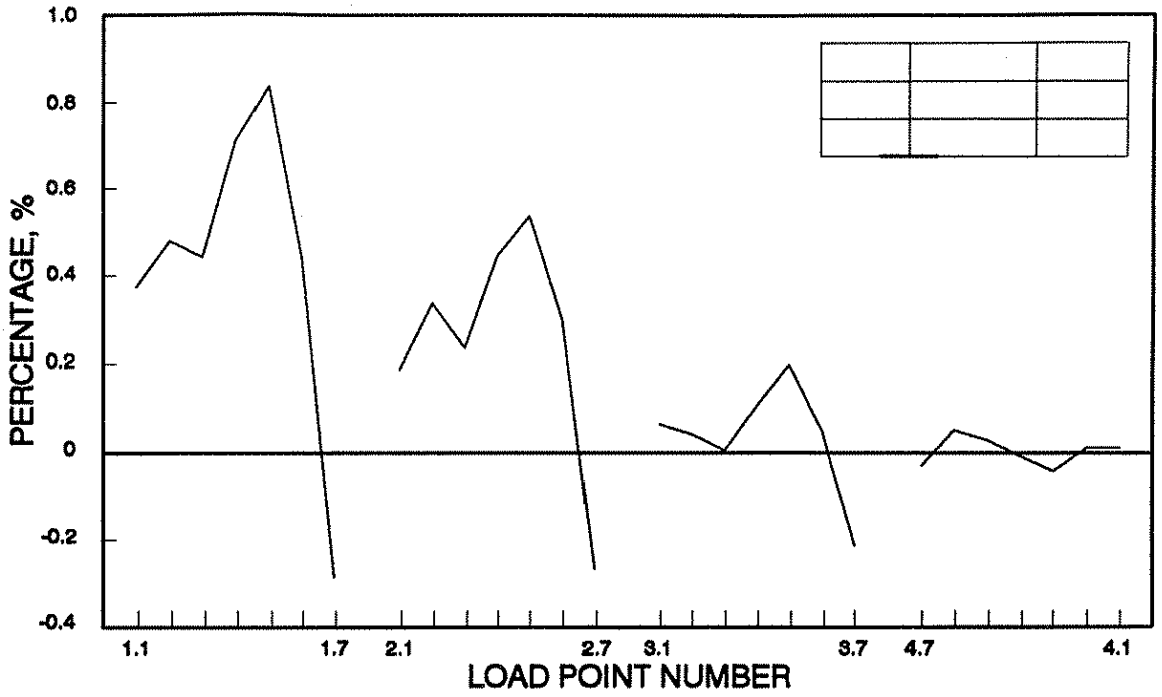

a. TRUSS 2

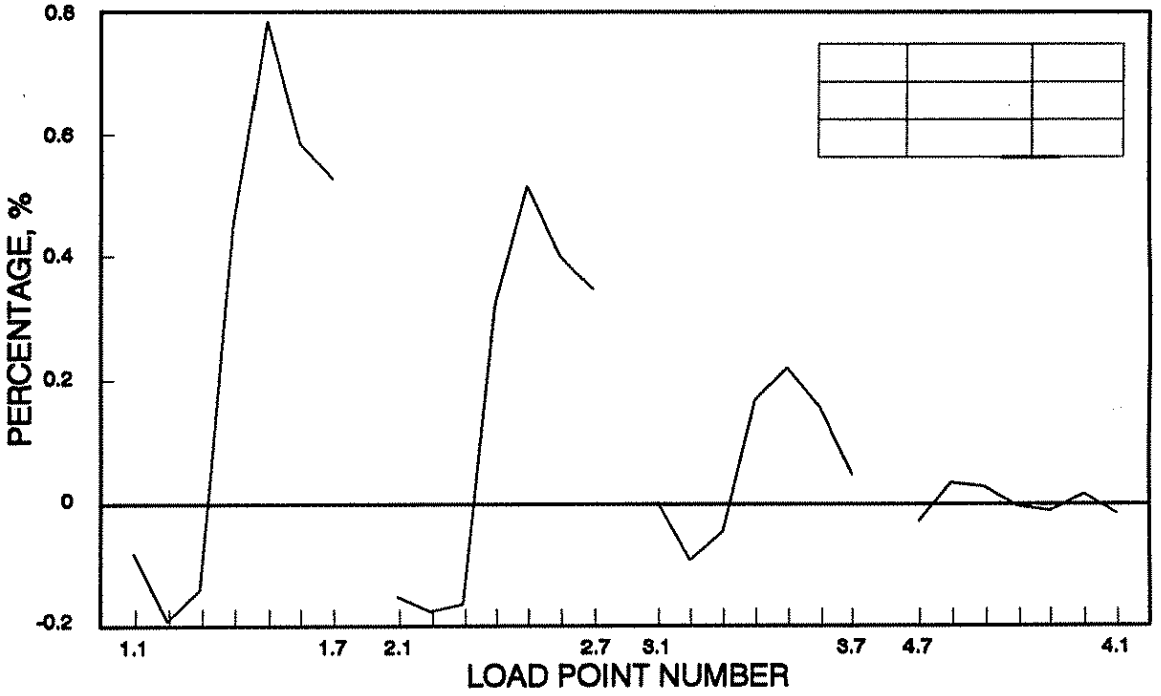

b. TRUSS 4

Fig. 5.28. Percent change in south truss tendon forces due to vertical loading.

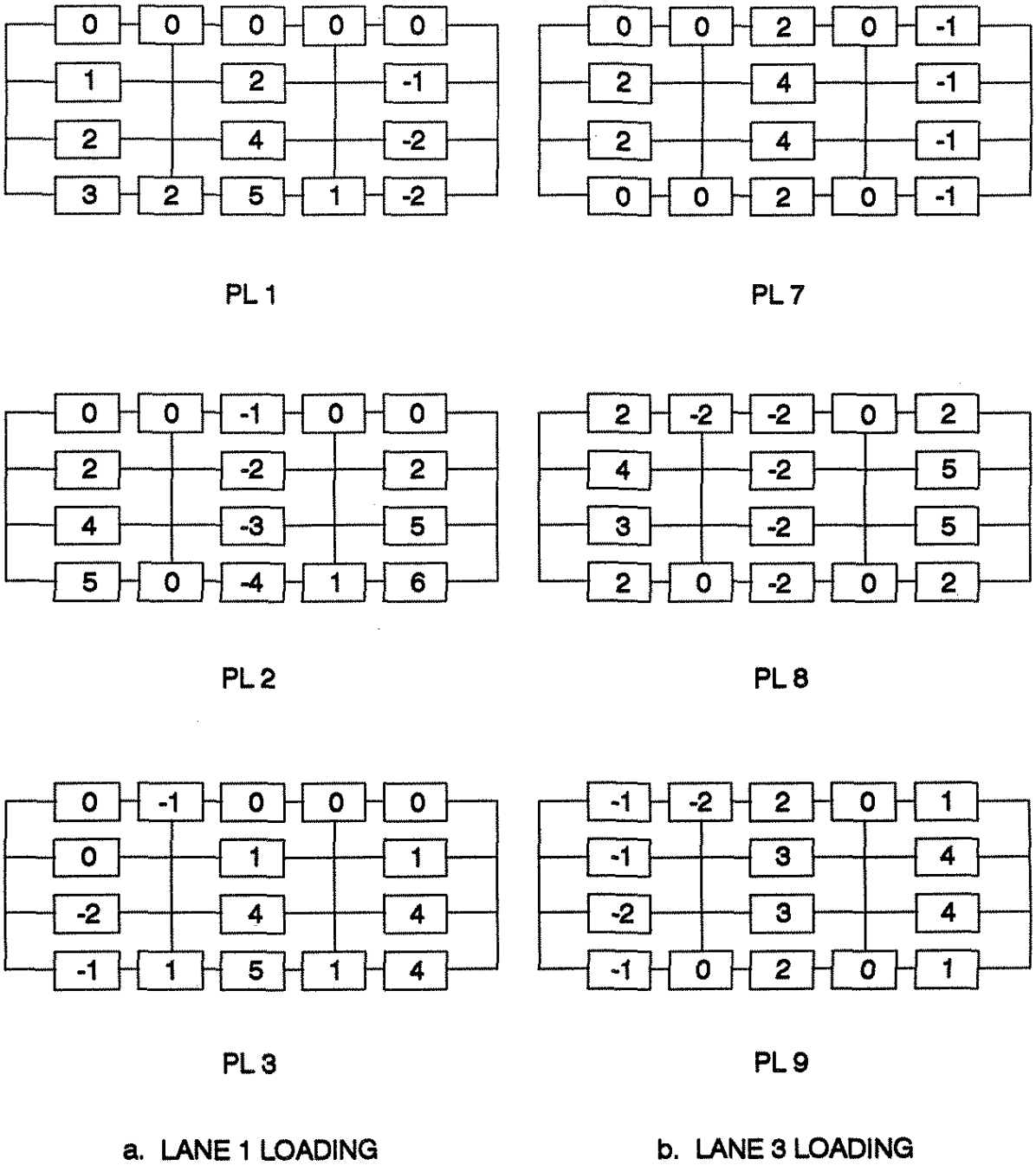

Fig. 5.29. Change in strengthening force (kips) due to pattern loading.

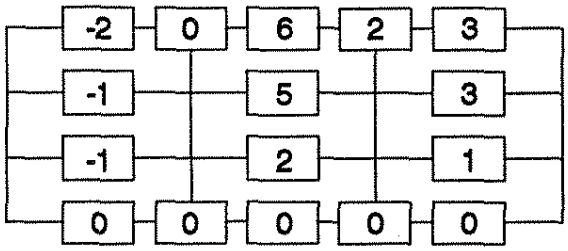

PL 10

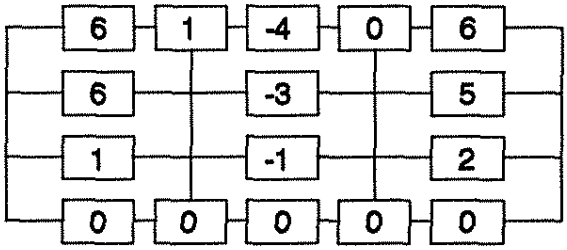

PL 11

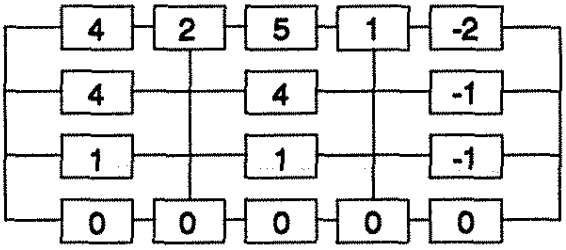

PL 12

c. LANE 4 LOADING

Fig. 5.29. continued.

in reverse order because the direction of Lane 4 was opposite the other three lanes. The maximum increase in tendon force for the interior stringer tendon was 7.0% while the maximum decrease was 1.7%. Both of these values occurred when the vehicle was located in Lane 1. The driver's side wheel line was 1.2 ft south of stringer 2 for Lane 1 loading and 1.8 ft north of stringer 2 for Lane 2 loading. As shown, the data for Lane 2 yielded results only slightly smaller than Lane 1 loading for the interior stringer tendon. The changes in tendon force for the exterior stringer were larger than for the interior stringer for Lane 1 loading. The maximum increase was 12% while the maximum decrease was 2.9% associated with Lane 1.

Similar plots were constructed for the west span as shown in Figs. 5.26a and 5.26b. For the interior stringer, Lane 1 and 2 again yielded very similar results; the maximum changes were a 6.6% increase and a 2.5% decrease. Figure 5.26b shows a maximum increase of 9.6% and decrease of 3.8%, both from Lane 1 loading. Note how both Figs. 5.25 and 5.26 show the effect of the lateral location of the vehicle on the tendon forces.

Figures 5.27 and 5.28 represent the percent change in truss tendon forces when the bridge is subjected to vertical loading. The largest percent increase for any truss tendon was 0.84% and the largest percent decrease was 0.31%. This represents only a 1 or 2 kip change in force.

For the single vehicle load cases, the loaded span deflects downward and the adjacent unloaded span(s) deflect upward. Because one truss bearing is in the loaded span (causing an increase in tendon force) and the other is in the adjacent unloaded span (causing a decrease in tendon force) the net effect causes the very small change in tendon force.

The effect discussed above is illustrated by Fig. 5.27a which shows the change in Truss 1 tendon force due to loading at load point 4.3. For this loading the middle span deflects downward and the end spans upward; the middle span deflects more than the end spans. Figure 5.27a indicates a 0.81% increase in tendon force.

Actual changes in tendon force for some of the strengthened pattern load tests are presented in Fig. 5.29. Lane 2 has been omitted because of its similarity to Lane 1. Analysis of this figure shows that the changes in truss tendon force ranged from -2 kips to +2 kips. For the end spans, the range was -2 kips to +6 kips and for the middle span -4 kips to +6 kips.

The tendon forces change depending upon the change in the elastic curve of the bridge. In a continuous bridge, the change in these forces can be either positive or negative (increase or decrease). This is different than what occurs when strengthening a simple span bridge. In such a case, the post-tensioning force for simple spans increases when additional vertical load is applied, except when the load is applied at a large eccentricity from the longitudinal centerline of the bridge. The tendon force on a continuous span bridge can either increase or decrease depending on the position of the loading.

5.5. Guardrail Strains

Previous research work reported in HR-308 [1], established that the guardrails resist part of the vertical load applied to the bridge. The bridge tested in that work was similar to the current bridge being investigated. The intent of monitoring guardrail strains in this study was to quantify the

load carrying contribution of the guardrails. The location of the strain gages on the guardrails was shown in Fig. 3.1 (see Sec. 3.1). This section discusses the guardrail strains measured during load testing.

The data presented in Figs. 5.30 and 5.31 are for the unstrengthened bridge. The figures illustrate the stringer strains and the corresponding guardrail strains for a given loading condition. In some instances, the guardrail strains exceeded 50 MII which is a significant percentage of the stringer strains. This observed behavior demonstrates that the bridge guardrail is carrying a portion of the applied loads. This can be explained by the fact that the guardrails along with the exterior stringers are acting as vierendeel trusses along the side of the bridge.

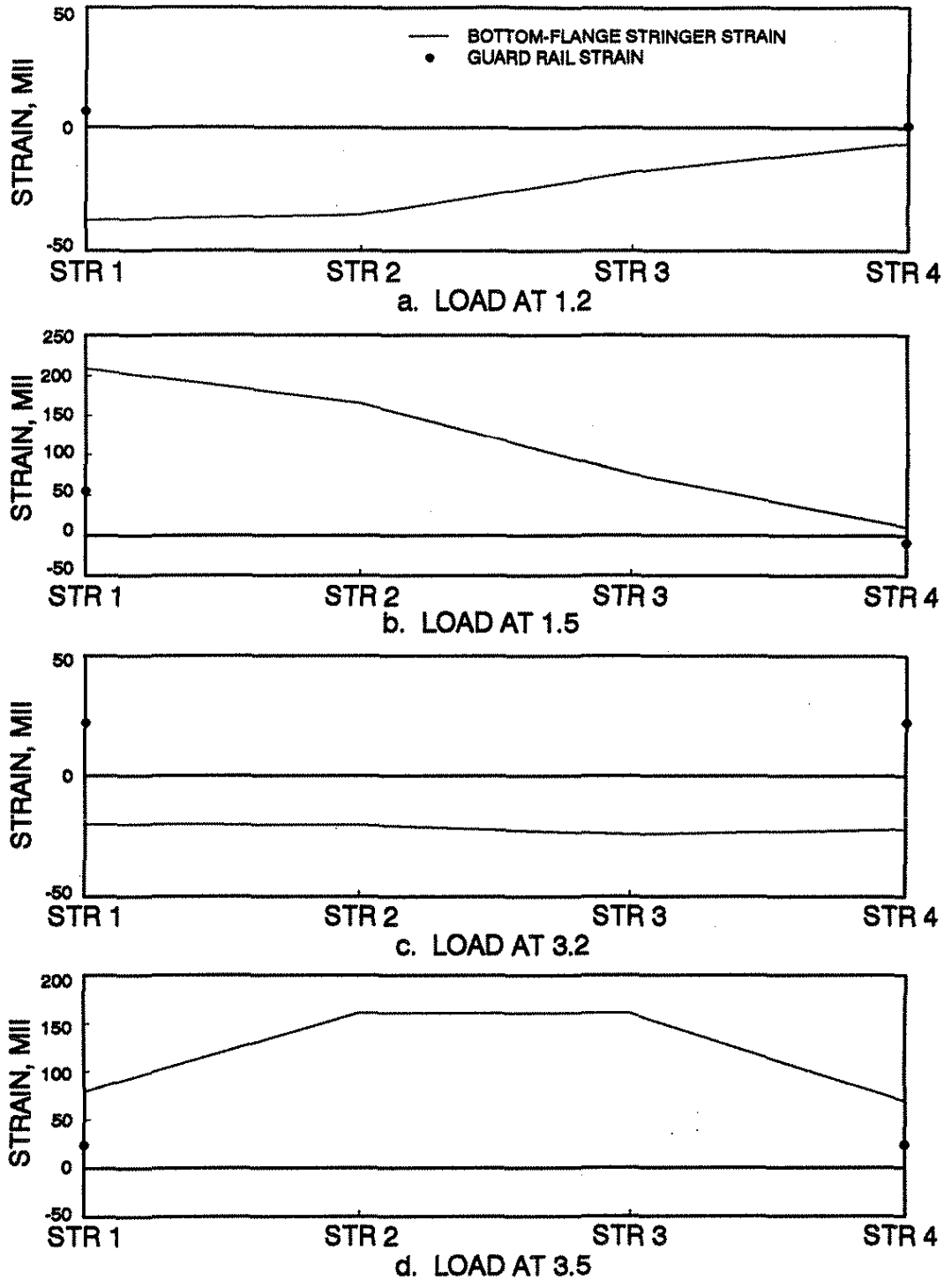

Fig. 5.30. Guardrail strains at midspan of middle span, no strengthening.

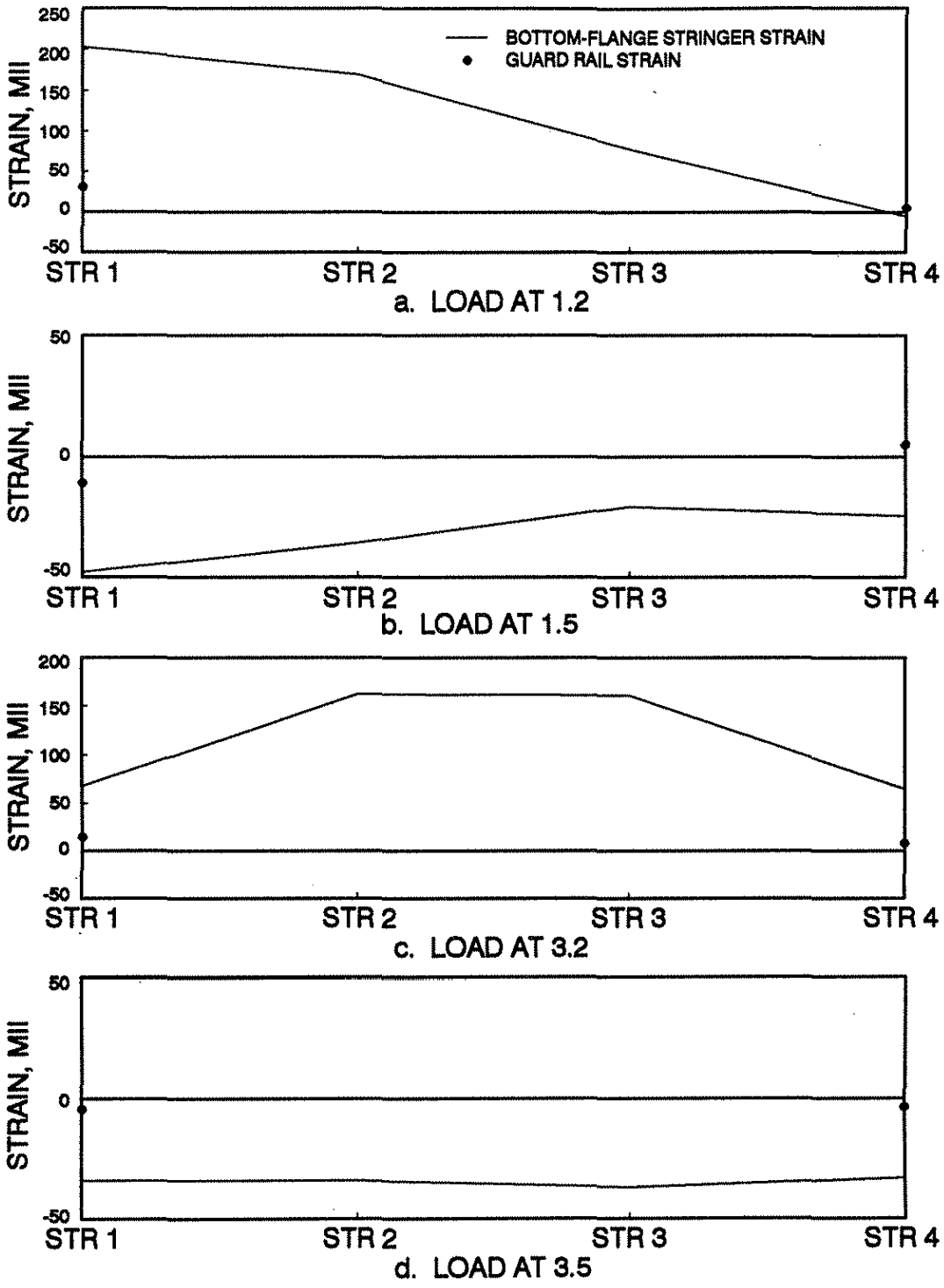

Fig. 5.31. Guardrail strains at midspan of west span, no strengthening.

6. SUMMARY AND CONCLUSIONS

6.1. Summary

This report documents the research that has been performed on the strengthening of a continuous-span, steel-stringer bridge. The research program consisted of two parts: Part 1 - Development of a Design Manual, Part 2 - Field Tests.

A comprehensive literature review pertaining to bridge strengthening was previously performed. Because these reviews are readily available, only articles published after January, 1990 have been included in this report.

The research team, in coordination with the Office of Bridge Design at the Iowa DOT, selected the bridge to be strengthened. This bridge is a three-span, continuous, steel-stringer, concrete-deck bridge from the V12 series. The bridge is located in Cerro Gordo County approximately 12 miles south of Mason City, Iowa. Exterior stringers are W21x62 and the interior stringers are W24x76.

The bridge was analyzed for overstresses considering Iowa legal loads using continuous beam analysis procedures. A 1/4 symmetry finite element model of the bridge was also developed to calibrate the beam analysis and to determine the strengthening forces required to achieve the desired stress reductions. The strengthening system consisted of post-tensioning in the positive moment regions of the stringers and superimposed trusses at the intermediate supports of the exterior stringers.

The field work included application of the post-tensioning brackets and tendons in the positive moment regions and the

truss tubes, brackets, and tendons at the piers. Shear connectors were added in the positive moment regions to satisfy the current AASHTO design specification [21].

Field tests were performed to evaluate the structural behavior of the strengthened bridge when subjected to the strengthening forces as well as live loads. Load tests with heavily loaded trucks were performed before and after strengthening. Strain gages and direct current displacement transducers were used to measure the effect of the applied loads.

A design methodology for the strengthening of continuous-span, composite, steel-stringer bridges has been developed. A design manual [25] has been prepared to assist in the design of strengthening systems for three-span continuous bridges. The manual contains an explanation of the design methodology and an example to illustrate the design procedure developed.

6.2. Conclusions

Based on the research performed and presented in this report the following conclusions have been made:

1. A linear bridge response was exhibited from the application of the superimposed truss forces.
2. The superimposed truss system acting alone slightly increased the stiffness of the bridge.
3. Field data showed that stresses were reduced in the negative moment regions at the piers due to the superimposed truss forces. Also, due to longitudinal distribution of these forces, a reduction in positive moment region stresses was observed.

4. Transverse distribution of the superimposed truss forces occurred as evidenced by the reduction in interior stringer strains (stresses) when the bridge was truss strengthened only.
5. Changes in post-tensioning tendon forces due to vertical loading of the fully strengthened bridge can be either positive (force increase) or negative (force decrease).
6. Changes in superimposed truss tendon forces due to vertical loading of the fully strengthened bridge were insignificant.
7. Guardrail strains indicated that a significant portion of the vertical load was being resisted by the guardrails.
8. The design methodology developed in this report and utilized in the associated design manual is an effective means of designing a strengthening system for continuous-span, composite, steel-stringer bridges.

7. RECOMMENDED FURTHER RESEARCH

On the basis of the literature reviewed and the work completed in the area of bridge strengthening (for this project as well as previous projects), it would be logical to consider continuing related research as follows:

1. Data from the investigation as well as from other investigations have determined that the guardrails are supporting a significant portion of the live load. The various guardrail configurations, connections, etc. should be reviewed and analyzed so that their structural contribution to the capacity of the bridge can be taken into account in the rating process. Modifications that could increase the structural contribution of the guardrail to the capacity of the bridge should also be investigated.
2. Although approximate procedures have been developed for determining the ultimate strength of the two strengthening procedures, these procedures should be extended and possibly modified to be consistent with the AASHTO LRFD Specifications.
3. With consideration of the new AASHTO Manual for Maintenance Inspection of Bridges, a practical method for evaluating the strength provided by the strengthening system should be developed for use by bridge rating engineers.
4. The combination of post-tensioning the positive moment regions and superimposed trusses was successful in eliminating the overstresses in the positive and negative moment regions of the bridge investigated in this project. However, since the trusses require more material and installation time, post-tensioning of the negative moment regions should be investigated as a possible alternative to the trusses.

5. To date, all post-tension strengthening research has been tested and implemented on steel stringers. The post-tension strengthening procedures developed should be tested on reinforced concrete and prestressed concrete beams. Such a strengthening scheme could also be used for repairing damaged beams. A preliminary study to determine the current state-of-the-art and the feasibility of the strengthening procedures is appropriate.
6. The use of prestressing should be reviewed for use in new designs. Based on preliminary analysis, it appears post-tensioning of steel stringers in new bridges can result in a considerable weight savings. A theoretical as well as laboratory investigation of this concept should be initiated.

8. ACKNOWLEDGEMENTS

The study presented in this report was conducted by the Bridge Engineering Center under the auspices of the Engineering Research Institute of Iowa State University. The research was sponsored by the Highway Division, Iowa Department of Transportation, and the Highway Research Board under Research Project HR 333.

The authors wish to extend sincere appreciation to the engineers of the Iowa DOT for their support, cooperation, and counseling. A special thanks is extended to the following individuals for their help in various phases of the project:

- William A. Lundquist (Bridge Engineer, Iowa DOT)
- John P. Harkin (Chief Structural Engineer, Iowa DOT)
- Kevin B. Jones (Special Investigations Engineers, Iowa DOT)
- Dirk Jablonski (County Engineer, Cerro Gordo County)
- Douglas L. Wood (Structures Laboratory Supervisor, ISU)

Appreciation is also extended to Jessie G. Barrido of Dywidag Systems International (DSI), Lemont, Illinois, who donated the Dywidag threadbars used on the bridge. The epoxy coating of the bars by Midwest Pipe Coating, Inc., Schererville, Indiana, is also appreciated.

Special thanks are accorded to the numerous undergraduate students in Civil Engineering at ISU and to structural engineering graduate students, Rick Janik, Matthew Johnson, Brian McCurnin, and Shekhar Scindia for their assistance in various phases of the project.

9. REFERENCES

1. Klaiber, F. W., Dunker, K. F., S. M. Planck, W. W. Sanders, Jr. "Strengthening of an Existing Continuous-Span, Steel-Beam, Concrete Deck Bridge by Post-Tensioning." Final Report. ISU-ERI-Ames-90210. Ames: Engineering Research Institute, Iowa State University, Ames, IA, 1990.

2. Klaiber, F. W., Wipf, T. J., Dunker, K. F., Abu-Kishk, R. B., Planck, S. M. "Alternate Methods of Bridge Strengthening." Final Report. ISU-ERI-Ames-89262. Ames: Engineering Research Institute, Iowa State University, Ames, IA, 1989.

3. El-Arabaty, H. *Strengthening of Continuous Span Composite Bridges Using Post-Tensioning and Superimposed Trusses*. PhD. Dissertation, Iowa State University, Ames, Iowa, 1993.

4. Dunker, K. F., F. W. Klaiber, F. K. Daoud, W. E. Wiley, W. W. Sanders, Jr. "Strengthening of Existing Continuous Composite Bridges." Final Report. ISU-ERI-Ames-88007. Ames: Engineering Research Institute, Iowa State University, Ames, IA, 1987.

5. Dunker, K. F., F. W. Klaiber, W. W. Sanders, Jr. "Design Manual for Strengthening Single-Span Composite Bridges by Post-Tensioning." Final Report-Part III. ISU-ERI-Ames-85229. Ames: Engineering Research Institute, Iowa State University, Ames, IA, 1985.

6. Klaiber, F. W., D. J. Dedic, K. F. Dunker, W. W. Sanders, Jr. "Strengthening of Existing Single Span Steel Beam and Concrete Deck Bridges." Final Report-Part I. ISU-ERI-Ames-83185. Ames: Engineering Research Institute, Iowa State University, Ames, IA, 1983.

7. Dunker, K. F., F. W. Klaiber, B. L. Beck, W. W. Sanders, Jr. "Strengthening of Existing Single-Span Steel-Beam and Concrete Deck Bridges." Final Report-Part II. ISU-ERI-Ames-85231. Ames: Engineering Research Institute, Iowa State University, Ames, IA, 1985.

8. Klaiber, F. W., K. F. Dunker, W. W. Sanders, Jr. "Feasibility Study of Strengthening Existing Single Span Steel Beam Concrete Deck Bridges." Final Report. ISU-ERI-Ames-81251. Ames: Engineering Research Institute, Iowa State University, Ames, IA, 1981.

9. Klaiber, F. W., K. F. Dunker, T. J. Wipf, W. W. Sanders, Jr. "Methods of Strengthening Existing Highway Bridges." National Cooperative Highway Research Program Report 293, Transportation Research Board, 1987, pp. 114.

10. Klaiber, F. W., K. F. Dunker, T. J. Wipf, Fanous, F. S. "Strengthening of Existing Bridges by Post-Tensioning.", *Symposium on Practical Solutions for Bridge Strengthening & Rehabilitation, Proceedings*. Bridge Engineering Center, Iowa State University, 1993, pp. 143-152.

11. Saadatmanesh, H., P. Albrecht, B. M. Ayyub. "Guidelines for Flexural Design of Prestressed Composite Beams." *Journal of Structural Engineering*, ASCE, 115, No. 11, November, 1989, pp. 2944-2961.

12. Ayyub, B. M., Y. G. Sohn, H. Saadatmanesh. "Prestressed Composite Girders. I: Experimental Study for Negative Moment." *Journal of Structural Engineering*, ASCE, 118, No. 10, October, 1992, pp. 2743-2762.

13. Ayyub, B. M., Y. G. Sohn, H. Saadatmanesh. "Prestressed Composite Girders. II: Analytical Study for Negative Moment." *Journal of Structural Engineering*, ASCE, 118, No. 10, October, 1992, pp. 2763-2782.

14. Ayyub, B. M., Y. G. Sohn, H. Saadatmanesh. "Prestressed Composite Girders Under Positive Moment." *Journal of Structural Engineering*, ASCE, 116, No. 11, November, 1990, pp. 2931-2951.

15. Tong, W., H. Saadatmanesh. "Parametric Study of Continuous Prestressed Composite Beams." *Journal of Structural Engineering*, ASCE, 118, No. 1, January, 1992, pp. 186-206.

16. Mancarti, G. D. "Strengthening Short Span Bridges for Increased Live Loads.", *Proceedings of the Third International Conference on Short and Medium Span Bridges*, Canadian Society of Civil Engineers, Volume II, 1990, pp. 169-180.

17. Albrecht, P., W. Li. "Fatigue Strength of Prestressed Composite Beams." Final Report. NSF Project ECE-85-13684, University of Maryland, College Park, MD 1990.

18. Saadatmanesh, H., M. R. Ehsani. "RC Beams Strengthened with GFRP Plates. I: Experimental Study." *Journal of Structural Engineering*, ASCE, 117, No. 11, November, 1991, pp. 3417-3433.

19. An, W., H. Saadatmanesh. "RC Beams Strengthened with FRP Plates. II: Analysis and Parametric Study." *Journal of Structural Engineering*, ASCE, 117, No. 11, November, 1991, pp. 3434-3455.

20. Seible, F., Priestley, M. J. N., and Krishnan, K., "Bridge Superstructure Rehabilitation and Strengthening." *Transportation Research Record*, No. 1290, Volume 1, 1991, pp. 59-67.

21. American Association of State Highway and Transportation Officials. *Standard Specifications for Highway Bridges*, 14th Edition. Washington: American Association of State Highway and Transportation Officials, 1989.

22. Dedic, D. J. *Push-out and Composite Beam Tests of Shear Connectors*. M. S. Thesis, Iowa State University, Ames, Iowa, 1983.

23. Standard Design, Continuous 3-Span I-Beam Bridges, 24 ft Roadway, Concrete Floor, Steel Rail, H-15 Loading. Ames: Iowa State Highway Commission, 1957.

24. Standard Design, 28 ft Roadway, Continuous I-Beam Bridges, Concrete Floor, Steel Rail, H-20 Loading. Ames: Iowa State Highway Commission, 1960.

25. Klaiber, F. W., F. S. Fanous, T. J. Wipf, H. El-Arabaty. "Design Manual for Strengthening of a Continuous-Span Composite Bridge." ISU-ERI-Ames-94404. Ames: Engineering Research Institute, Iowa State University, Ames, IA, 1993.

APPENDIX A

INSTRUMENTATION DETAILS

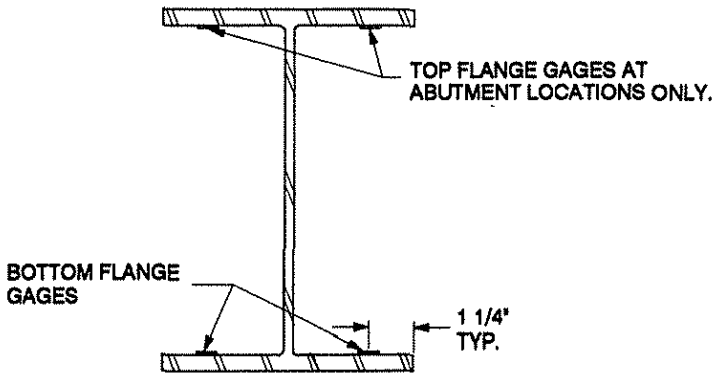

a. STRINGER FLANGES

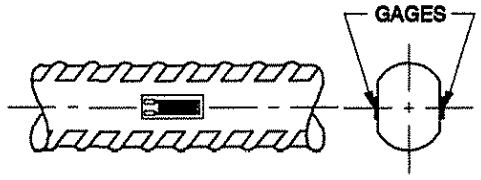

b. TENDONS

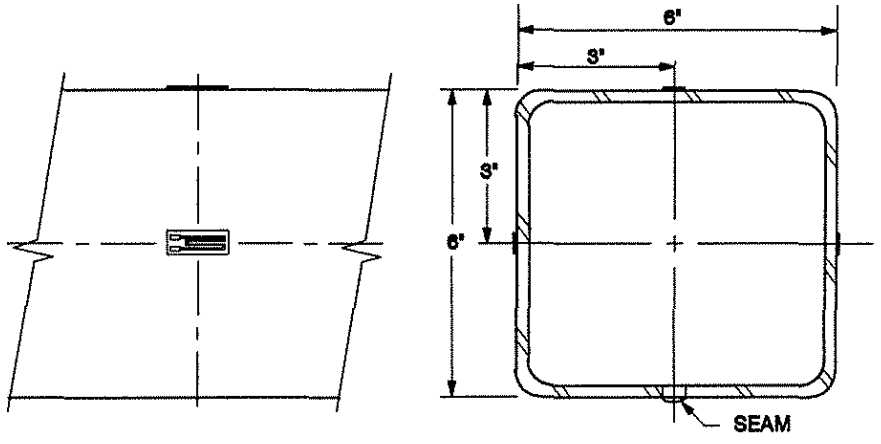

c. SUPERIMPOSED TRUSS TUBES

Fig. A.1. Strain gage instrumentation details.

APPENDIX B

BRACKET DETAILS

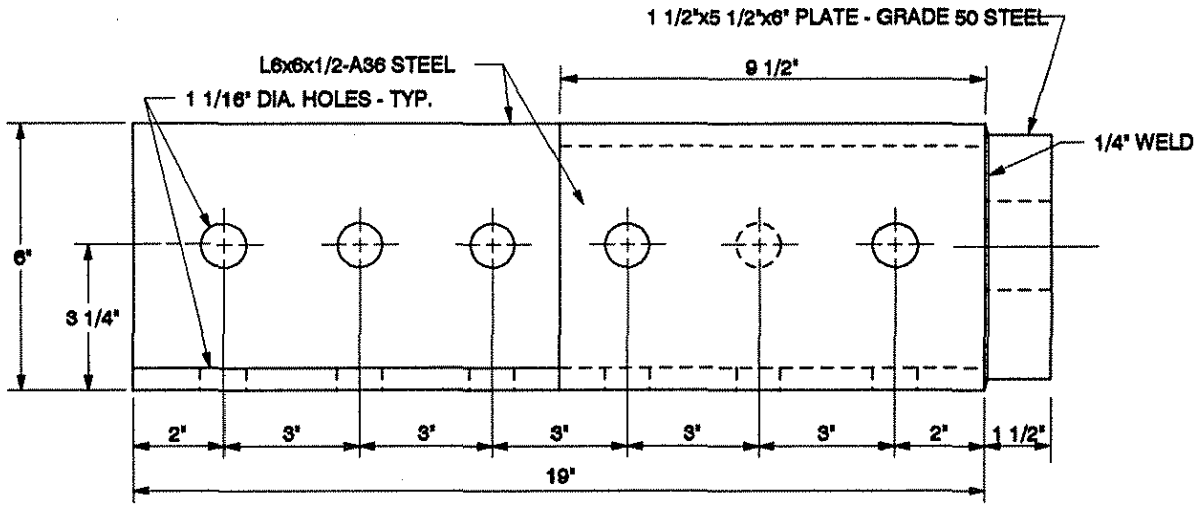

a. SIDE VIEW

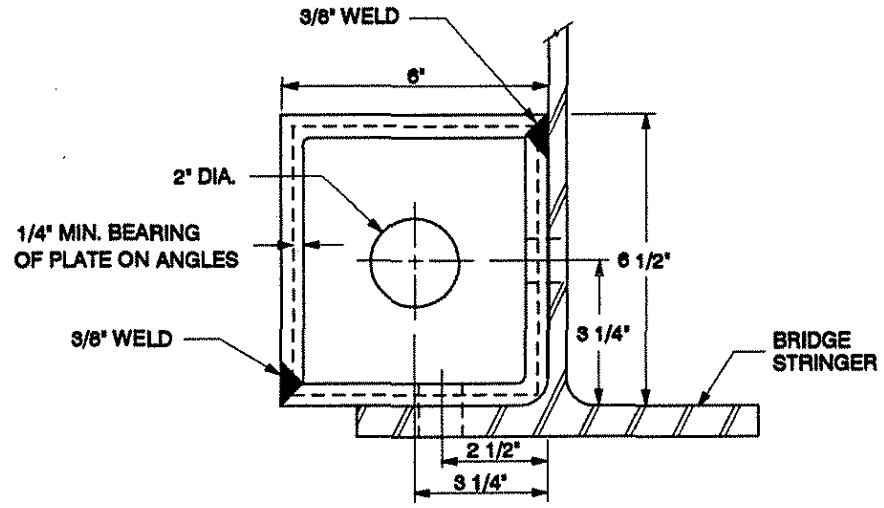

b. END VIEW

Fig. B.1. Post-tensioning Bracket A.

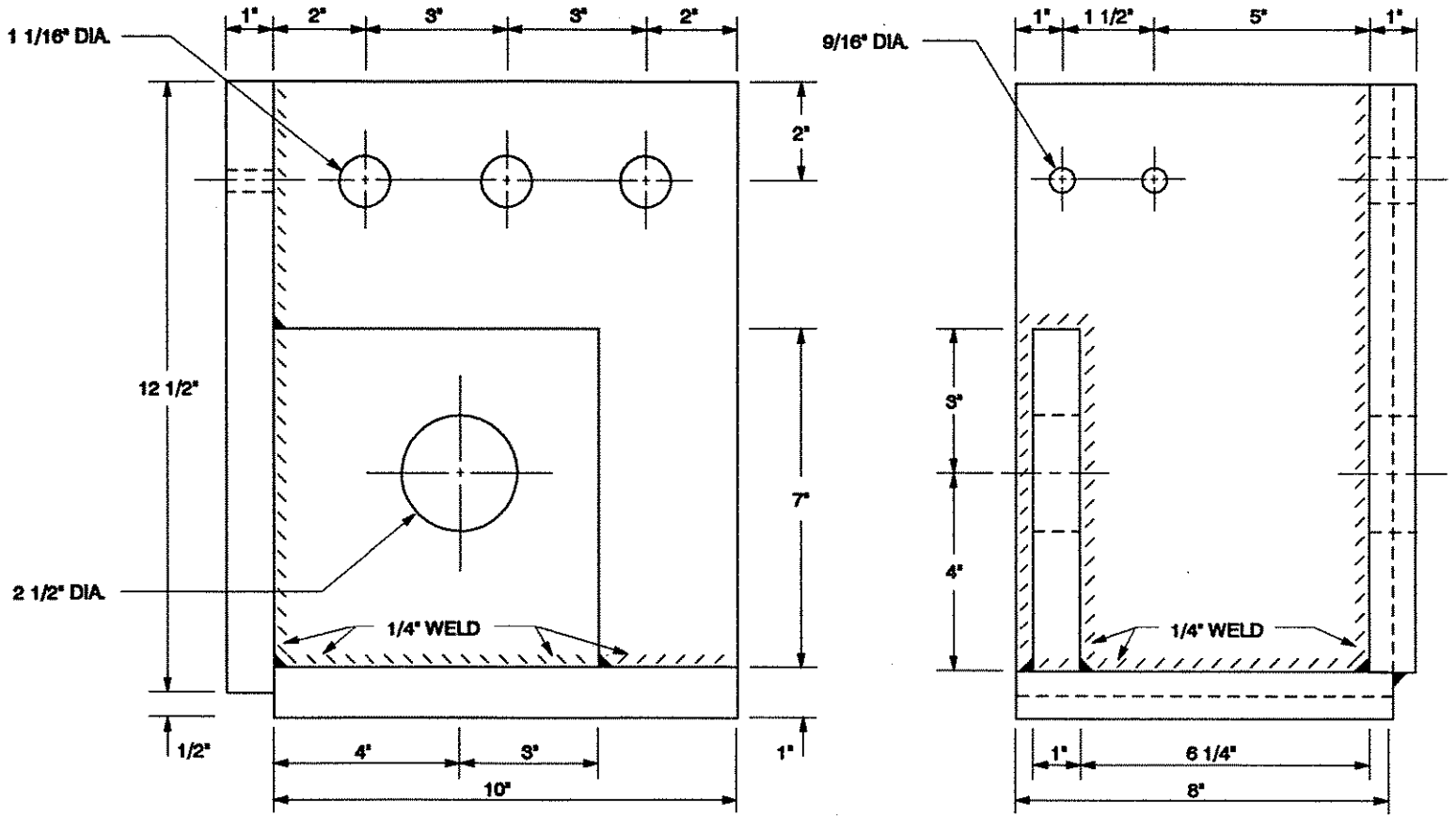

Fig. B.2. Truss pin Bracket B.

APPENDIX C

TRUSS DETAILS

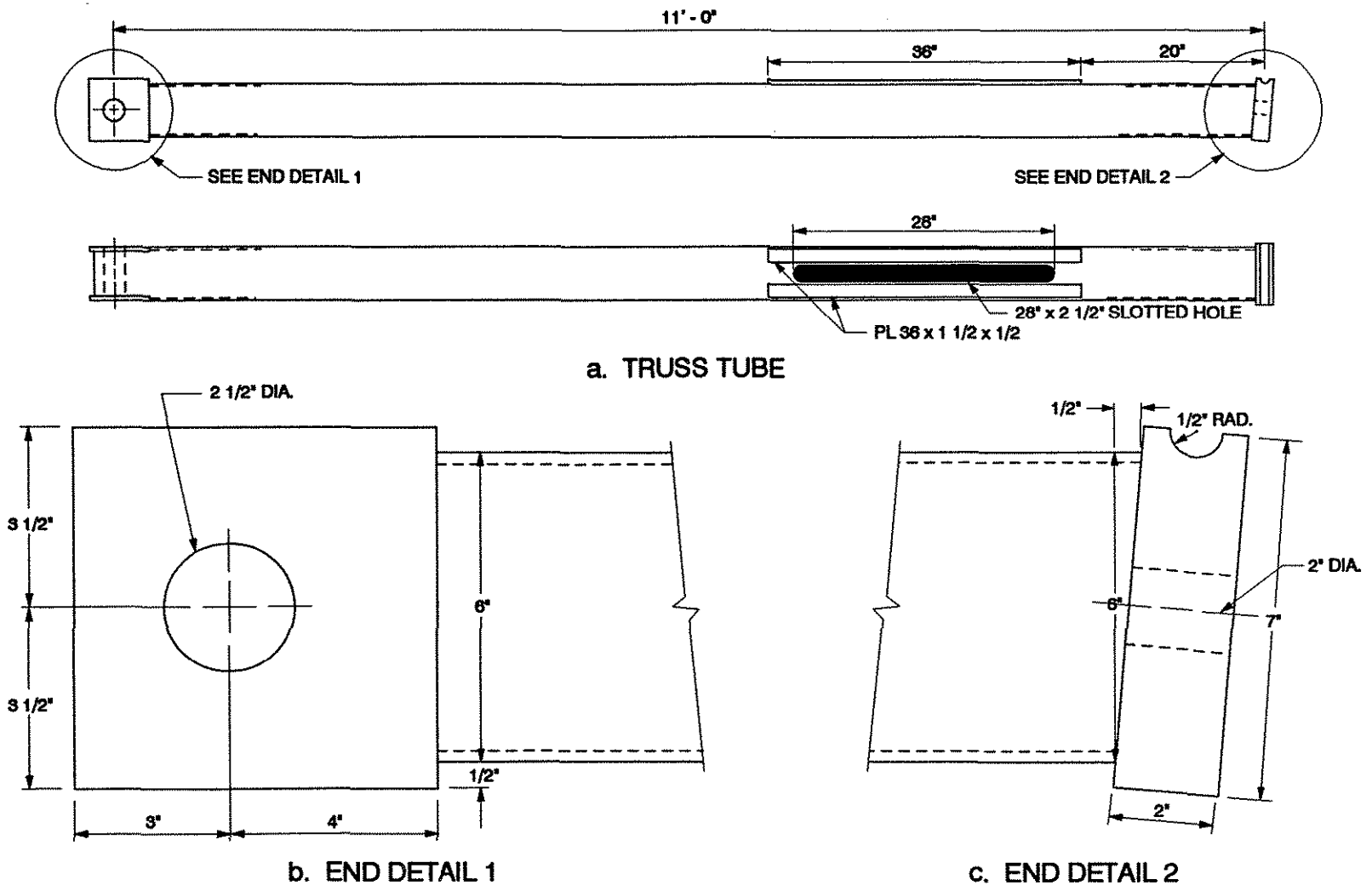

Fig. C.1. Truss tube

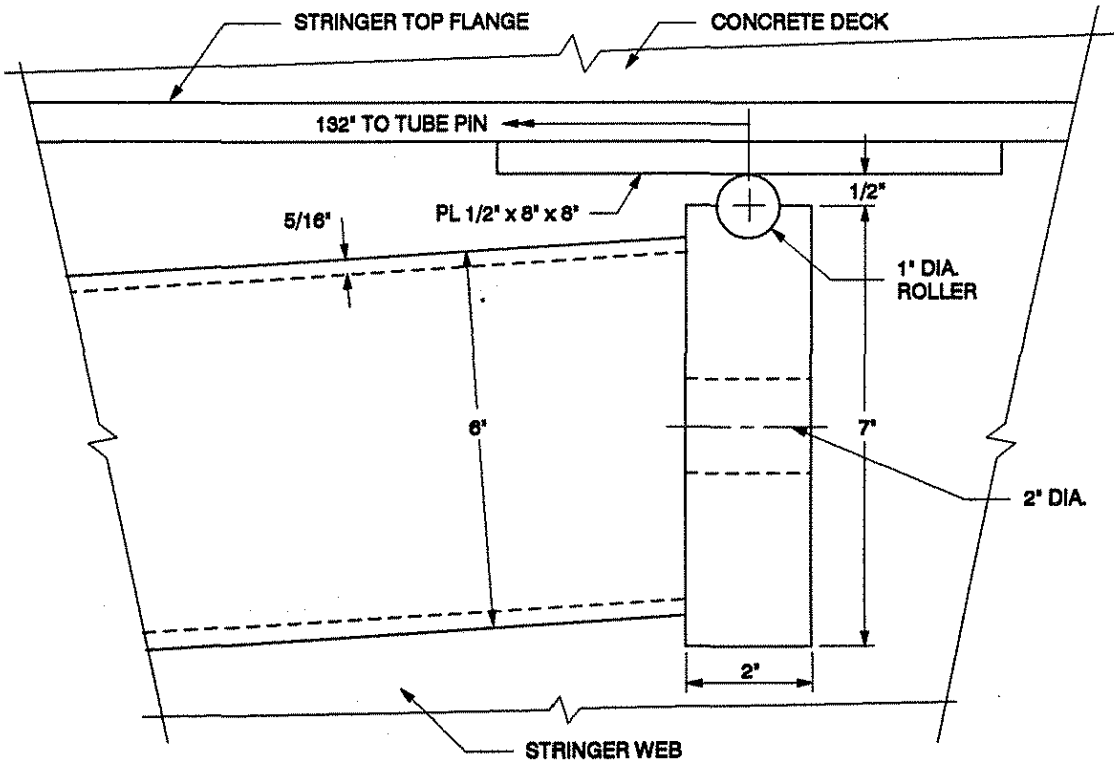

Fig. C.2. Truss bearing detail.

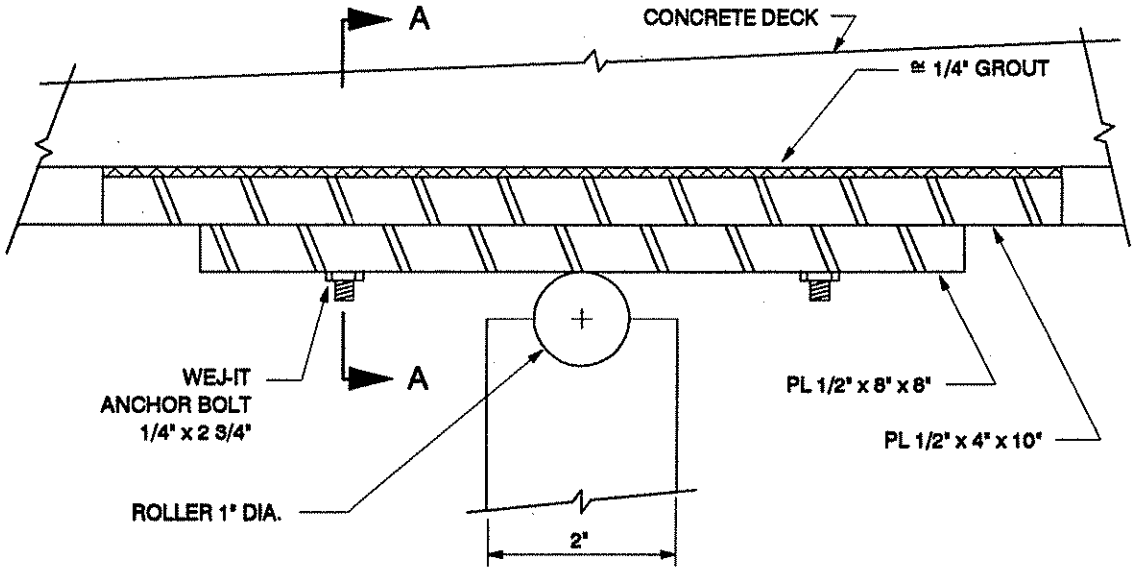

a. LONGITUDINAL BEARING PLATE SECTION

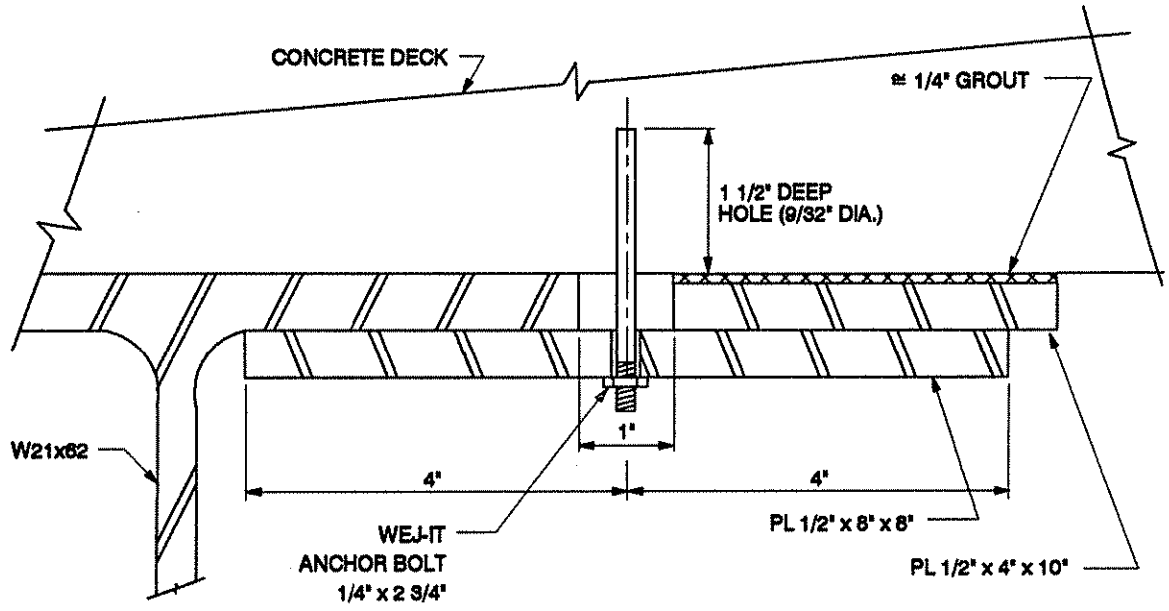

b. TRANSVERSE BEARING PLATE SECTION: SECTION A-A

Fig. C.3. Bearing plate assembly.